2014

Localization and security algorithms for wireless sensor networks and the usage of signals of opportunity

Gustavo Andres Chacon Rojas
Louisiana State University and Agricultural and Mechanical College

LOCALIZATION AND SECURITY ALGORITHMS FOR WIRELESS SENSOR NETWORKS AND THE AND THE USAGE OF SIGNALS OF OPPORTUNITY

A Dissertation

Submitted to the Graduate Faculty of the
Louisiana State University and
Agricultural and Mechanical College
in partial fulfillment of the
requirements for the degree of
Doctor of Philosophy

in

The School of Electrical Engineering and Computer Sciences

by
Gustavo Andres Chacon Rojas
B.Sc., University of Chile, 2006
M.Sc., University of Chile, 2006
May 2014

"... and when your deepest thoughts are broken,
keep on dreaming boy,
cause when you stop dreamin' it's time to die."

Acknowledgments

First of all, I would like to express my gratitude to my professor advisor, Dr. Morteza Naraghi-Pour, for the opportunity to work with him, for the confidence given to me, and overall for his patience with the ideas we discussed. The knowledge and experience gained during his courses and the research we worked on have influenced me in different and positive ways, specially from the mathematical point of view. I also appreciate the opportunity for developing electronic circuits and systems, for which the ideas he provided had a great impact in the final results.

Also, I would like to thank to many of the professors of the Division of Electrical & Computer Engineering at LSU. Specially to Dr. Guoxiang Gu, Dr. Shuangqing Wei and Dr. Xuebin Liang for the knowledge and experience provided during their courses, which enriched my vision in different areas of Electrical Engineering. Moreover, I appreciate for being part of the committee of this Dissertation, providing me comments and support in the development of it. I would also like to thank Mr. John Scalzo for the opportunity of teaching part of a course during two semesters, from which I have gained a very rich experience for the future. I would like to thank Dr. Chester Wilmot for his time and comments during this dissertation.

I thank and appreciate the great support of my whole family, specially my parents, Maria and Gustavo, and my brothers and sister. The encouraging during my Ph.D. studies were one the best support I could have ever had, for that I will always be grateful. This academic achievement is dedicated to my parents, without them I would not have made it possible.

Besides the professors from the Division of Electrical & Computer Engineering, I would like to thank the staff of the department, making the campus living situation more friendly. Specially, I would like to mention Beth Cochran and Sandy Saale.

Finally and no because of that less important, I would like to thank all my friends for their support and making me laugh when I most needed. Besides my friends being far away, I greatly appreciate the support of Paul Callahan, James Kimura-Green, Michael Mackenzie, Thomas LaPann, Christopher Bergeron and Justin Taylor, among many more.

Table of Contents

Acknowledgments iii

List of Tables vii

List of Figures x

Abstract xi

1 Introduction and Related Work 1
1.1 Related Work 3
1.1.1 Positioning System based on Narrowband Signals of Opportunity 3
1.1.2 Localization of Node in Wireless Sensor Network 5

2 Positioning System based on Narrowband Signals of Opportunity . . . 12
2.1 Problem Formulation 12
2.2 Proposed Algorithm 13
2.2.1 Localization with Time Difference of Arrival 13
2.2.2 Time Difference of Arrival Estimation for Narrowband Signals 21
2.3 Simulation Results 33

3 Localization of Nodes in Wireless Sensor Networks 39
3.1 Distributed Nodes Localization in WSN 39
3.1.1 Problem Formulation 39
3.1.2 Proposed Algorithm 41
3.1.3 Simulation Results 52
3.2 Distributed Mobile Nodes Localization in WSN 61
3.2.1 Mobility Model 62
3.2.2 Modification of DRGD for Mobile Sensors 63
3.2.3 Simulation Results 65
3.3 Centralized Node Localization in WSN with Outlier Communication Links 68
3.3.1 Simulation Results 74

4 Conclusion 83

Appendix A: Proof and Discussion of Lemma 1 86

Appendix B: CRLB and MLE for Localization using TDOA 89

References 91

Vita 103

List of Tables

2.1 Distance from base/mobile to FM transmitters. 35

2.2 Mean and variance for estimated TDOAs under SNR = 20 dB 36

2.3 Mean and variance for estimated TDOAs under SNR = 10 dB 37

3.1 Summary of Algorithm 2. 53

3.2 Average CPU execution time (in seconds) for localization using SOCP, SA and DRGD. 60

3.3 Localization Algorithm in Presence of Outlier Edges 75

List of Figures

2.1 Schematic illustration of TDOA 15

2.2 Graph of $|S_\ell(\omega)|$ over $[0,\ 2M\pi]$ in the case of odd M illustrated for $M = 3$ 24

2.3 Graph of $|S_\ell(\omega)|$ over $[0,\ 2M\pi]$ in the case of even M illustrated for $M = 4$. 24

2.4 Block diagram for reconstruction of $\{s(n)\}$ based on $\{s_\ell(n)\}$ 26

2.5 Graph of $|\tilde{S}_\ell(\omega)|$ over $[0,\ 2\pi]$ with BPF illustrated for $M = 3$ 26

2.6 General diagram of a typical FM receiver. 33

2.7 Scheme of the position of the FM transmitters, Base and Mobil. . . . 35

2.8 Outage curve for localization accuracy averaged over 1000 emsemble runs 38

3.1 (a) The Network topology. (b) Initial positions for the localization algorithms. (c) Localization results using relaxation and SOCP. (d) Localization results using SDP. (e) Localization results using SA. (f) Localization results using the proposed DRGD. 55

3.2 (a) The Network topology. (b) Localization results using relaxation and SOCP. (c) Localization results using SDP. (d) Localization results using SA. (e) Localization results using the proposed DRGD. 56

3.3 (a) The Network topology. (b) Localization results using relaxation and SOCP. (c) Localization results using SDP. (d) Localization results using SA. (e) Localization results using the proposed DRGD. 57

3.4 RMSE for the localization of 20 networks with similar characteristics to Figure 3.2-(a) using SOCP, SDP, SA and DRGD. 58

3.5 RMSE for the localization of 20 networks with similar characteristics to Figure 3.3-(a) using SOCP, SDP, SA and DRGD. 59

3.6 (a) The Network topology. (b) Localization results using relaxation and SOCP. (c) Localization results using SDP. (d) Localization results using SA. (e) Localization results using the proposed DRGD. 60

3.7 (a) The Network topology. (b) Localization results using relaxation and SOCP. (c) Localization results using SDP. (d) Localization results using SA. (e) Localization results using the proposed DRGD. 61

3.8 (a) The Network topology. (b) Localization results using relaxation and SOCP. (c) Localization results using SDP. (d) Localization results using SA. (e) Localization results using the proposed DRGD. 62

3.9 (a) The Network topology. (b) Localization results using relaxation and SOCP. (c) Localization results using SDP. (d) Localization results using SA. (e) Localization results using the proposed DRGD. 63

3.10 CPU execution time-to-convergence vs. the number of anchors using DRGD. 64

3.11 Depiction of the mobility model and the initial position assumed in Table 3.1 for the blind nodes. 65

3.12 Topology of the network with the initial position of the blind and anchor nodes. 66

3.13 One-step movement of the blind nodes. Actual starting and final positions are shown by circles and squares, respectively, along with the initial position (cross) assumed for each node according to (3.39) and the final estimated position from the algorithm (+ sign) for $V_{\max} = 0.1$. 67

3.14 One-step movement of the blind nodes. Actual starting and final positions are shown by circles and squares, respectively, along with the initial position (cross) assumed for each node according to (3.39) and the final estimated position from the algorithm (+ sign) for $V_{\max} = 0.7$. 68

3.15 Trajectories of the blind nodes (blue circles) and the estimated trajectories (red crosses) using the modified DRGD algorithm, $V_{\max} = 0.1$. . 69

3.16 Trajectories of the blind nodes (blue circles) and the estimated trajectories (red crosses) using the modified DRGD algorithm, $V_{\max} = 0.7$. . 79

3.17 Topology of the sensor network, where blue links represent the edges, black squares correspond to anchor nodes, and blue circles correspond to blind nodes. 80

3.18 Real position of the blind nodes (blue circle), the estimated position of the blind nodes (red cross) and the communication links considered non-outliers (blue links) 80

3.19 Real position of the blind nodes (blue circle), the estimated position of the blind nodes (red cross), the communication links considered outliers (in black links), and the true outlier communication links (red links) . 81

3.20 Topology of the sensor network, where blue links represent the edges, black squares correspond to anchor nodes, and blue circles correspond to blind nodes. 81

3.21 Real position of the blind nodes (blue circle), the estimated position of the blind nodes (red cross) and the communication links considered non-outliers (blue links) 82

3.22 Real position of the blind nodes (blue circle), the estimated position of the blind nodes (red cross), the communication links considered outliers (in black links), and the true outlier communication links (red links) . 82

4.1 PDF $f_Z(z)$ versus Gaussian PDF with x-axis scaled by σ^{-1}, y-axis by σ, and $\kappa = 10\sigma$. 88

Abstract

In this dissertation we consider the problem of localization of wireless devices in environments and applications where GPS (Global Positioning System) is not a viable option. The first part of the dissertation studies a novel positioning system based on narrowband radio frequency (RF) signals of opportunity, and develops near optimum estimation algorithms for localization of a mobile receiver. It is assumed that a reference receiver (RR) with known position is available to aid with the positioning of the mobile receiver (MR). The new positioning system is reminiscent of GPS and involves two similar estimation problems. The first is localization using estimates of time-difference of arrival (TDOA). The second is TDOA estimation based on the received narrowband signals at the RR and the MR. In both cases near optimum estimation algorithms are developed in the sense of maximum likelihood estimation (MLE) under some mild assumptions, and both algorithms compute approximate MLEs in the form of a weighted least-squares (WLS) solution. The proposed positioning system is illustrated with simulation studies based on FM radio signals. The numerical results show that the position errors are comparable to those of other positioning systems, including GPS.

Next, we present a novel algorithm for localization of wireless sensor networks (WSNs) called distributed randomized gradient descent (DRGD), and prove that in the case of noise-free distance measurements, the algorithm converges and provides the true location of the nodes. For noisy distance measurements, the convergence properties of DRGD are discussed and an error bound on the location estimation error is obtained. In contrast to several recently proposed methods, DRGD does not require that blind nodes be contained in the convex hull of the anchor nodes, and can accurately localize the network with only a few anchors. Performance

of DRGD is evaluated through extensive simulations and compared with three other algorithms, namely the relaxation-based second order cone programming (SOCP), the simulated annealing (SA), and the semi-definite programing (SDP) procedures. Similar to DRGD, SOCP and SA are distributed algorithms, whereas SDP is centralized. The results show that DRGD successfully localizes the nodes in all the cases, whereas in many cases SOCP and SA fail. We also present a modification of DRGD for mobile WSNs and demonstrate the efficacy of DRGD for localization of mobile networks with several simulation results. We then extend this method for secure localization in the presence of outlier distance measurements or distance spoofing attacks. In this case we present a centralized algorithm to estimate the position of the nodes in WSNs, where outlier distance measurements may be present.

Chapter 1
Introduction and Related Work

Location-based services are a new paradigm in computing/networking which are expected to bring life-changing experience in many areas including work, health, entertainment, personal and social life, and safety and security. A key function of location-based services is the localization of a wireless device. While global positioning system (GPS) has had an overwhelming success in this area, for many applications or scenarios GPS may not be a viable option. In many environments such as indoors, under a forest canopy or in urban canyons the GPS signal may not be available or too weak for reliable positioning. In addition, in applications where cost is of primary concern, a GPS device may not be suitable. An example is in wireless sensor networks (WSNs) where hundreds or thousands of inexpensive sensor nodes must be localized and the cost of a sensor node is expected to be below that of a GSP chip. Finally GPS signals are susceptible to jamming.

With the proliferation of wireless devices, and the societal reliance on such devices for a myriad of applications, positioning of such devices has become an essential and in some cases a critical functionality. In this dissertation we consider two localization algorithms tailored to slightly different applications in wireless networks. The first approach relies on ambient signals such as AM and FM radio, TV, or WiFi signals often referred to as signals of opportunity (SOP). Here a reference receiver (RR) is used to help localize a mobile receiver (MR). The time difference-of-arrival (TDOA) between the signals of opportunity at the two receivers is first estimated. In this application at least four SOP signals are required. One signal is used to eliminate the clock offset between the two receivers and at least three sig-

nals for the estimation of the three position variables in the Cartesian coordinate system. The FM radio signal is considered in the simulations which show position errors comparable to other positioning systems including GPS.

Next we consider localization of the sensor nodes in a wireless sensor network (WSN). WSNs consist of a large number of tiny battery powered sensors that are deployed in the sensor field which, despite their limited resources, can nevertheless network themselves and communicate their collected information with a central station over wireless links. Wireless sensor networks (WSN) have applications in many military and civilian areas including intrusion detection and surveillance, medical monitoring, emergency response, environmental monitoring, target detection and tracking, and battlefield assessment. For the information collected by the sensor nodes to be of any value the information must be tagged with the location of the reporting sensor. Therefore self-localization of the sensors in a WSN has been the topic of intensive research studies in recent years. In Chapter 3 we present a distributed algorithm for the localization of the nodes in a WSNs. This algorithm uses the pairwise distances between all the nodes to calculate the positions. Numerical results are obtained for a large number of different network topologies which show the efficacy of the proposed algorithm compared with those existing methods in the literature. We also extend our proposed method to localization of WSNs when some distance measurements are highly unreliable. This may arise due to the challenges of distance measurement techniques. For example it is well known that distance estimations based on received signal strength in indoors can be highly unreliable due to multipath fading effects. Distance errors may also be due to mischief caused by an adversary who falsifies its reported distances.

In the remainder of this chapter we present a review of the literature on the two problems considered in this dissertation and more details on our solutions for these two problems.

1.1 Related Work

1.1.1 Positioning System based on Narrowband Signals of Opportunity

Collaborative localization using wireless sensor networks has been an active area of research [1, 2]. Recently, however, research activity in this area has been somewhat diminished due to the overwhelming success of the global positioning system (GPS). On the other hand GPS has its own limitations, including low signal power, inability to penetrate natural or man-made structures, and susceptibility to multipath fading. As such, GPS is believed to be less effective in urban canyons, forested areas and mountainous regions, and it usually fails for localization inside building structures. Another concern is the vulnerability of GPS to jamming and spoofing which poses a threat to many law enforcement and military applications.

There are several alternatives for localization in the absence of GPS. The one that interests us in this dissertation is collaborative localization based on signals of opportunity (SOP). Such signals are not intended for localization purposes and include broadcast radio, TV, and wireless LAN (WLAN) signals. The early work in this field can be traced to [3, 4] where AM radio signals are used for positioning. Later work in [5, 6, 7] explores FM radio signals. In [5] the authors utilize the received signal strength (RSS) from FM radio stations and a radio map (a database of RSS measurements at a number of reference locations) to estimate the location of a mobile receiver. The accuracy of this scheme hinges on the availability of an accurate and dense radio map whose construction is difficult as it requires a large number of measurements. Moreover, in many application (e.g., law enforcement or

military) prior construction of such a database is not feasible. RSS of FM radio signals is also used in [6, 7] for location estimation with [7] also using a simulated signal strength map. Unfortunately the resulting location estimation error is too high rendering these schemes unsuitable for most applications.

Compared to GPS signals, both AM and FM are narrowband signals. Even though they have considerably higher signal strength than GPS signals, there are no effective signal processing algorithms to achieve positioning accuracy comparable with that of GPS. In [8, 9] the authors have considered the RSS from WLAN base stations for indoor location estimation. They also rely on a database of reference RSS measurements. In [10] the authors exploit the multi-carrier structure of WLAN signals for time-difference of arrival (TDOA) measurements which are then used for localization. However, for wideband signals multipath fading degrades the accuracy of the localization methods particularly in an indoor environment.

We are motivated by the work in [5, 3, 4, 6, 7], because of the ubiquity of AM and FM radio signals. The relatively low carrier frequency allows for penetration into building structures, and the narrow bandwidth of these signals enables localization resilient to multipath fading. In addition, narrowband signals can be digitized using fewer bits (lower rates) and therefore, require lower critical resources such as storage capacity, transmission bandwidth and energy when used in collaborative localization schemes.

We present effective signal processing algorithms for localization using FM SOP. Our algorithms are reminiscent of those used in GPS but with significant departure dictated by the narrowband and TDOA features of SOP. To be specific, for localization based on SOP, a reference receiver (RR) with a known location is assumed. The TDOA between the FM radio signals received at the RR and the MR is utilized for localization of the mobile. The number of unknowns includes the

three position parameters of the MR in the Cartesian coordinate system, as well as the clock synchronization error between the MR and the RR.

The positioning system proposed in this dissertation consists of two similar estimation problems. The first involves localization based on n ($n \geq 4$) estimated TDOAs. The second involves estimation of the n TDOAs based on narrowband FM signals. This is in sharp contrast with GPS which relies on the estimation of n time delays based on wideband pseudo random sequences. In addition to the novel positioning system proposed in this dissertation, our main contributions also include development of near optimum algorithms in the sense of MLE for both of the aforementioned estimation problems, assuming independent and identically distributed (i.i.d.) Gaussian noise sequences.

1.1.2 Localization of Node in Wireless Sensor Network

Global positioning system (GPS) has had an overwhelming success in localization. However, for localization in WSNs, GPS may not be a viable option. In many environments such as indoors, forested areas or urban canyons the GPS signal may be too weak or not even available. In addition, for a network of hundreds or thousands of nodes, fitting each sensor with a GPS device is too costly. Therefore recently many research studies are devoted to developing cost-effective self-localization schemes for WSNs [11, 12].

Range-based localization uses the distance measurements between the neighboring nodes which may be obtained in a number of ways including estimates of: time of arrival (TOA), time difference of arrival (TDOA) or received signal strength (RSS), [13, 14]. It is well known that knowledge of the distance profile of the network may not be sufficient to uniquely localize all the nodes. Unique localizability requires that the network's underlying graph be globally rigid [15, 16].The prob-

ability that a network is localizable can be improved by including a number of *anchors*[1] which can assist in localizing the non-anchor (blind) nodes.

Localization algorithms may be classified as centralized or distributed. Centralized algorithms require a great deal of communication between the sensors and a central processor (fusion center) and therefore are not suitable for resource-constrained WSNs. In contrast, in distributed algorithms each node computes its position based on information available from its neighbors (i.e., those within its radio range). Therefore, this approach is more efficient in resource utilization and is also scalable in terms of the size of the network.

Sensor network localization is often stated as an optimization problem with an objective function that depends on the distances and positions of the sensors[2]. The main difficulty with this approach is that even in the absence of measurement errors, it is a non-convex optimization problem with many local minima. Recently a number of approaches are proposed which relax the non-convex problem in order to obtain a convex problem that can be efficiently solved using techniques such as the interior point method [19]. Two prominent approaches use semidefinite programing (SDP), [20, 21, 22], and second-order cone programming (SOCP) [23, 24, 25]. While the original versions of these algorithms were centralized [20, 21, 23], more recently some distributed approaches have been proposed [26, 24, 27].

For a brief review of the advantages and disadvantages of SDP and SOCP we refer to [20, 27]. Here we would like to point out a few of the shortcomings which have not been previously discussed. The approach in [26] is not truly a distributed method. Instead the network is partitioned into several clusters which are then in-

[1]It is assumed that the anchor nodes are aware of their own (global) positions, say, by manual configuration or through GPS.

[2]Two alternative methods are presented in [17, 18].

dependently solved by SDP. Now the sensors whose positions are accurately computed are designated as "ghost anchors" and are used to decide the un-positioned sensors. This scheme is then iterated. It can be seen that this approach breaks up the centralized problem into a number of (centralized) sub-problems for which a solution can be obtained from SDP. Furthermore, both SDP and SOCP rely on a sophisticated optimization package (SeDuMi was used in [20, 24]) which cannot be easily deployed on a sensor node with limited resources.

Another difficulty with the relaxation methods is that even when the original problem is uniquely localizable, the relaxed problem may not be. Suppose that the localization problem is to be solved in $\Re^d$ where $d \geq 1$. In [20] the authors derive conditions under which the solution of the relaxed problem is the same as that of the original problem. However, these conditions are difficult to verify as they imply that the original problem cannot be uniquely localized in a higher dimensional space $\Re^l$ where $l > d$ (see [20] for more details). In fact as pointed out in [20], in the presence of measurement errors, SDP with interior point method results in a solution in a higher dimensional space which must then be rounded onto $\Re^d$. A simple projection of the solution onto $\Re^d$ results in the crowding of the estimated positions in the center of the field and in [21] the authors propose a method to address this issue. The above problem is also present in SOCP relaxation approach, [24], where spurious solutions may be introduced as a result of the relaxation. An example of this is shown in Section 3.1.1.

Extensive simulations show that in the relaxation methods, the estimated positions of the blind nodes are always in the convex hull of the anchors. Therefore when the actual positions of the nodes are outside of this convex hull, the estimation errors are often very large. A solution is to carefully deploy a large number of anchors on the periphery of the geographic area to ensure that no blind nodes

are outside of the convex hull of the anchors. This, however, increases the cost of the network and imposes a constraint on the network deployment strategy. In particular, random scattering of the nodes in the sensor field which has been envisioned for some applications, [28], fails to satisfy this constraint. Another issue with relaxation methods is that the dual solution obtained from the interior point method is not guaranteed to be the same as the solution of the primal problem. This is due to the gap between the cost functions which highly depends on the parameters chosen in the implementation of the interior point method [19].

Zhu et al. proposed a distributed localization algorithm in [29], based on the gradient descent algorithm which requires that blind nodes be contained in the convex hull of their neighbors. In [30], the authors proposed a convex/non-convex formulation. Each node solves a convex optimization problem using a subset of its neighbors. Once a solution is reached, a refinement of the position is carried out (non-convex part) based on a *search* process. Convergence of the algorithm is not guaranteed.

Probabilistic approaches such as simulated annealing (SA) have long been used for numerical optimization of non-convex problems to allow convergence (with probability one) to the global optimum [31, 32]. Simulated annealing-based algorithms have been proposed for localization in sensor networks in [33, 34]. However, convergence of these algorithms has not been established and the accuracy of the final result strongly depends on the selected parameters. Moreover, as pointed out in [32], SA may fail if the *basin of attraction* of a local minimum (maximum) is *sufficiently* wide.

It should point out that, for the sake of brevity, our survey of previous work here is short of complete and only contains the previous work related to our work. For a more complete survey we refer to [34, 27, 13] and the references therein. One of

the major difficulties with range-based localization is that all the pairwise distance measurements may not be reliable. This issue is different from noisy measurements or errors occurring during the calculation of the distances. Algorithms which are robust to such measurement noise or distance calculation errors have been previously developed [26, 20]. In the case under consideration here, some reported distance measurements are significantly different from their true values. This may be a result of Byzantine or malicious nodes inserted into the network by an adversary for distance spoofing attacks. These nodes report false distance or position information to their neighbors in order to defeat the localization algorithm. Large distance errors may also arise as a result of faulty measurements. For example it is well know that in indoor environments, due to multipath fading effects, some RSS measurements may be highly inaccurate. We refer to such distance measurements as outliers [35].

Secure positioning has been the subject of several studies in recent years. Different attack types and outliers are discussed in [36] and techniques to prevent or/and deal with such issues are presented. Theoretical approaches to deal with the presence of outliers or corrupted distances have been developed in [37, 38, 39]. These approaches are based on the rigidity property of the network, establishing limitations of the triangle inequality for localization purposes and conditions to uniquely estimate the position of the nodes in the presence of outlier distances. In [40, 41], the authors provide a bound for the required anchor nodes for localization, and describe algorithms that satisfy this condition.

Several algorithms have also been developed to detect malicious nodes or outlier distance measurements, and to use this information in order to avoid such nodes or distances in a localization algorithm. In [42, 43], the authors detect malicious nodes by comparing the estimated distances with the round-trip time of the transmitted

information, which is then used to develop a reputation metric for classifying the nodes.

In [44] outlier distances are detected using the distribution of RSS. Consistencies of the estimated positions with known model and observations are developed in [45] in order to detect malicious nodes. In [46] an algorithm is developed to detect malicious nodes by examining the regions where the nodes claim to be located. A similar algorithm is developed in [47], which also includes a voting process used to develop a reputation metric. A hypothesis testing method is presented in [48] using the RSS measurements in order to detect outlier distances. The authors in [49] identify malicious nodes by comparing the distributions of the TOA of the transmitted signal, and using the expectation-maximization (EM) algorithm to determine the reliability of the links. The TOA of the received signal is also used in [50] to identify the malicious nodes and in [51], an algorithm to detect wormwhole attacks is developed based on TOA of the signals and the measured distances.

Two methods are developed for localization of WSNs in the presence of threats in [52]. The first method filters out malicious signals by examining the consistency amoung multiple signals and the second method use a voting procedure based on the overlap between the regions where the nodes claim to reside. In [53, 54, 55] authors use cryptography and intersection of regions to estimate the positions of the nodes.

Several authors have formulated the localization problem as an (constrained) optimization algorithm. In [56] the localization problem is cast as a minimization of the median of the square of the difference between measured distances and the distances from estimated positions using RSS. The approach in [57] verifies

the triangularization properties between sets of distances. A similar algorithm is presented in [58], by incorporating TDOA of the transmitted signals.

An important issue of these approaches is the fact that the blind nodes estimate their position using information directly from the anchor nodes, i.e., it is assumed that they have communication capabilities with the anchor nodes. Although the large amount of proposed algorithms for localization or threats detection in WSNs in presence of outlier distances and/or nodes, almost none of them has stated the localization algorithm as an optimization problem for networks where the blind nodes may not have communication capabilities with the anchor nodes.

Chapter 2

Positioning System based on Narrowband Signals of Opportunity

This chapter presents a localization algorithm in which the position of a device is estimated using the available commercial signals and the position of an auxiliary device as reference. Section 2.1 describes and states the localization problem. Section 2.2 details and analyzes the development of the localization algorithm. Finally, Section 2.3 provides simulation results, analyzing the performance of the algorithm.

2.1 Problem Formulation

The main problem stated in this research is the localization of a mobile device (denoted by *MR*), by using Signals of Opportunity (SoP).

In order to achieve the mentioned objective, at least 4 sources of SoP are required, and a localization reference, denoted by *Reference Rover (RR)*. The location of the source of the SoP must be known as well.

The position of the RR is assumed to be known, through GPS (for example). In addition, the SoPs must be received by RR and MR.

Based on this setting, the objective can be decomposed into two subproblems: the first one consists in estimating the position of MR based on certain measurements provided by the SoP arrived to MR and RR, the position of the RR, and the positions of the SoP sources. This subproblem can be stated as a Least Square.

The second subproblem is to estimate certain measurements from on the SoPs to be use for localization purposes. Time Difference of Arrival (TDOA) of the SoP arriving to Rover and Mobile is considered as such measurement, which will lead to a estimation of the distance between the RR and MR for each SoP.

The SoP considered in this project are commercial Frequency Modulated Radio (FM) signals. It is assumed that the position of the FM signal transmitters is known. The choice of this type of signals is due to its availability in large urban and rural regions, being able to be received in indoor environments without the need of the line of sight between receiver and transmitter.

It is important to mention that the transmission of the signals is assumed to be through a flat fading channel. Moreover, the localization procedure is though for low speed mobile and references. Also, it is assumed that the mobile and reference can interchange information such that the position of the rover can be estimated in the reference.

2.2 Proposed Algorithm

The following subsections describe the methodology previously mentioned. Firstly, a procedure is described for localization of the rover using TDOA from FM signals that have arrived to RR and MR. Later, an algorithm to estimate the TDOA used in the localization previously mentioned, which is designed for narrowband signals.

2.2.1 Localization with Time Difference of Arrival

Localization based on signals of opportunity assumes that the RR, whose position is precisely known, receives the same signals as those received by the MR. In general there is a synchronization error between the two time clocks at the RR and the MR. This clock synchronization error is assumed to be constant during the time window that we collect the signals of opportunity used to compute the TDOA. This assumption is valid as the clocks will not have a significant drift during this short time window. In fact the same assumption is also made in the case of GPS. As a result, there are four unknown parameters involved in estimating the position of the mobile receiver: the position parameters of the mobile in the three-

dimensional Cartesian coordinate system, plus the clock synchronization error. For this reason, SOP broadcasted from a total of at least four different locations are needed in localizing the mobile, yielding at least four equations in order to remove the time synchronization error and to resolve the mobile's position effectively.

Let (x_b, y_b, z_b) be the known position of the reference receiver, and let (x_m, y_m, z_m) be the unknown position of the mobile receiver to be estimated. By convention, the position of the ith broadcast tower of the signal of opportunity is assumed to be fixed and known, denoted by (x_i, y_i, z_i), where $1 \leq i \leq n$ and $n \geq 4$. For convenience denote

$$d_m(x_i, y_i, z_i) = \sqrt{(x_m - x_i)^2 + (y_m - y_i)^2 + (z_m - z_i)^2} \tag{2.1}$$

as the distance from the mobile to the ith broadcast tower. If d_{b_i} denotes the distance from the RR to the ith broadcast tower, then

$$d_{b_i} = \sqrt{(x_b - x_i)^2 + (y_b - y_i)^2 + (z_b - z_i)^2}$$

and d_{b_i} is known for $1 \leq i \leq n$. There holds

$$d_m(x_i, y_i, z_i) + \Delta d = d_{b_i} + c(\delta t_i + \varepsilon), , \qquad 1 \leq i \leq n, \tag{2.2}$$

with c the speed of light, ε the clock synchronization error, Δd the error in distance due to the clock synchronization error and δt_i the ith TDOA as shown in Figure 2.1.

Although (2.2) reveals a nonlinear relation between the TDOAs and the mobile's position, a pseudo-linear model exists [59, 60]. Without loss of generality, (x_1, y_1, z_1) is taken as the reference tower. By eliminating the synchronization error in (2.2), the following equation

$$d_m(x_1, y_1, z_1) + c\delta t_{i,1} + d_{i,1} = d_m(x_i, y_i, z_i)$$

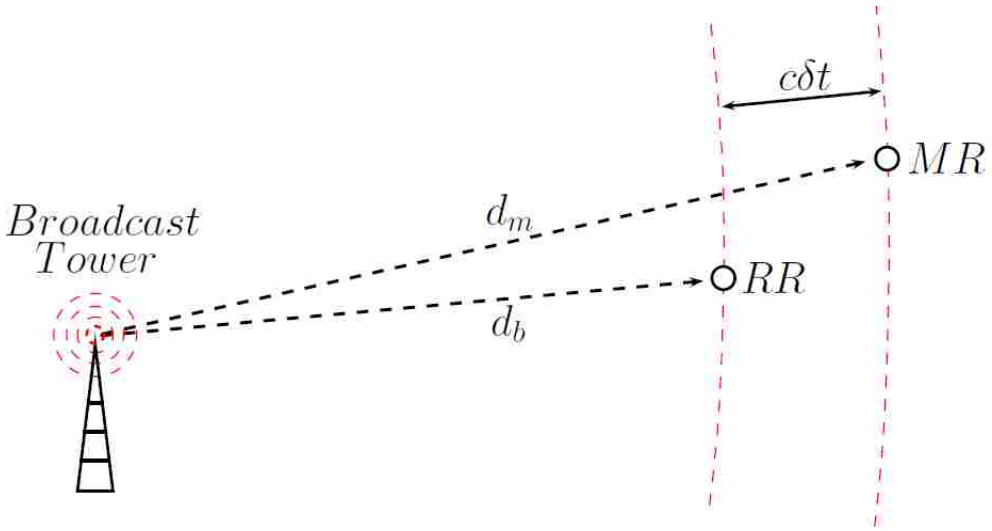

FIGURE 2.1. Schematic illustration of TDOA

is obtained for $2 \leq i \leq n$ where $\delta t_{i,1} = \delta t_i - \delta t_1$ and $d_{i,1} = d_{b_i} - d_{b_1}$. Squaring the two sides and using (2.1) yields

$$(x_m - x_i)^2 + (y_m - y_i)^2 + (z_m - z_i)^2 \left[d_m(x_1, y_1, z_1) + c\delta t_{i,1} + d_{i,1}\right]^2 . \tag{2.3}$$

Denote $r_k = \sqrt{x_k^2 + y_k^2 + z_k^2}$, $d_{m,1} = d_m(x_1, y_1, z_1)$, $a_i = c\delta t_{i,1} + d_{i,1}$, and

$$b_i = r_i^2 - r_1^2 - a_i^2 - 2(x_{i,1}x_1 + y_{i,1}y_1 + z_{i,1}z_1) \tag{2.4}$$

where $x_{i,1} = x_i - x_1$, $y_{i,1} = y_i - y_1$, and $z_{i,1} = z_i - z_1$. The equations in (2.3) for $2 \leq i \leq n$ can be rearranged and packed into the following pseudo-linear model:

$$\begin{bmatrix} b_2 \\ b_3 \\ \vdots \\ b_n \end{bmatrix} = 2 \begin{bmatrix} x_{2,1} & y_{2,1} & z_{2,1} & a_2 \\ x_{3,1} & y_{3,1} & z_{3,1} & a_3 \\ \vdots & \cdots & \cdots & \vdots \\ x_{n,1} & y_{n,1} & z_{n,1} & a_n \end{bmatrix} \begin{bmatrix} x_{m,1} \\ y_{m,1} \\ z_{m,1} \\ d_{m,1} \end{bmatrix} \tag{2.5}$$

satisfying $d_{m,1}^2 = x_{m,1}^2 + y_{m,1}^2 + z_{m,1}^2$.

For convenience, let $\mathbf{p}_m = \begin{bmatrix} x_{m,1} & y_{m,1} & z_{m,1} \end{bmatrix}'$ where $'$ indicates the transpose operation, and let $\mathbf{a}$ and $\mathbf{b}$ be column vectors with a_{i+1} and b_{i+1} denoting the ith

element of $\mathbf{a}$ and $\mathbf{b}$, respectively. There holds

$$\mathbf{b} - 2\mathbf{a}d_{m,1} = G\mathbf{p}_m, \qquad d_{m,1}^2 = \mathbf{p}_m'\mathbf{p}_m, \tag{2.6}$$

in which the matrix G of size $(n-1) \times 3$ is specified by the right hand side of (2.5). A closed-form solution of $\mathbf{p}_m$ to (2.6) is derived in [61, 60] in the case when noise-free measurements of TDOA $\{\delta t_{i,1}\}$ are available. The solution procedure is quite simple and first writes $\mathbf{p}_m = (G'G)^{-1}G'(\mathbf{b} - 2\mathbf{a}d_{m,1})$, as if $d_{m,1}$ is known. Using $d_{m,1}^2 = \mathbf{p}_m'\mathbf{p}_m$ with the expression of $\mathbf{p}_m$ substituted in then gives

$$d_{m,1}^2 = (\mathbf{b} - 2\mathbf{a}d_{m,1})'G(G'G)^{-2}G'(\mathbf{b} - 2\mathbf{a}d_{m,1}).$$

It can be easily verified that the above is the same as $\alpha x^2 + \beta x + \gamma = 0$ with $x = d_{m,1}$ and

$$\alpha = 1 - 4\mathbf{v}_a'\mathbf{v}_a, \qquad \beta = 2\mathbf{v}_b'\mathbf{v}_a, \qquad \gamma = -\mathbf{v}_b'\mathbf{v}_b,$$

where $\mathbf{v}_a = (G'G)^{-1}G'\mathbf{a}$ and $\mathbf{v}_b = (G'G)^{-1}G'\mathbf{b}$. Hence there are two possible roots and the one with positive real value can be used for $d_{m,1}$ which in turn gives the solution for $\mathbf{p}_m$. See [61] for the discussion on the existence of the positive real root in the noise-free case.

Clearly the solution procedure becomes more complex when the measurements of TDOA involve errors which are inevitable. In fact the simple procedure discussed earlier is inapplicable in general due to the existence of possible complex roots when noises are present in TDOAs. For this reason an effective two-stage LS algorithm is proposed in [59] to estimate the position vector in the case of noisy TDOAs. However, its optimality is difficult to analyze. This dissertation makes use of our earlier result ([62] for GPS-based localization) in deriving an approximate MLE in the case of i.i.d. Gaussian noise. To be specific, assume that the measurements $\{\widehat{\delta t}_i\}_{i=1}^n$ are given by

$$\widehat{\delta t}_i = \delta t_i + v_i \quad \Longrightarrow \quad \widehat{\delta t}_{i,1} = \delta t_{i,1} + v_{i,1} \tag{2.7}$$

for $2 \leq i \leq n$ where $\{v_i\}_{i=1}^n$ are i.i.d. Gaussian with mean 0 and variance σ_v^2. The notation $\Rightarrow$ stands for "imply" or "give rise to". As a result $v_{i,1} = v_i - v_1$ for $2 \leq i \leq n$ are also Gaussian with mean zero but are not independent anymore. In fact the covariance of $\{v_{i,1}\}_{i=2}^n$ is given by the following $(n-1) \times (n-1)$ matrix

$$C_{i,1} = \sigma_v^2 \begin{bmatrix} 2 & 1 & \cdots & 1 \\ 1 & \ddots & \ddots & \vdots \\ \vdots & \ddots & \ddots & 1 \\ 1 & \cdots & 1 & 2 \end{bmatrix} =: \sigma_v^2 C_0. \tag{2.8}$$

Hence the joint probability density function (PDF) of $\{v_{i,1}\}$ can be easily obtained as in (4.5) of the Appendix (where the Cramer-Rao lower bound (CRLB) is also derived for the error covariance associated with localization based on SOP using TDOAs). It is important to point out that obtaining the exact MLE solution involves maximization of the joint PDF which is in fact quite complex. Hence an alternative is sought in this dissertation. Under the noisy measurements of TDOA, a_i and b_i in (2.4) are replaced respectively by

$$\widehat{a}_i = a_i + cv_{i,1}, \qquad \widehat{b}_i = \widehat{\beta}_i + \mu c^2 \sigma_v^2,$$

with $\widehat{\beta}_i = b_i - 2ca_i v_{i,1} - c^2 v_{i,1}^2$, which are the $(i-1)$th element of $\widehat{\mathbf{a}}$ and $\widehat{\mathbf{b}}$ for $2 \leq i \leq n$, leading to the noisy pseudo-linear model

$$\widehat{\mathbf{b}} - 2\widehat{\mathbf{a}} d_{m,1} = G\mathbf{p}_m + \widehat{\mathbf{v}}, \qquad d_{m,1}^2 = \mathbf{p}_m' \mathbf{p}_m, \tag{2.9}$$

where $\mu \geq 0$ is a real parameter. For $1 \leq i < n$, the ith element of $\widehat{\mathbf{v}}$ is given by

$$\widehat{v}_i = -2c(d_{m,1} + a_{i+1}) v_{i+1,1} - c^2 (v_{i+1,1}^2 - \mu \sigma_v^2).$$

Let $\mathrm{E}\{\cdot\}$ denote expectation. If $\mu = 2$, it can be verified that $\mathrm{E}\{\widehat{v}_i\} = 0$ and

$$\frac{\mathrm{E}\{\widehat{v}_{i-1}\widehat{v}_{j-1}\}}{2c^2\sigma_v^2} = \begin{cases} 4(d_{m,1} + a_i)^2 + 4c^2\sigma_v^2, & \text{if } i = j, \\ 2(d_{m,1} + a_i)(d_{m,1} + a_j) + c^2\sigma_v^2, & \text{if } i \neq j, \end{cases} \tag{2.10}$$

for $i, j \geq 2$ using $\mathrm{E}\{v_{i,1}^2\} = 2\sigma_v^2$, $\mathrm{E}\{v_{i,1}^3\} = 0$, and $\mathrm{E}\{v_{i,1}^4\} = 12\sigma_v^4$. The following lemma shows that the joint distribution of $\{\widehat{v}_i\}_{i=1}^{n-1}$ is approximately Gaussian. The proof and discussion are moved to the Appendix.

Lemma 1. *Let* $Z_i = -2\kappa_i U_i + U_i^2 - \sigma^2$ *where* $\kappa_i \neq 0$ *and* $\{U_i\}_{i=1}^{n-1}$ *are jointly* Gaussian *with mean zero and covariance* $C > 0$. *If the ratio of* $|\kappa_i|$ *to* σ *is sufficiently large for each* i, *then* $\{Z_i\}_{i=1}^{n-1}$ *admit an approximate joint* Gaussian *distribution with common mean* $-\sigma^2$ *and covariance* $D_\kappa C D_\kappa$ *where* $D_\kappa = 2\mathrm{diag}(\kappa_1, \cdots, \kappa_{n-1})$.

For application to our problem, $U_i = \widehat{v}_{i,1}/2c^2$. The large ratio condition amounts to

$$\frac{|d_{m,1} + a_i|}{c\sigma_v} = \frac{|d_{m,1} + d_{i,1} + c\delta t_{i,1}|}{c\sigma_v} = \frac{d_m(x_i, y_i, z_i)}{c\sigma_v} >> 1$$

which holds for each $i \geq 2$. In fact $c\sigma_v$ can be regarded as the distance resolution in TDOA estimates, and it has to be within $\mathcal{O}(1)$ in unit of meter in order to have acceptable localization error.

Theorem 1. *Suppose that* $\{\widehat{v}_i\}_{i=1}^{n-1}$ *are jointly Gaussian with mean zero and covariance* $\widehat{C}$ *whose* (i,j)*th entry is specified in* (2.10). *Then the* MLE *solution to the constrained pseudo-linear equation in* (2.9) *is the constrained minimizer* $\widehat{\mathbf{p}}_m$ *that solves*

$$\begin{aligned} \min_{d_{m,1} = \|\mathbf{x}\|} \left\| \widehat{\mathbf{b}} - 2\widehat{\mathbf{a}} d_{m,1} - G\mathbf{x} \right\|_{\widehat{C}^{-1}}^2 \\ = \left\| \widehat{\mathbf{b}} - 2\widehat{\mathbf{a}} d_{m,1} - G\widehat{\mathbf{p}}_m \right\|_{\widehat{C}^{-1}}^2 \end{aligned} \tag{2.11}$$

where $\|\mathbf{x}\|_Q^2 = \mathbf{x}' Q \mathbf{x}$ *and* $\|\mathbf{x}\|^2 = \mathbf{x}'\mathbf{x}$.

Proof. The hypothesis on $\{\widehat{v}_i\}_{i=1}^{n-1}$ implies the joint PDF:

$$f_{\widehat{V}}\left(\{\widehat{v}_i\}_{i=1}^{n-1}\right) = \frac{\exp\left[-\frac{1}{2}\left\|\widehat{\mathbf{b}} - 2\widehat{\mathbf{a}} d_{m,1} - G\mathbf{p}_m\right\|_{\widehat{C}^{-1}}^2\right]}{\sqrt{(2\pi)^{n-1}\det(\widehat{C})}}. \tag{2.12}$$

The MLE solution aims at computing $\mathbf{p}_m$ that maximizes $f_{\widehat{V}}\left(\{\widehat{v}_i\}_{i=1}^{n-1}\right)$ under the constraint $d_{m,1} = \|\mathbf{p}_m\|$, which is equivalent to minimizing $\left\|\widehat{\mathbf{b}} - 2\widehat{\mathbf{a}} d_{m,1} - G\mathbf{p}_m\right\|_{\widehat{C}^{-1}}^2$

subject to $d_{m,1} = \|\mathbf{p}_m\|$. As such, the MLE solution satisfies (2.11) and this concludes the proof. □

Theorem 1 shows that under the Gaussian assumption, the MLE solution to localization using TDOAs amounts to computing the constrained WLS solution in (2.11). Although the exact Gaussian distribution does not hold for $\{\widehat{v}_i\}_{i=1}^{n-1}$ in practice, they are approximately Gaussian by Lemma 1. Hence the constrained WLS solution is an approximate MLE. To derive this solution, denote

$$\begin{aligned} H &= \left[\begin{array}{cc} G & 2\widehat{\mathbf{a}} \end{array}\right], \quad \underline{\theta}_p = \left[\begin{array}{c} \mathbf{p}_m \\ d_{m,1} \end{array}\right] \\ \Longrightarrow \quad & \widehat{\mathbf{b}} - 2\widehat{\mathbf{a}} d_{m,1} - G\mathbf{p}_m = \widehat{\mathbf{b}} - H\underline{\theta}_p. \end{aligned}$$

Lagrange multiplier is a standard method for constrained optimization. Let λ be real and

$$J = \frac{1}{2}\left[\left(H\underline{\theta}_p - \widehat{\mathbf{b}}\right)' \widehat{C}^{-1}\left(H\underline{\theta}_p - \widehat{\mathbf{b}}\right) + \lambda \underline{\theta}_p' Q \underline{\theta}_p\right]$$

where $Q = \mathrm{diag}(1,1,1,-1)$. The necessary condition for optimality yields the condition

$$\begin{aligned} H'\widehat{C}^{-1}[H\underline{\theta}_p - \widehat{\mathbf{b}}] + \lambda Q\underline{\theta}_p = 0 \quad &\Longleftrightarrow \\ \underline{\theta}_p = [H'\widehat{C}^{-1}H + \lambda Q]^{-1} H'\widehat{C}^{-1}\widehat{\mathbf{b}}. & \end{aligned} \tag{2.13}$$

An optimal solution needs to satisfy the constraint $\underline{\theta}_p' Q \underline{\theta}_p = 0$ leading to

$$\widehat{\mathbf{b}}'\widehat{C}^{-1}H[H'\widehat{C}^{-1}H + \lambda Q]^{-1}Q[H'\widehat{C}^{-1}H + \lambda Q]^{-1}H'\widehat{C}^{-1}\widehat{\mathbf{b}} = 0. \tag{2.14}$$

The solution algorithm hinges on the computation of the real root λ from the above equation and there can be more than one such real root. The result of simultaneous diagonalization in [63] can be employed for this purpose. Because $\widehat{C} = \widehat{C}' > 0$ and $Q = Q'$, there exists a nonsingular matrix S such that $H'\widehat{C}^{-1}H = SD_{\widehat{C}}S'$ and $Q = SD_Q S'$ where $D_{\widehat{C}}$ and D_Q are both diagonal. It is noted that $D_{\widehat{C}}$ and D_Q

have the same inertia as $\widehat{C}$ and Q, respectively. It follows that (2.14) is equivalent to

$$(S^{-1}H'\widehat{C}^{-1}\widehat{\mathbf{b}})'M_\lambda D_Q^{-1}M_\lambda(S^{-1}H'\widehat{C}^{-1}\widehat{\mathbf{b}}) = 0. \tag{2.15}$$

where $M_\lambda = (\lambda I + D_{\widehat{C}}D_Q^{-1})^{-1}$ is diagonal. Let $D_Q^{-1} = \mathrm{diag}(q_1, q_2, \cdots, q_\ell)$ with $\ell = 4$. It has the same number of negative and positive elements as $D = D_{\widehat{C}}D_Q^{-1} = \mathrm{diag}(d_1, d_2, \cdots, d_\ell)$ by the positivity of $\widehat{C}$ and $D_{\widehat{C}}$. In fact $q_i d_i > 0$. The matrices S and D can be obtained by eigenvalue decomposition of $H'\widehat{C}^{-1}HQ^{-1} = SDS^{-1}$. Let γ_i be the ith element of $S^{-1}H'\widehat{C}^{-1}\widehat{\mathbf{b}}$ and $\underline{\gamma} = \begin{bmatrix} \gamma_1 & \gamma_2 & \cdots & \gamma_\ell \end{bmatrix}$. Then (2.15) is equivalently converted into

$$\underline{\gamma}M_\lambda D_Q^{-1}M_\lambda\underline{\gamma}' = \sum_{i=1}^{\ell}\frac{q_i\gamma_i^2}{(\lambda + d_i)^2} = 0. \tag{2.16}$$

Because Q is indefinite, there is at least one strictly positive and one strictly negative element from $\{q_i\}_{i=1}^{\ell}$. Hence the above equation has at least one real root. On the other hand, there are only finitely many real λ values satisfying (2.16). In fact all the roots of the nonlinear equation in (2.16) are roots of the following polynomial with degree $2(\ell - 1) = 6$:

$$\sum_{i=1}^{\ell} q_i\gamma_i^2\prod_{k\neq i}(\lambda + d_k)^2 = 0. \tag{2.17}$$

Let $\{\lambda_k\}_{k=1}^{r}$ be the r real roots of (2.17). It can be shown that

$$\begin{aligned} M_Q &:= H(H'\widehat{C}^{-1}H + \lambda_k Q)^{-1}H'\widehat{C}^{-1} - I \\ &= HQ^{-1}(\lambda_k I + H'\widehat{C}^{-1}HQ^{-1})^{-1}H'\widehat{C}^{-1} - I \\ &= -\lambda_k(\lambda_k I + HQ^{-1}H'\widehat{C}^{-1})^{-1} \\ &= -\lambda_k\widehat{C}(\lambda_k\widehat{C} + HQ^{-1}H')^{-1}. \end{aligned}$$

Hence by (2.13),

$$H\underline{\theta}_p - \widehat{\mathbf{b}} = M_Q\widehat{\mathbf{b}} = -\lambda_k\widehat{C}(\lambda_k\widehat{C} + HQ^{-1}H')^{-1}\widehat{\mathbf{b}}.$$

Substituting the above into the performance index leads to

$$J = \frac{1}{2}\lambda_k^2 \widehat{\mathbf{b}}'(\lambda_k \widehat{C} + HQ^{-1}H')^{-1}\widehat{C}(\lambda_k \widehat{C} + HQ^{-1}H')^{-1}\widehat{\mathbf{b}}.$$

Let λ_{opt} be one of the r real roots that minimizes J over $\{\lambda_k\}_{k=1}^r$. Then in light of (2.13), the optimal $\underline{\theta}_p$ is obtained as $\underline{\theta}_p = \underline{\theta}_{\text{opt}}$ given by

$$\underline{\theta}_{\text{opt}} = [H'\widehat{C}^{-1}H + \lambda_{\text{opt}}Q]^{-1}H'\widehat{C}^{-1}\widehat{\mathbf{b}}.$$

Remark 1. The entries of $\widehat{C}$ are functions of $d_{m,1}$ and δt_i's which are unknown. The TDOAs δt_i's can be replaced by $\widehat{\delta t}_i$'s obtained from measurements. This causes negligible error if σ_v^2 is small. On the other hand, $d_{m,1}$ has to be determined iteratively. That is, the solution $\widehat{\mathbf{p}}_m$ may be initially obtained under $\widehat{C} = I$, which can then be replaced to compute new solution $\widehat{\mathbf{p}}_m$ under more accurate $\widehat{C}$. Only a few iterations are needed in order to obtain a near MLE solution. □

2.2.2 Time Difference of Arrival Estimation for Narrowband Signals

The challenge in localization based on narrowband (real) signals of opportunity lies in estimation of TDOA efficiently and accurately. Specifically, let $[\Omega_L,\ \Omega_H)$ be the support of the frequency response of the signal of opportunity where $\Omega_H > \Omega_L > 0$. The narrowband nature of the signal implies that $\Omega_H - \Omega_L << \Omega_L$ and thus the SOP is a bandpass signal. Let k be the integer-valued time index, and $\{s_m(k)\}$ and $\{s_b(k)\}$ be sampled signals of the same continuous-time signal received at the mobile and reference, respectively, under the same sampling frequency $\Omega_S \geq 2\Omega_H$. There holds $S_b(\Omega) = e^{j\Omega\delta t}S_m(\Omega)$ at all frequency Ω, if the TDOA δt is multiple of the sampling period, where Ω is the physical frequency, and $S_m(\Omega)$ and $S_b(\Omega)$ are discrete-time Fourier transforms (DTFT) of $\{s_m(k)\}$ and $\{s_b(k)\}$, respectively. Hence TDOA can be estimated using the existing results on estimation of time delay. However, bandpass signals can be sampled at much lower sampling frequency

$\Omega_s << 2\Omega_H$ without aliasing, provided that $\Omega_s > 2(\Omega_H - \Omega_L)$ [64], which leads to considerably more efficient proceddure for the estimation of TDOA. Indeed TDOA requires that both $\{s_m(k)\}$ and $\{s_b(k)\}$ be available in the same location in order to estimate the TDOA. This requires that at least one of the sampled signals be transmitted. A lower sampling frequency implies that fewer number of bits need to be transmitted thereby reducing the transmission energy and bandwidth. However, $S_b(\Omega) = e^{j\Omega\delta t}S_m(\Omega)$ does not hold anymore, at least not for all Ω, if the sampling frequency $\Omega_s < 2\Omega_H$. The reason lies in the fact that the TDOA δt is not likely to be multiple of the sampling period. This problem is studied in this section. We employ a multirate approach based on polyphase analysis.

Let $\{s(k)\}_{k=-\infty}^{\infty}$ be sampled at $\Omega_S \geq 2\Omega_H$. Its DTFT with normalized frequency is given by

$$S(\omega) = \sum_{k=-\infty}^{\infty} s(k)e^{-jk\omega}, \qquad \omega = \Omega T_S := \Omega(2\pi/\Omega_S).$$

Thus $\omega_H = \Omega_H T_S$ and $\omega_L = \Omega_L T_S$. Consider the M polyphase components

$$\{s_\ell(k)\}_{k=-\infty}^{\infty} = \{s(kM+\ell)\}_{k=-\infty}^{\infty}$$

where ℓ is some integer. For $\ell \in \{0, 1, \cdots, M-1\}$,

$$S_\ell(\omega) = \sum_{t=-\infty}^{\infty} s_\ell(k)e^{-jk\omega} = \sum_{k=-\infty}^{\infty} s(kM+\ell)e^{-jk\omega}$$

is the DTFT of the ℓth polyphase of $\{s(k)\}$. Denote $W_M = e^{-j2\pi/M}$. It is easy to show that [65]

$$S_\ell(\omega) = \frac{e^{j\ell\omega/M}}{M} \sum_{i=0}^{M-1} W_M^{-i\ell} S\left(\frac{\omega + 2i\pi}{M}\right). \tag{2.18}$$

Lemma 2. *Suppose that $S(\omega)$ has support $[\omega_L,\ \omega_H) \subset [0,\ \pi]$ with $0 < \omega_L < \omega_H \leq \pi$ and $\omega_H \approx \pi$. Denote $\lfloor\cdot\rfloor$ as the operation of taking the integer part. Then*

$$\text{(i)}\ \ M = \left\lfloor \frac{\omega_H}{\omega_H - \omega_L} \right\rfloor > 1 \quad \Longrightarrow \quad \text{(ii)}\ \ \omega_L \geq (M-1)(\omega_H - \omega_L),$$

and no aliasing exists for the DTFT *of the ℓth polyphase of $\{s(k)\}$. Moreover, there holds*

$$\begin{aligned} S_\ell(\omega) &= \frac{e^{j\ell(\omega+2i_\omega\pi)/M}}{M} S\left(\frac{\omega+2i_\omega\pi}{M}\right) \\ &= e^{j\ell(\omega+2i_\omega\pi)/M} S_0(\omega) \end{aligned} \tag{2.19}$$

for each $\omega \in [0,\ 2\pi)$ and some $i_\omega \in \{0, 1, \cdots, M-1\}$ that depends only on ω.

Proof. Recall that $\{s(k)\}$ is real, and $S(\omega)$ is periodic with period 2π. Over the frequency range of $[0,\ 2\pi]$, $S(\omega)$ has a symmetric support

$$[\omega_L,\ \omega_H) \cup (2\pi - \omega_H,\ 2\pi - \omega_L]$$

with respect to $\omega = \pi$. The width of the total support, denoted by W, from ω_L to $2\pi - \omega_L$ is no more than $2\pi/M$. This is easy to see from the fact that

$$W = 2(\omega_H - \omega_L) \le \frac{2\omega_H}{M} \le \frac{2\pi}{M}$$

since $\omega_H \le \pi$ and from (i), $\omega_H \ge M(\omega_H - \omega_L)$. Furthermore, (ii) follows straightforwardly from (i).

Consider the first case when M is odd. Then the fundamental period $[0,\ 2\pi]$ of $S(\omega)$ can be divided into M equal size intervals with $\left[\frac{2i\pi}{M},\ \frac{2(i+1)\pi}{M}\right]$ as the ith one for $0 \le i < M$. The support of $S(\omega)$ is located strictly inside the interval corresponding to $i = (M-1)/2$ and $S(\omega) = 0$ over the other $(M-1)$ intervals. As a result, $S_\ell(\omega)$ in (2.18) has M copies of $S(\omega)$ over $[0,\ 2M\pi]$ without aliasing. See the illustration in Figure 2.2 below. Hence the formula in (2.19) holds for each $\omega \in [0,\ 2\pi)$ and some $i_\omega \in \{0, 1, \cdots, M-1\}$ which depends only on ω.

When M is even, the fundamental period of $[0,\ 2\pi]$ can be divided into $(M+1)$ intervals with the first and the last having equal lengths of π/M specified by $[0,\ \pi/M]$ and $[(2M-1)\pi/M,\ 2\pi]$, respectively. The remaining $(M-1)$ intervals

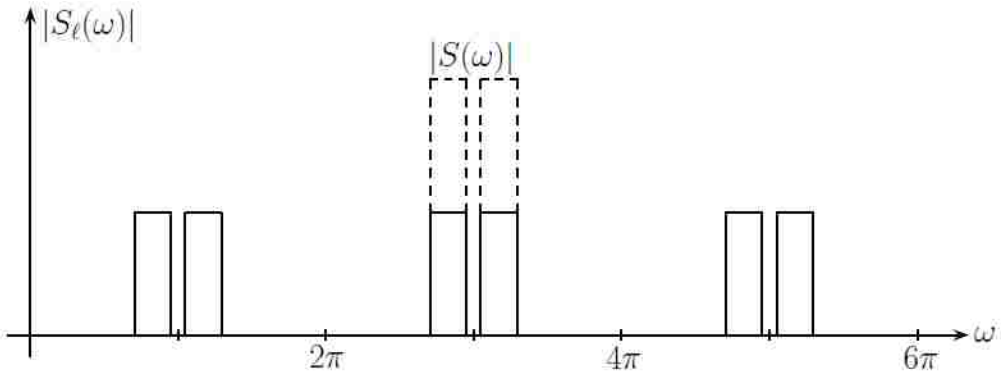

FIGURE 2.2. Graph of $|S_\ell(\omega)|$ over $[0,\ 2M\pi]$ in the case of odd M illustrated for $M = 3$

are given by

$$\left[\frac{(2i-1)\pi}{M},\ \frac{(2i+1)\pi}{M}\right], \qquad i = 1, 2, \cdots, M-1,$$

which have equal lengths of $2\pi/M$. Again the support of $S(\omega)$ lies in the center interval with $i = M/2$ and $S(\omega) = 0$ over other intervals. Hence again no aliasing exists for $S_\ell(\omega)$ in (2.18) in the case of even M as illustrated in Figure 2.3. It is interesting to observe that the center interval is the same as $\left[\frac{(M-1)\pi}{M},\ \pi\right]$. The proof of the lemma is now complete. □

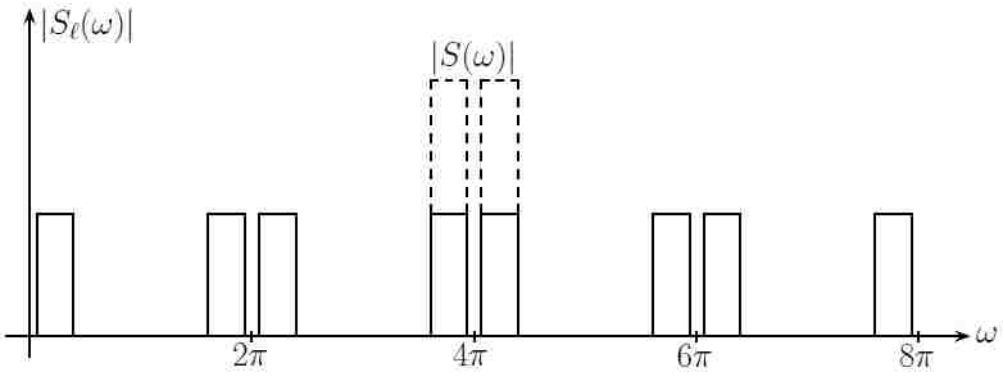

FIGURE 2.3. Graph of $|S_\ell(\omega)|$ over $[0,\ 2M\pi]$ in the case of even M illustrated for $M = 4$.

A few observations are made. The first regards the value of i_ω in (2.19). In light of the periodicity of $S_\ell(\omega)$ with period of 2π, and summation index $i = 0$ corresponding to the center copy, $i_\omega = \frac{M-1}{2}$ in the case of odd M for $\omega \in [0,\ 2\pi]$.

When M is even, i_ω for $\omega \in [0,\ 2\pi]$ is given by

$$i_\omega = \begin{cases} \frac{M}{2}, & \text{if } \omega \in [0,\ \pi), \\ \frac{M}{2} - 1, & \text{if } \omega \in (\pi,\ 2\pi], \end{cases} \tag{2.20}$$

by the proof of Lemma 2. The second regards the minimum sampling frequency. Denote Ω as the physical frequency, Ω_S as the sampling frequency for $\{s(k)\}$, and Ω_s as the sampling frequency for $\{s_\ell(k)\}$. Then $\Omega_S = M\Omega_s$. Denote $W_B = (\Omega_H - \Omega_L)$. Let $\Omega_{\min}$ be the minimum sampling frequency that ensures (2.19), i.e., no aliasing for $\{s_\ell(n)\}$. Then

$$2W_B < \Omega_{\min} \leq 2(1 + 1/M)W_B.$$

The above agrees with the the result in [64]. The third observation from Lemma 2 is that

$$S_\ell(\omega + 2\pi) = \frac{e^{j\ell[\omega+2(i_\omega+1)\pi]/M}}{M} S\left(\frac{\omega + 2(i_\omega + 1)\pi}{M}\right).$$

That is, ω replaced by $\omega + 2\pi$ on the left is equivalent to i_ω replaced by $(i_\omega + 1)$ on the right. The final observation regards reconstruction of $\{s(k)\}$ based on $\{s_\ell(k) = s(kM + \ell)\}_{k=-\infty}^{\infty}$. Upsampler or expander with ratio M can be applied first to yield the following new sequence:

$$\tilde{s}_\ell(k) = \begin{cases} s_\ell(k), & \text{if } k \text{ is multiple of } M, \\ 0, & \text{elsewhere.} \end{cases} \tag{2.21}$$

Its DTFT at $\omega \in [0,\ 2\pi]$ satisfies

$$\tilde{S}_\ell(\omega) = S_\ell(M\omega) = \frac{e^{j\ell\left(\omega + \frac{2i_\omega\pi}{M}\right)}}{M} S\left(\omega + \frac{2i_\omega\pi}{M}\right) \tag{2.22}$$

where $i_\omega = \frac{M-1}{2}$ for odd M, and i_ω has the expression in (2.20) for even M. Bandpass filtering can then be applied to $\{\tilde{s}_\ell(k)\}$ to reconstruct $\{s(k)\}$. Such a procedure is implemented by the interpolator consisting of an upsampler of ratio

M followed by a bandpass filter (BPF). The BPF has amplitude M and linear phase $-\ell\omega$ over the passband in $\left(\frac{(M-1)\pi}{M},\ \pi\right)$ by (2.22), and $i_\omega = 0$ for the center copy of the image. If zero phase bandpass filter is used, the filtered output needs to be shifted by k samples. The reconstruction is illustrated in the Figure 2.4.

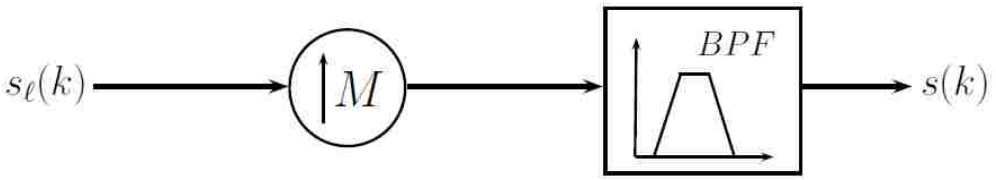

FIGURE 2.4. Block diagram for reconstruction of $\{s(n)\}$ based on $\{s_\ell(n)\}$

It is well known that upsampling induces the imaging effect [65]. The BPF filtering of $\{\tilde{s}_\ell(k)\}$ removes the extra copies and restores $\{s(k)\}$ as illustrated in Figure 2.5.

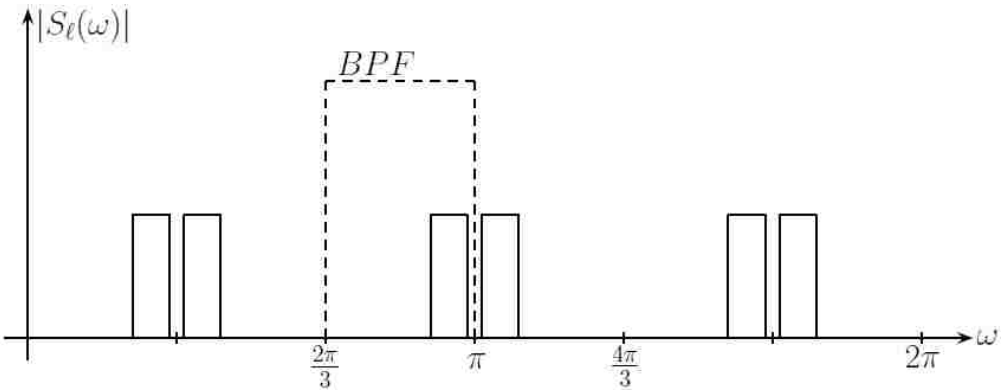

FIGURE 2.5. Graph of $|\tilde{S}_\ell(\omega)|$ over $[0,\ 2\pi]$ with BPF illustrated for $M = 3$

The next result follows from Lemma 2.

Corollary 1. *Let integer M be the downsampling ratio. Suppose that $\omega_H > (1 - 1/M)\pi$ where $\pi \geq \omega_H > \omega_L > 0$, and condition (i) of* Lemma 2 *holds. Then there exists no aliasing for the* DTFT *of the kth polyphase of $\{s(k)\}$, if and only if $\omega_L \geq (1 - 1/M)\pi$.*

This condition implies the expression of (2.19) *for $\omega \in [0,\ 2\pi)$ and some integer i_ω.*

Proof. For sufficiency, assume that $\omega_L \geq (1 - 1/M)\pi$, i.e., $M \leq \pi/(\pi - \omega_L)$. Consider

$$g(x) = \frac{x}{x - \omega_L} = 1 + \frac{\omega_L}{x - \omega_L}.$$

Clearly $g(x)$ is monotonically decreasing for $x > \omega_L$. It follows that

$$M \leq \frac{\pi}{\pi - \omega_L} \leq \frac{\omega_H}{\omega_H - \omega_L}$$

which implies that $M \leq \left\lfloor \frac{\omega_H}{\omega_H - \omega_L} \right\rfloor$ by the fact that M is integer-valued. We need to consider only the largest possible M that yields condition (i) in Lemma 2. Hence no aliasing exists for the DTFT of the kth polyphase of $\{s(k)\}$ and the relation in (2.19) is true. Conversely $s_\ell(\omega)$ consists of M shifted copies of $S(\omega/M)$ over $[0,\ 2M\pi]$ or $S(\omega)$ over $[0,\ 2\pi]$ which do not overlap. In the case of odd M, the ith copy of $S(\omega)$ is located within $[\frac{2i\pi}{M},\ \frac{2(i+1)\pi}{M}]$. The hypothesis on ω_H implies that $\omega_H \in \left(\frac{M-1}{M}\pi,\ \frac{M+1}{M}\pi\right]$. Together with the assumption of no aliasing yields $\omega_L \geq (1 - 1/M)\pi$. The case of even M can be argued similarly and is omitted. □

The condition in Corollary 1 is easier to use and can be translated into

$$\Omega_L \geq (1 - 1/M)\Omega_S/2$$

in physical frequencies with Ω_S the sampling frequency for $\{s(k)\}$. Together with $2M(\Omega_H - \Omega_L) \leq \Omega_S$ for no aliasing, we have the following inequality:

$$2M(\Omega_H - \Omega_L) \leq \Omega_S \leq 2M\Omega_L/(M - 1). \tag{2.23}$$

The result from Lemma 2 can now be used to compute the time offset ℓ between the two polyphase components $\{s_\ell(k)\}$ and $\{s_0(k)\}$ by computing the phase slope or group delay of

$$S_\ell(\omega)S_0^*(\omega) = \frac{e^{j\frac{\ell[\omega + 2i_M\pi]}{M}}}{M}\left|S\left(\frac{\omega + 2i_M\pi}{M}\right)\right|^2 \tag{2.24}$$

for all $\omega \in [0,\ \pi]$ where $i_M = (M-1)/2$ for odd M, $i_M = M/2$ for even M, and superscript * denotes conjugation. Recall the first observation made after the proof of Lemma 2. However, Lemma 2 and (2.24) do not provide an answer for the case when ℓ is not an integer which is crucial in estimation of TDOA.

Let $s_c(t)$ be the continuous-time signal with t real-valued from which $\{s_\ell(k)\}$ and $\{s_0(k)\}$ are obtained through sampling with sampling frequency $\Omega_s = 2\pi/T_s$ and $T_s = MT_S$. Suppose that

$$s_\ell^\epsilon(k) = s_c[(kM + \ell + \epsilon_0)T_S], \quad \epsilon_0 \in [0,\ 1) \tag{2.25}$$

where $k = 0, \pm 1, \pm 2, \cdots$ and $0 < \ell < M$. We are interested in knowing $S_\ell^\epsilon(\omega)$, DTFT of $\{s_\epsilon(k)\}$, in terms of $S_0(\omega)$, DTFT of $\{s_0(k)\} = \{s_c(kT_s)\}$. The next result holds.

Theorem 2. *Let $s_c(t)$ be bandpass continuous-time signal whose frequency response has a support over $[\Omega_L,\ \Omega_H)$, and $\{s_\ell^\epsilon(k)\}$ in (2.25) and $\{s_0(k) = s_c(kT_s)\}$ be samples of $s_c(t)$ under the same sampling frequency $\Omega_s = 2\pi/T_s$. Let $M > 0$ be the smallest integer such that $\Omega_S = M\Omega_s \geq 2\Omega_H$. Then there exists no aliasing for frequency responses of $\{s_0(k)\}$ and $\{s_\ell^\epsilon(k)\}$. In addition the* DTFT *of $\{s_\ell^\epsilon(k)\}$ is related to the* DTFT *of $\{s_0(k)\}$ according to*

$$S_\ell^\epsilon(\omega) = e^{j(\ell+\epsilon_0)(\omega+2i_\omega\pi)/M} S_0(\omega) \ \ \forall\ \omega \in [0,\ \pi), \tag{2.26}$$

for some integer i_ω dependent on ω.

Proof. The hypothesis implies that no aliasing exists for DTFTs of $\{s_0(k)\}$ and $\{s_\ell^\epsilon(k)\}$, in light of Lemma 2 and Corollary 1. To prove the theorem, consider first the case when $\ell = 0$. It follows from no aliasing that

$$\hat{S}_0(\Omega) = \sum_{i=-\infty}^{\infty} S_c(\Omega + i\Omega_s) = S_c(\Omega + i_\Omega \Omega_s)$$

for all $\Omega \in [0,\ \Omega_s/2)$ and for some i_Ω dependent on Ω. On the other hand, the frequency response of $\{s_0^\epsilon(n)\}$ is given by

$$\begin{aligned}\hat{S}_0^\epsilon(\Omega) &= \sum_{i=-\infty}^{\infty} S_c(\Omega + i\Omega_s) e^{j\epsilon_0 T_S(\Omega + i\Omega_s)} \\ &= e^{j\epsilon_0 T_S(\Omega + i_\Omega \Omega_s)} S_c(\Omega + i_\Omega \Omega_s) \\ &= e^{j\epsilon_0 T_S(\Omega + i_\Omega \Omega_s)} \hat{S}_0(\Omega)\end{aligned}$$

for all $\Omega \in [0,\ \Omega_S/2)$ by again the fact of no aliasing. Since the normalized frequency $\omega = \Omega T_s = \Omega\Omega_s/2\pi$, we have $\Omega = 2\pi\omega/\Omega_s$. Hence $S_0(\omega) = \hat{S}_0(2\pi\omega/\Omega_s)$, and

$$\begin{aligned}S_0^\epsilon(\omega) &= \hat{S}_0^\epsilon\left(\frac{2\pi\omega}{\Omega_s}\right) = e^{j\frac{\epsilon_0(T_s\Omega + i_\Omega T_s \Omega_s)}{M}} \hat{S}_0\left(\frac{2\pi\omega}{\Omega_s}\right) \\ &= e^{j\frac{\epsilon_0(\omega + 2i_\Omega \pi)}{M}} S_0(\omega)\end{aligned}$$

are DTFTs of $\{s_0(n)\}$ and $\{s_0^\epsilon(n)\}$, respectively, by $T_S = T_s/M$ from which the relations

$$\begin{aligned}S_0^\epsilon(\omega) &= e^{j\epsilon_0(\omega + 2i_\omega \pi)/M} S_0(\omega) \quad \Longrightarrow \\ S_\ell^\epsilon(\omega) &= e^{j\epsilon_0(\omega + 2i_\omega \pi)/M} S_\ell(\omega)\end{aligned}$$

follow where $i_\omega = i_\Omega$ depends on ω. Applying Lemma 2 yields

$$\begin{aligned}S_\ell^\epsilon(\omega) &= \frac{e^{j(\ell+\epsilon_0)(\omega + 2i_\omega \pi)/M}}{M} S\left(\frac{\omega + 2i_\omega \pi}{M}\right) \\ &= e^{j(k+\epsilon_0)(\omega + 2i_\omega \pi)/M} S_0(\omega)\end{aligned}$$

which concludes the proof. □

The result of Theorem 2 implies that the formula in (2.24) can now be replaced by

$$S_\ell^\epsilon(\omega) S_0^*(\omega) = \frac{e^{j\frac{(\ell+\epsilon_0)(\omega + 2i_M \pi)}{M}}}{M} \left| S\left(\frac{\omega + 2i_M \pi}{M}\right) \right|^2 \tag{2.27}$$

for all $\omega \in [0,\ \pi]$, which admits the linear phase with slope of $(\ell + \epsilon_0)/M$. For application to TDOA estimate, both the reference and mobile receive the same

narrowband SOP under the same sampling frequency. Without loss of generality, the signal at the mobile can be modeled by $\{\alpha s_0(k)\}$ while the signal at the RR by $\{\beta s_\ell^\epsilon(k)\}$ where α and β satisfying $0 < \alpha, \beta \leq 1$ are some constants in order to take the path loss of the radio signal into account. For narrowband signals, frequency dependent fading can be ignored (which may not hold for wideband signals). Because (α, β) affect only SNR, the relation in (2.27) will be employed next to develop near MLE solution to TDOA estimation of which the true value of TDOA is given by $\delta t = (\ell+\epsilon_0)T_S = (\ell+\epsilon_0)T_s/M$ for some integer ℓ and $\epsilon_0 \in [0,\ 1)$. The following provides an approximate MLE to TDOA estimation.

Theorem 3. *Let* $\{\widehat{s}_0(k)\}$ *and* $\{\widehat{s}_\ell^\epsilon(k)\}$ *be measurements of the sampled bandpass signals* $\{s_0(k)\}$ *and* $\{s_\ell^\epsilon(k)\}$ *at the reference receiver and mobile receiver, respectively. Denote* $\Psi_0(\omega)$, *and* $\Psi_{\ell_\epsilon}(\omega)$ *as the power spectral density* (PSD) *functions of* $\{s_0(k)\}$ *and* $\{s_\ell^\epsilon(k)\}$, *respectively, and* $\Psi_{0,\ell_\epsilon}(\omega)$ *the cross-*PSD *of* $\{s_0(k)\}$ *and* $\{s_\ell^\epsilon(k)\}$. *Define*

$$W(\omega) = \frac{|\Psi_{0,\ell_\epsilon}(\omega)|^2}{\Psi_0(\omega)\Psi_{\ell_\epsilon}(\omega) - |\Psi_{0,\ell_\epsilon}(\omega)|^2}.$$

Finally let $\widehat{\Psi}_{0,\ell_\epsilon}(\omega) = |\widehat{\Psi}_{0,\ell_\epsilon}(\omega)|e^{j\widehat{\varphi}(\omega)}$ *be the estimated cross* PSD *based on the measured signals* $\{\widehat{s}_0(k)\}$ *and* $\{\widehat{s}_\ell^\epsilon(k)\}$. *Then under high* SNR, *approximate* MLE $\widehat{\delta t}_{\text{ML}}$ *for* TDOA *is given by*

$$\widehat{\delta t}_{\text{ML}} = \underset{\delta t}{\text{argmin}} \int_0^\pi \left[(\omega + 2i_M\pi)\delta t - \widehat{\varphi}(\omega)\right]^2 W(\omega)\ d\omega. \tag{2.28}$$

Proof. By equation (44) in [66] with modification to discrete-time signals, the MLE maximizes the real-valued cost function

$$J_1 = \int_{-\pi}^{\pi} \frac{\widehat{\Psi}_{0,\ell_\epsilon}(\omega)}{|\Psi_{0,\ell_\epsilon}(\omega)|} W(\omega) e^{-j(\omega+2i_\omega\pi)\delta t}\ d\omega. \tag{2.29}$$

Under the high SNR assumption, there holds $\Psi_{0,\ell_\epsilon}(\omega) \approx \widehat{\Psi}_{0,\ell_\epsilon}(\omega)$ and

$$\begin{aligned} J_1 &\approx \int_{-\pi}^{\pi} \frac{\widehat{\Psi}_{0,\ell_\epsilon}(\omega)}{|\widehat{\Psi}_{0,\ell_\epsilon}(\omega)|} W(\omega) e^{-j(\omega+2i_\omega\pi)\delta t}\, d\omega \\ &\approx \int_{-\pi}^{\pi} \cos\left[(\omega+2i_\omega\pi)\delta t - \widehat{\varphi}(\omega)\right] W(\omega)\, d\omega \\ &\approx \int_{-\pi}^{\pi} \left\{1 - .5\left[(\omega+2i_\omega\pi)\delta t - \widehat{\varphi}(\omega)\right]^2\right\} W(\omega)\, d\omega \end{aligned}$$

where $\cos(x) \approx 1 - x^2/2$ is used. Hence maximization of J_1 is equivalent to minimization of

$$J_2 = \int_0^{\pi} \left[(\omega+2i_M\pi)\delta t - \widehat{\varphi}(\omega)\right]^2 W(\omega)\, d\omega$$

considering that the signals are real and $i_\omega = i_M$ is a constant dependent only on whether M is even or odd by $\omega \in [0,\ \pi)$. The formula in (2.28) thus holds. □

Theorem 3 shows that the MLE is approximately a WLS solution. Indeed measured signals always have a finite number of samples. As long as $\delta t = (\ell+\epsilon_0)T_S << T_D$, where T_D is the duration of the received signals at the RR and mobile, and is considerably smaller than 1 second, we can regard the signal duration adequately long. Hence with suitable windowing, FFT (fast algorithm for discrete Fourier transform) can be employed to estimate the cross PSD. If $\{\omega_i\}_{i=1}^L$ is the total frequency samples over the signal bandwidth, then the minimization in (2.28) can be replaced by

$$J_{\delta t}(\delta t) = \sum_{i=1}^{L} \left[(\omega_i+2i_M\pi)\delta t - \widehat{\varphi}(\omega_i)\right]^2 \widehat{W}(\omega_\ell) \tag{2.30}$$

where $\widehat{W}(\omega_i)$ is based on estimated PSDs and cross-PSD. The minimizer to $J_{\delta t}(\cdot)$ can be easily computed and is an approximate MLE to TDOA. The details are omitted.

Remark 2. (i) The estimation error based on near MLE in Theorem 3 is approximately Gaussian distributed. Indeed by (2.29),

$$\frac{\widehat{\Psi}_{0,\ell_\epsilon}(\omega)}{|\Psi_{0,\ell_\epsilon}(\omega)|} \approx e^{j\varphi(\omega)} + \mathcal{O}\left(\frac{2}{\sqrt{\mathrm{SNR}(\omega)}} + \frac{1}{\mathrm{SNR}(\omega)}\right)$$

where SNR is now function of frequency and $1/\mathrm{SNR}(\omega)$ is linear with respect to noise power. The proof of Theorem 3 and the first order approximation for $\ln(1+x) \approx x$ yield

$$\widehat{\varphi}(\omega) \approx \varphi(\omega) + \mathcal{O}\left(\frac{2}{\sqrt{\mathrm{SNR}(\omega)}} + \frac{1}{\mathrm{SNR}(\omega)}\right).$$

In light of Lemma 1, the above is approximately Gaussian under high SNR. We thus have an approximate linear approximation problem in the presence of Gaussian noise. MLE for such an estimation problem is the WLS solution as in Theorem 3, leading to Gaussian distributed estimation error [67].

(ii) It needs to be commented that a different estimation procedure can be developed by using an interpolator illustrated in Figure 2.4 to first upsample and filter the signals, which may generate more accurate signals at a higher sampling frequency $\Omega_S \geq 2\Omega_H$. The interpolated signals can then be used to estimate the TDOA using the same estimation algorithm in Theorem 3. This new procedure will increase the computational complexity considerably, especially when M is a large integer. The resolution of the TDOA estimate is limited by the CRLB and cannot be improved by the interpolator alone.

(iii) Although Ω_s can be as low as $2(\Omega_H - \Omega_L)$, this is not suggested due to consideration of SNR. Specifically the total signal and noise powers are fixed in practice. If $\Omega_s = 2(\Omega_H - \Omega_L)$, the total noise power is entirely distributed over the signal bandwidth, leading to poor SNR. On the other hand, if $\Omega_s >> 2(\Omega_H - \Omega_L)$, then only a small fraction of the noise power is distributed over the signal bandwidth in

which the TDOA is estimated. Hence large sampling frequency will result in better SNR. For this reason, the sampling frequency is primarily limited by the data rate of the wireless channel used to transmit the sampled signals to the computing center. □

2.3 Simulation Results

FM radio signals will be used in this section to illustrate our proposed positioning system based on narrowband signals. A typical FM receiver is shown in Figure 2.6 [68]. The received signal $s_{FM}(t)$ is filtered using a tunable bandpass filter whose center frequency is adjusted by the frequency of a local oscillator. The resulting radio-frequency signal $s_{RF}(t)$ is mixed with the local oscillator signal which has a frequency equal to $\omega_c + \omega_{IF}$, where ω_c is the the carrier frequency of the desired radio station and ω_{IF} is the fixed *intermediate frequency* (IF). The mixing process produces an image of the bandpass-filtered signal centered at the IF frequency. After passing through bandpass filters in the IF stage at ω_{IF}, adjacent-channel interferences are suppressed greatly [68], producing the signal $s_{IF}(t)$. Finally the FM demodulator (e.g., a phase lock loop) is used to obtain the information signal $m(t)$. Our approach employs $s_{IF}(t)$ implying that the demodulator can be excluded, yielding a simpler receiver than the full FM radio.

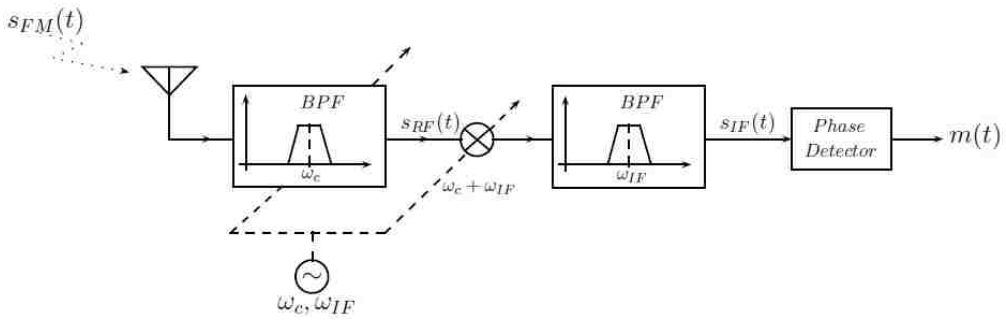

FIGURE 2.6. General diagram of a typical FM receiver.

In the United States, Federal Communications Commission (FCC) has established the intermediate frequency for FM radio broadcasting as 10.7 MHz, with a separation of 200 KHz between carrier frequencies from different stations. The peak frequency deviation of the FM signal is 75 KHz. Moreover, a minimum distance must be observed between FM transmitters (antennas) depending on the class of the radio station and the adjacent channels in the frequency spectrum.

In our simulation study, IF signals at four different carrier frequencies, equal to 100.7 MHz, 100.9 MHz, 101.1 MHz, and 103.3 MHz, are employed, which ensure the 200 MHz separation dictated by FCC. These four signals are from four different FM radio stations, assumed to be transmitted from four different broadcast towers. The positions of the four corresponding transmitter antennas of the broadcast towers are specified by their coordinates given by

$$\mathbf{p}_{E_1} = \begin{bmatrix} 0 \\ 0 \\ 0.1 \end{bmatrix}, \quad \mathbf{p}_{E_2} = \begin{bmatrix} 0 \\ 72 \\ 0.1 \end{bmatrix},$$

$$\mathbf{p}_{E_3} = \begin{bmatrix} 72 \\ 72 \\ 0.1 \end{bmatrix}, \quad \mathbf{p}_{E_4} = \begin{bmatrix} 50 \\ 0 \\ 0.1 \end{bmatrix}$$

with the units in kilometer (KM). Figure 2.7 shows the positions of these four antennas, together with the positions of the RR and MR given by

$$\mathbf{p}_b = \begin{bmatrix} 28 \\ 40 \\ 0 \end{bmatrix}, \quad \mathbf{p}_m = \begin{bmatrix} 40 \\ 25 \\ 0 \end{bmatrix}.$$

Table 2.1 summarizes the distances in KM from the RR and MR to each FM transmitter $\{E_i\}_{i=1}^4$:

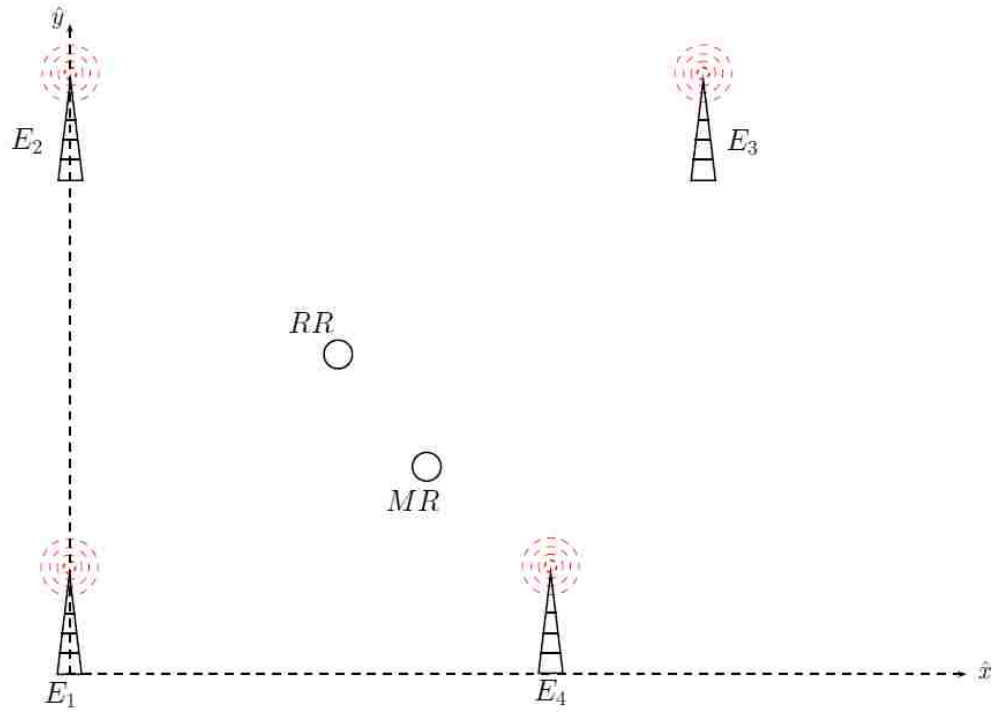

FIGURE 2.7. Scheme of the position of the FM transmitters, Base and Mobil.

TABLE 2.1. Distance from base/mobile to FM transmitters.

	E_1	E_2	E_3	E_4
RR	48.8263	42.5207	54.4060	45.6509
MR	47.1700	61.7172	56.8569	26.9260

In accordance with Section 2, the TDOAs $\{\delta t_i\}_{i=1}^4$ are defined by $\delta t_i = (d_{m_i} - d_{b_i})/c$ with c the speed of light, and d_{m_i} and d_{b_i} the distance from the transmitter E_i to the mobile and RR, respectively. It follows that

$$\delta t_1 = -5.521\mu\text{s}, \qquad \delta t_2 = 63.988\mu\text{s},$$
$$\delta t_3 = 8.1787\mu\text{s}, \qquad \delta t_4 = -62.416\mu\text{s}.$$

The bandwidth of the baseband FM signal is assumed to be equal to 15 KHz. We used a modulating signal $m(t)$ composed of 20 sinusoidal signals with unit amplitude given by

$$m(t) = \sin(2\pi f_{\max} t) + \sum_{k=1}^{19} \sin(2\pi f_k t + \varphi_k), \tag{2.31}$$

where $0 < f_1 < f_2 < \cdots < f_{\max} = 15$ KHz. The FM signal is then obtained as

$$s_{FM}(t) = \cos\left(\omega_c t + 2\pi k_f \int_{-\infty}^{t} m(\tau)\ d\tau\right). \tag{2.32}$$

By setting $k_f = 3000$, the peak frequency deviation satisfies the FCC's requirement. The frequencies $\{f_k\}_{k=1}^{19}$ and phases $\{\varphi_k\}_{k=1}^{19}$ are generated randomly for each broadcast station with uniform distributions on $(0,\ 15\text{KHz})$, and $(-\pi,\ \pi)$, respectively. The sampling frequency used at the MR and RR is taken to be 400 KHz which results in the sampling period of 2.5 μs.

In our simulation study a total of 1000 ensemble runs are carried out for each FM signal under two different SNR values, namely 20 dB, and 10 dB. In each ensemble run, four different FM baseband signals are generated as discussed above, which are modulated, and transmitted. The received signals at the mobile and RR are corrupted by independent white Gaussian noise processes, and are processed as in Figure 2.6. After the four IF signals are received and sampled at both the RR and mobile over the period of 10 milliseconds, the corresponding TDOAs are computed and the position of the mobile is then estimated using the two approximate MLE algorithms proposed in the previous two sections. Table 2.2 summarizes the simulation results for TDOA estimation under SNR of 20 dB.

TABLE 2.2. Mean and variance for estimated TDOAs under SNR = 20 dB

FM Tx	δt_i (μs)	$\mathrm{E}\{\widehat{\delta t}_i\}$ (μs)	$\mathrm{var}\{\widehat{\delta t}_i - \delta t_i\}$ (ns^2)
E_1	-5.521	-5.519	118.2
E_2	63.988	63.980	1,469.1
E_3	8.179	8.175	154.9
E_4	-62.416	-62.413	1,418.2

Table 2.3 shows the statistics of the TDOA estimates for the SNR value of 10 dB, while keeping the rest of the parameters the same as those in Table 2.2.

It is easy to see that variances of the TDOA estimation error are dominated by $\widehat{\delta t}_i$ at E_2 and E_4 because of the large differences between the distances of the two

TABLE 2.3. Mean and variance for estimated TDOAs under SNR = 10 dB

FM Tx	δt_i (μs)	E$\{\widehat{\delta t}_i\}$ (μs)	var$\{\widehat{\delta t}_i - \delta t_i\}$ (ns^2)
E_1	-5.521	-5.517	790.1
E_2	63.988	63.980	$2,112.8$
E_3	8.179	8.176	878.8
E_4	-62.416	-62.413	$2,110.5$

towers to the RR and mobile. This phenomenon has been constantly observed by our simulation results. After the TDOAs $\{\widehat{\delta t}_i\}_{i=1}^4$ are estimated, the localization procedure in Section 2 is applied to compute the mobile position. The performance measure of the position error is the outage curve [2] shown in Figure 2.8. It shows that for SNR of 20 dB, the position errors are smaller than 30 meters for about 94% of the position estimations, smaller than 20 meters for about 82% of the position estimations, and 10 meters for about 53% of the position estimations. The performance deteriorates as SNR decreases. For SNR of 10 dB, the location errors are smaller than 30 meters for about 86% of the position estimations, smaller than 20 meters for about 69% of the position estimations, and smaller than 10 meters for about 32% of the position estimations. Our simulation results demonstrate the comparable performance to many existing positioning systems, including GPS, even though the underlying SOP have much smaller bandwidth.

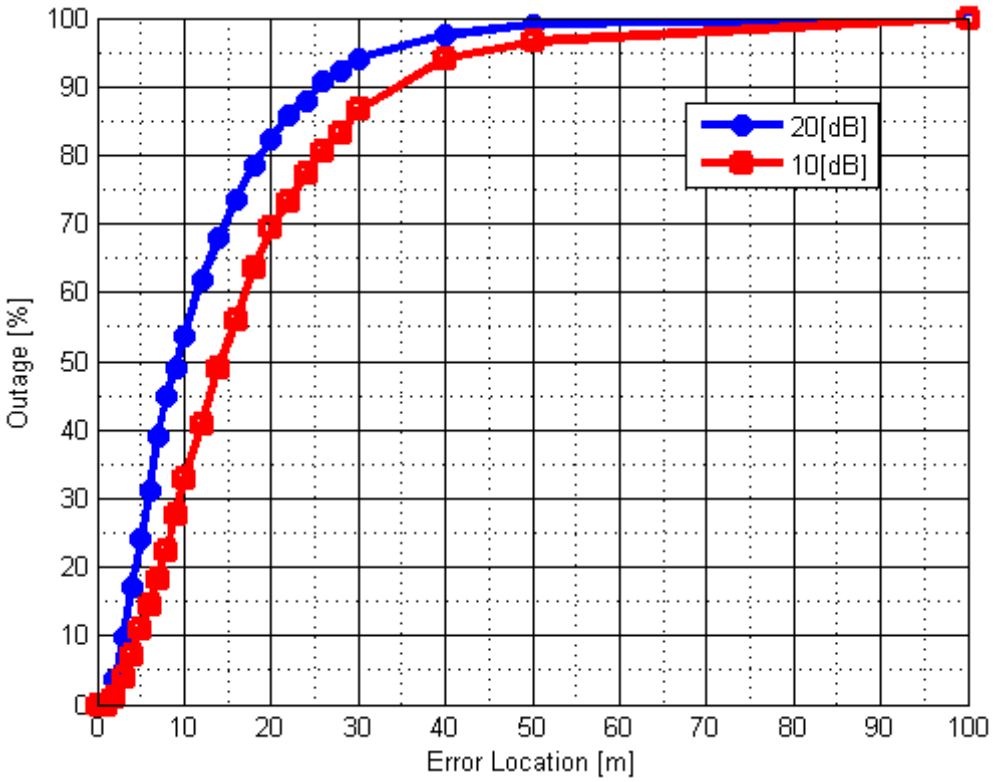

FIGURE 2.8. Outage curve for localization accuracy averaged over 1000 emsemble runs

Chapter 3

Localization of Nodes in Wireless Sensor Networks

This chapter presents the localization of nodes in WSNs. Section 3.1 presents a distributed localization approach, in which each node estimates its position based on information from their neighbors, whose positions may not be known. In Section 3.2, the second algorithm describes the localization algorithm based on the previous algorithm, but considering mobility capability of the nodes. Later, Section 3.3 describes a centralized localization algorithm in presence of outliers, which is also based on theoretical approaches stated in the first algorithm.

Each Section provides analysis of the developed algorithm, as well as simulation results.

3.1 Distributed Nodes Localization in WSN

3.1.1 Problem Formulation

Consider a network of M nodes with n blind nodes and $m = M - n$ anchor nodes in $\Re^d$ $(d > 1)$. Let $\mathbf{p}_i$ denote the (unknown) position of blind node i for $i = 1, 2 \cdots, n$ and let $\mathbf{a}_i$ be the (known) position of the ith anchor for $i = n+1, \cdots, M$. Let d_{ij} denote the distance between nodes i and j which is assumed to be known for $i, j = 1, 2, \cdots, M$. The localization problem is to determine the positions $\{\mathbf{p}_i\}_{i=1}^{n}$ such that all the pairwise distance relations are satisfied.

It is assumed that the network is localizable and is equipped with only a few anchor nodes [1]. Moreover, the blind nodes are not required to be contained in the

[1]It should be pointed out that localizability of the network is not the subject of this research. Necessary and sufficient conditions for unique localizability are derived in [69]. I would like to note that as pointed out in [69], network localizability is not a significant issue in practice, as many applications can function properly as long as a sufficient number of anchor nodes are available.

convex hull of the anchor nodes, and $\mathbf{p}_i \neq \mathbf{p}_j . \forall i, j = 1, \ldots, n$ with $i \neq j$, and $\mathbf{p}_i \neq \mathbf{a}_j$, $\forall i = 1, \ldots, n$ and $j = n+1, \ldots, M$.

Let R_r denote the radio range of each node and let $\mathcal{E} \triangleq \{(i,j) : \|\mathbf{p}_i - \mathbf{p}_j\| \leq R_r, i < j, i, j = 1, 2, \cdots, n\}$ and $\mathcal{F} \triangleq \{(i,j) : \|\mathbf{p}_i - \mathbf{a}_j\| \leq R_r, i = 1, 2, \cdots, n, j = n+1, \cdots, M\}$ denote all pairs of sensor/sensor and sensor/anchor nodes that are within range of each other, respectively, where $\|.\|$ denotes the Euclidean norm. We assume that the nodes are able to estimate the distances to their neighbor nodes (e.g. using Signal Strength Indicator). The method for which the nodes estimate the mentioned distance is out of the scope of this dissertation.

In the following we describe the problem with the relaxation methods where spurious solutions may be introduced as a result of relaxing the constraints. In [20] the localization problem is stated as the following non-linear optimization problem.

$$\min_{\mathbf{p}_1, \cdots, \mathbf{p}_n} J(\underline{\mathbf{p}}) \triangleq \frac{1}{2} \sum_{(i,j) \in \mathcal{E}} \left| \|\mathbf{p}_i - \mathbf{p}_j\|^2 - d_{ij}^2 \right| + \frac{1}{2} \sum_{(i,j) \in \mathcal{F}} \left| \|\mathbf{p}_i - \mathbf{a}_j\|^2 - d_{ij}^2 \right| \qquad (3.1)$$

In [24] the problem in (3.1) is relaxed to obtain the following convex optimization problem which is then solved using the second-order cone programming method.

$$\min_{\mathbf{p}_1, \cdots, \mathbf{p}_n, y_{ij}} \sum_{(i,j) \in \mathcal{E}} |y_{ij} - d_{ij}^2|, \quad \text{such that} \quad y_{ij} \geq ||\mathbf{p}_i - \mathbf{p}_j||^2, \ \forall \ (i,j) \in \mathcal{E} \qquad (3.2)$$

Since the unknowns $\{\mathbf{p}_i\}_{i=1}^n$ do not explicitly appear in the objective function in (3.2), it is rather trivial to obtain a solution for (3.2) which yields a value of zero for the objective function (simply pick n positions that are very close to each other and let $y_{ij} = d_{ij}^2$ for all i, j) while the constraints are satisfied with strict inequality. Therefore, although the original problem is uniquely localizable, the relaxed problem may not be.

Our approach in this dissertation is based on a novel randomized gradient descent method. Therefore we define the objective function as

$$F(\underline{\mathbf{p}}) \triangleq \frac{1}{2}\sum_{(i,j)\in\mathcal{E}}\left(\|\mathbf{p}_i-\mathbf{p}_j\|-d_{ij}\right)^2+\frac{1}{2}\sum_{(i,j)\in\mathcal{F}}\left(\|\mathbf{p}_i-\mathbf{a}_j\|-d_{ij}\right)^2 \tag{3.3}$$

where $\underline{\mathbf{p}}=\left[\mathbf{p}_1^T,\ldots,\mathbf{p}_n^T\right]^T$ and where $\mathbf{p}_i$ is a $d\times 1$ column vector. The optimization problem is then formulated as

$$\min_{\underline{\mathbf{p}}} F(\underline{\mathbf{p}}) \tag{3.4}$$

We note that $F(\underline{\mathbf{p}})$ is continuous and bounded below ($F(\underline{\mathbf{p}})\geq 0, \forall\underline{\mathbf{p}}$), and $F(\underline{\mathbf{p}})\rightarrow\infty$ as $\|\underline{\mathbf{p}}\|\rightarrow\infty$. Furthermore, $F(\underline{\mathbf{p}})$ has a finite number of minima. The latter property will be used in proving the convergence of our algorithm. Note that a gradient-based method is not applicable to (3.1) or (3.2) since the objective functions are not differentiable. As stated previously, we assume that the network is uniquely localizable and therefore (3.4) has a unique optimal solution $\underline{\mathbf{p}}^*$ such that $F(\underline{\mathbf{p}}^*)=0$.

3.1.2 Proposed Algorithm

The optimization in (3.4) can be implemented using a distributed gradient descent method. Denote the set of blind and anchor neighbors of blind node i by $\mathbb{G}_i$, and $\mathbb{H}_i$, respectively, i.e.,

$$\mathbb{G}_i \triangleq \{j : \|\mathbf{p}_i-\mathbf{p}_j\|\leq R_r, j\neq i, j=1,\ldots,n\} \tag{3.5}$$

$$\mathbb{H}_i \triangleq \{j : \|\mathbf{p}_i-\mathbf{a}_j\|\leq R_r, j=n+1,\ldots,M\}\,. \tag{3.6}$$

The component of the gradient of $F(\underline{\mathbf{p}})$ corresponding to position $\mathbf{p}_i$ is given by

$$\nabla_i F(\underline{\mathbf{p}}) = \sum_{j\in\mathbb{G}_i}\frac{(\mathbf{p}_i-\mathbf{p}_j)\gamma_{ij}}{\|\mathbf{p}_i-\mathbf{p}_j\|}+\sum_{j\in\mathbb{H}_i}\frac{(\mathbf{p}_i-\mathbf{a}_j)\delta_{ij}}{\|\mathbf{p}_i-\mathbf{a}_j\|}, \tag{3.7}$$

where $\gamma_{ij}\triangleq\|\mathbf{p}_i-\mathbf{p}_j\|-d_{ij}$ and $\delta_{ij}\triangleq\|\mathbf{p}_i-\mathbf{a}_j\|-d_{ij}$. From (3.7), we see that $\nabla_i F(\underline{\mathbf{p}})$ depends only on the information (distances and positions) from neighbors

of node i. For node i define the objective function

$$f_i(\underline{\mathbf{p}}; \mathcal{A}, \mathcal{B}) \triangleq \frac{1}{2} \sum_{j \in \mathcal{A}} \left(\|\mathbf{p}_i - \mathbf{p}_j\| - d_{ij} \right)^2 + \frac{1}{2} \sum_{j \in \mathcal{B}} \left(\|\mathbf{p}_i - \mathbf{a}_j\| - d_{ij} \right)^2 \tag{3.8}$$

where $\mathcal{A} \subseteq \mathbb{G}_i$ and $\mathcal{B} \subseteq \mathbb{H}_i$. From (3.7) and (3.8) we see that

$$\nabla_i f_i(\underline{\mathbf{p}}; \mathbb{G}_i, \mathbb{H}_i) = \nabla_i F(\underline{\mathbf{p}}) \tag{3.9}$$

where $\nabla_i f_i(\underline{\mathbf{p}}; \mathbb{G}_i, \mathbb{H}_i)$ is the gradient of $f_i(\underline{\mathbf{p}}; \mathbb{G}_i, \mathbb{H}_i)$ with respect to $\mathbf{p}_i$. This shows that the Gradient Descent (GD) algorithm for the objective function $F(\underline{\mathbf{p}})$ can be implemented as a (synchronous) distributed algorithm. Based on the observation in (3.9) we present the following.

3.1.2.1 Distributed Gradient Descent Algorithm

3.1.2.1.1 Algorithm 1

At each step, each blind node i solves a "local" optimization problem to minimize the objective function $f_i(\underline{\mathbf{p}}, \mathbb{G}_i, \mathbb{H}_i)$ using the GD method. The kth iteration of the algorithm is given by

$$\hat{\mathbf{p}}_i(k+1) = \hat{\mathbf{p}}_i(k) - \alpha_k \nabla_i f_i(\hat{\underline{\mathbf{p}}}(k); \mathbb{G}_i, \mathbb{H}_i), \tag{3.10}$$

where $\alpha_k \in \Re^+$, $\hat{\mathbf{p}}_i(k)$ stands for the position of node i at iteration k of the algorithm, and $\hat{\underline{\mathbf{p}}}(k) = \left[\hat{\mathbf{p}}_1^T(k), \ldots, \hat{\mathbf{p}}_n^T(k)\right]^T$. Algorithm 1, defined by (3.10), stops when a minimum of $F(\underline{\mathbf{p}})$ is reached, i.e., $\nabla_i F(\hat{\underline{\mathbf{p}}}(k)) = 0$ (equivalently $\|\hat{\mathbf{p}}_i(k+1) - \hat{\mathbf{p}}_i(k)\| = 0$), for all $i = 1, \ldots, n$, for some $k \geq 0$. □

In view of (3.7) and (3.9), Algorithm 1 is the same as the GD method applied to (3.4) and is guaranteed to converge to a minimum of (3.3) when the step sizes $\{\alpha_k\}$ satisfy the Wolfe conditions [70]. However, it should be noted that, since $F(\underline{\mathbf{p}})$ is non-convex and, in the case of a large number of blind nodes, it has many

local minima, the GD method described above may not converge to the optimal solution $\underline{\mathbf{p}}^*$.

Two issues must be addressed regarding the choice of the step sizes $\{\alpha_k\}$.

1. First, the convergence rate of the GD method depends on the choice of the step sizes $\{\alpha_k\}$. One method relies on the (exact) line search by setting

$$\alpha_k = \arg\min_{\alpha} F[\underline{\hat{\mathbf{p}}}(k) - \alpha \nabla F(\underline{\hat{\mathbf{p}}}(k))] \tag{3.11}$$

   However this approach requires a great deal of computation. Barzilai and Borwein have proposed an alternative method for the calculation of the step size according to

$$\tilde{\alpha}_k = \frac{\|\underline{\hat{\mathbf{p}}}(k) - \underline{\hat{\mathbf{p}}}(k-1)\|^2}{(\underline{\hat{\mathbf{p}}}(k) - \underline{\hat{\mathbf{p}}}(k-1))^T(\nabla F(\underline{\hat{\mathbf{p}}}(k)) - \nabla F(\underline{\hat{\mathbf{p}}}(k-1)))} \tag{3.12}$$

   which guarantees convergence of the GD and does not require any line search [71].

2. Next, The computation in (3.12) is centralized. For implementation in WSNs, a distributed algorithm is needed where each sensor can compute its own step size. Based on the consensus algorithm, [72, 73], and using the above result, a distributed method is presented for step size computations in [74], which can be used to estimate $\tilde{\alpha}_k$. Each node $i = 1, 2, \cdots, n$ runs the consensus iteration using information from its neighbors according to

$$\rho_i(q+1) \triangleq W_{ii}\rho_i(q) + \sum_{j \in \mathbb{G}_i \cup \mathbb{H}_i} W_{ij}\ \rho_j(q) \tag{3.13}$$

$$\psi_i(q+1) \triangleq W_{ii}\psi_i(q) + \sum_{j \in \mathbb{G}_i \cup \mathbb{H}_i} W_{ij}\ \psi_j(q) \tag{3.14}$$

for $q = 0, 1, \cdots$. The initial conditions are given by

$$\rho_i(0) \triangleq \|\hat{\mathbf{p}}_i(k) - \hat{\mathbf{p}}_i(k-1)\|^2 \tag{3.15}$$

$$\psi_i(0) \triangleq (\hat{\mathbf{p}}_i(k) - \hat{\mathbf{p}}_i(k-1))^T(\nabla_i f_i(\underline{\hat{\mathbf{p}}}(k); \mathbb{G}_i, \mathbb{H}_i) - \nabla_i f_i(\underline{\hat{\mathbf{p}}}(k-1); \mathbb{G}_i, \mathbb{H}_i)), \tag{3.16}$$

and

$$W_{ij} \triangleq \begin{cases} \frac{1}{\max\{|\mathbb{G}_i \cup \mathbb{H}_i|, |\mathbb{G}_j \cup \mathbb{H}_j|\}}, & (i,j) \in \mathcal{E} \cup \mathcal{F} \\ 1 - \sum_{k \in \mathbb{G}_i \cup \mathbb{H}_i} W_{ik}, & i = j \\ 0, & \text{otherwise} \end{cases} \tag{3.17}$$

where $|C|$ denotes the number of elements in the set C. Note that index q refers to the iterations of the distributed consensus algorithm that needs to be performed (to compute $\tilde{\alpha}_k$) once per each iteration k of the GD algorithm. It is shown in [74] that for all $i = 1, 2, \cdots, n$,

$$\lim_{q \to \infty} \frac{\rho_i(q)}{\psi_i(q)} = \tilde{\alpha}_k \tag{3.18}$$

3.1.2.2 **Distributed Randomized Gradient Descent (DRGD) Algorithm**

We now present an algorithm that allows the distributed GD algorithm to "escape" from any local minimum and converge to the optimal solution $\underline{\mathbf{p}}^*$. We start by describing some of the properties of the distributed Algorithm 1.

Lemma 3. *Suppose that Algorithm 1 has converged to a point* $\underline{\tilde{\mathbf{p}}} = \left[\tilde{\mathbf{p}}_1^T, \ldots, \tilde{\mathbf{p}}_n^T\right]^T$, *i.e.,* $\nabla_i f_i(\underline{\tilde{\mathbf{p}}}(k), \mathbb{G}_i, \mathbb{H}_i) = 0$ *for all* $i = 1, 2, \cdots, n$. *If* $\underline{\tilde{\mathbf{p}}} \neq \underline{\mathbf{p}}^*$, *then there exists at least one node* $\ell \in \{1, 2, \cdots, n\}$ *and two subsets of neighbors of* ℓ, $A_\ell \subset \mathbb{G}_\ell$, $B_\ell \subset \mathbb{H}_\ell$, *such that* $\nabla_{\mathbf{p}_\ell} f_\ell(\underline{\tilde{\mathbf{p}}}; A_\ell, B_\ell) \neq 0$.

Proof. If there is no such ℓ, then from (3.7) and (3.9) it follows that $\tilde{\gamma}_{ij} = \|\tilde{\mathbf{p}}_i - \tilde{\mathbf{p}}_j\| - d_{ij} = 0$ for $i, j = 1, 2, \cdots, n$ $(i \neq j)$ and $\tilde{\delta}_{ij} = \|\tilde{\mathbf{p}}_i - \mathbf{a}_j\| - d_{ij} = 0$ for all $i = 1, 2, \cdots, n$ and $j = n+1, n+2, \cdots, M$. This implies that $\underline{\tilde{\mathbf{p}}}$ is a solution

to the optimization problem in (3.4) which contradicts the assumption that $\underline{\mathbf{p}}^*$ is unique. □

Remark 3. Note that if Lemma 3 holds for a node ℓ, then there exists a node $s \in \mathbb{G}_\ell \cup \mathbb{H}_\ell$ such that $\nabla_\ell f_\ell(\underline{\tilde{\mathbf{p}}}; \mathbb{G}_\ell - \{s\}, \mathbb{H}_\ell - \{s\}) \neq 0$. Therefore if node ℓ removes s from its set of neighbors and restarts the GD iteration,

$$\hat{\mathbf{p}}_\ell(k+1) = \tilde{\mathbf{p}}_\ell(k) - \lambda \nabla_{\mathbf{p}_\ell} f_\ell(\underline{\tilde{\mathbf{p}}}(k); \mathbb{G}_\ell - \{s\}, \mathbb{H}_\ell - \{s\}), \tag{3.19}$$

where $\lambda > 0$, then $\hat{\mathbf{p}}_\ell(k+1) \neq \tilde{\mathbf{p}}_\ell(k)$. We will use this property to enable the algorithm to scape from the local minima of $F(\underline{\mathbf{p}})$. □

Lemma 4. *Suppose that Algorithm 1 has converged to the unique optimal solution* $\underline{\mathbf{p}}^*$. *Then for any* $\ell = 1, 2, \cdots, n$ *and any subsets* $A_\ell \subset \mathbb{G}_\ell$ *and* $B_\ell \subset \mathbb{H}_\ell$, $\nabla_\ell f_\ell(\mathbf{p}^*; A_\ell, B_\ell) = 0$.

Proof. We have $F(\underline{\mathbf{p}}^*) = 0$, implying that $\gamma_{ij} = \|\mathbf{p}_i^* - \mathbf{p}_j^*\| - d_{ij} = 0$, for all $i, j = 1, 2, \cdots, n$ $(i \neq j)$ and $\delta_{ij} = \|\mathbf{p}_i^* - \mathbf{a}_j\| - d_{ij} = 0$ for $i = 1, 2, \cdots, n$ and $j = n+1, n+2, \cdots, M$. The result follows from differentiating (3.8). □

The following definition is used in our subsequent discussion.

Definition 1. *Consider the function* $F : \Re^{nd} \longrightarrow \Re$ *in* (3.3) *and let* $\mathbf{x_0} \in \Re^{nd}$ *denote a (local) minimum of* $F(.)$. *A basin of attraction of* $\mathbf{x_0}$ *is the set of points* $\mathbf{x} \in \Re^{nd}$ *such that using* $\mathbf{x}$ *as the initial position for Algorithm 1 leads to the same minimum* $\mathbf{x_0}$.

Let $\mathcal{M} \subset \Re^{nd}$ denote the set of minima of $F(\underline{\mathbf{p}})$. Since, as mentioned previously, $F(\underline{\mathbf{p}})$ has a finite number of minima, $\mathcal{M}$ is finite. Let $\mathcal{M} = \{\mathbf{x}_1, \mathbf{x}_2, \cdots, \mathbf{x}_L, \mathbf{p}^*\}$ where $\mathbf{x}_j, j = 1, 2, \cdots, L$ are the local minima of $F(\underline{\mathbf{p}})$ and, as before, $\mathbf{p}^*$ is the unique global minimum. Also denote the attraction basin of $\mathbf{x}_j$ by U_j, and for

$i = 1, 2, \cdots, n$ let $\mathbf{x}_{j,i}$ denote the component of $\mathbf{x}_j$ corresponding to the ith node, i.e., $\mathbf{x}_j = [\mathbf{x}_{j,1}^T, \mathbf{x}_{j,2}^T, \cdots, \mathbf{x}_{j,n}^T]^T$. Based on Lemmas 3 and 4, we propose the following algorithm.

3.1.2.2.1 **Algorithm 2**

We start with some initial position vector $\underline{\hat{\mathbf{p}}}(0) = \left[\hat{\mathbf{p}}_1^T(0), \hat{\mathbf{p}}_2^T(0), \ldots, \hat{\mathbf{p}}_n^T(0)\right]^T$, where $\hat{\mathbf{p}}_i(0)$ is the initial position of the ith blind node. Using Algorithm 1, the nodes compute a (possibly local) minimum of $F(.)$ corresponding to the attraction basin in which the initial point $\underline{\hat{\mathbf{p}}}(0)$ resides. Denote this minimum by $\underline{\mathbf{p}}(1) = [\mathbf{p}_1^T(1), \mathbf{p}_2^T(1), \cdots, \mathbf{p}_n^T(1)]^T$. Note that $\underline{\mathbf{p}}(1) \in \mathcal{M}$. At this point each node $i = 1, 2, \cdots, n$ selects a proper subset of its neighbors, namely $A_i(1) \subset \mathbb{G}_i$ and $B_i(1) \subset \mathbb{H}_i$, at random and computes a new initial position vector $\hat{\mathbf{p}}_i(1)$ according to

$$\hat{\mathbf{p}}_i(1) = \mathbf{p}_i(1) - \Lambda_i(1)\nabla_i f_i(\underline{\mathbf{p}}(1); A_i(1), B_i(1)), \tag{3.20}$$

where $\Lambda_i(1)$, $i = 1, 2, \ldots, n$ are chosen randomly. Using Algorithm 1, the nodes compute a new (local) minimum $\underline{\mathbf{p}}(2) = [\mathbf{p}_1^T(2), \mathbf{p}_2^T(2), \cdots, \mathbf{p}_n^T(2)]^T$ with each node i using $\hat{\mathbf{p}}_i(1)$ as its initial position vector, and continue. The kth iteration of the algorithm uses the initial position vector $\underline{\hat{\mathbf{p}}}(k-1)$ and Algorithm 1 to compute a (possibly local) minimum $\underline{\mathbf{p}}(k)$. From this minimum the next initial position vector $\underline{\hat{\mathbf{p}}}(k)$ is computed for Algorithm 1 according to the following.

$$\hat{\mathbf{p}}_i(k) = \mathbf{p}_i(k) - \Lambda_i(k)\nabla_i f_i(\underline{\mathbf{p}}(k); A_i(k), B_i(k)). \tag{3.21}$$

We assume that the constants $\Lambda_i(k)$ are selected from a Gaussian distribution with zero mean and unit variance[2]. Furthermore, the sequences of $\{\Lambda_i(k)\}$ form a col-

[2]The selection of Gaussian distribution ensures that, with a positive probability, the constants $\Lambda_i(k)$ can assume arbitrarily large values. This on the other hand ensures that (with a positive probability) the algorithm will be able to escape from any local minimum. We should point out that any distribution with an infinite support such as Laplacian or exponential can also be used here.

lection of n independent processes, each of which is an independent and identically distributed (iid) process.

Algorithm 2 produces a random sequence of position vectors. In particular if we only consider the points of convergence of Algorithm 1, i.e., $\{\underline{\mathbf{p}}(k)\}$, then a random sequence of the minima of $F(.)$ is observed.

For $k = 1, 2, \ldots$ let $Y_k = \underline{\mathbf{p}}(k)$. Then $\{Y_k\}$ forms a random process with state space $\mathcal{M}$. Lemma 5 is used in our proof of convergence of Algorithm 2.

Lemma 5. *For any $\mathbf{x}_j \in \mathcal{M}$, and any $k = 1, 2, \cdots,$*

$$P(Y_{k+1} \neq \mathbf{x}_j | Y_k = \mathbf{x}_j) > 0 \tag{3.22}$$

Proof. Suppose at time k the process is in state $\mathbf{x}_j$, i.e., $Y_k = \mathbf{x}_j$. At this point each node i computes a new position $\hat{\mathbf{p}}_i(k)$ according to (3.21) resulting in a new position vector $\underline{\hat{\mathbf{p}}}(k) = [\hat{\mathbf{p}}_1^T(k), \hat{\mathbf{p}}_2^T(k), \cdots, \hat{\mathbf{p}}_n^T(k)]^T$ for the entire network. In view of Lemma 3 and given the finite number of nodes in the network, there is a positive probability that for some node ℓ, the subsets $A_\ell(k), B_\ell(k)$ are chosen such that $\nabla_\ell f_\ell(\underline{\mathbf{p}}(k); A_\ell(k), B_\ell(k)) \neq 0$. Now since $\Lambda_\ell(k)$ is a Gaussian random variable, it follows from (3.21) that $\hat{\mathbf{p}}_\ell(k) \neq \mathbf{x}_{j,\ell}$. Therefore, $\underline{\hat{\mathbf{p}}}(k) \neq \mathbf{x}_j$. Now if the new position vector $\underline{\hat{\mathbf{p}}}(k)$ is still in the basin of attraction of $\mathbf{x}_j$, i.e., $\underline{\hat{\mathbf{p}}}(k) \in U_j$, then Algorithm 1 will again converge to $\mathbf{x}_j$, i.e., $Y_{k+1} = \mathbf{x}_j$. However, there is also a positive probability that $\underline{\hat{\mathbf{p}}}(k) \notin U_j$. In particular, let ξ_j denote the width of the basin of attraction of $\mathbf{x}_j$ defined by

$$\xi_j = \sup\{\|\mathbf{g} - \mathbf{h}\| : \mathbf{g}, \mathbf{h} \in U_j\} \tag{3.23}$$

Now since $\Lambda_\ell(k)$ is a Gaussian random variable, it follows that

$$\nu_\ell \triangleq P\left[\Lambda_\ell(k) \nabla_\ell f_\ell(\underline{\mathbf{p}}(k); A_\ell(k), B_\ell(k)) > \xi_j\right] > 0$$

Therefore, it follows that $P(\underline{\hat{\mathbf{p}}}(k) \notin U_j) \geq \nu_\ell > 0$. Consequently Algorithm 1 which is now initialized with $\underline{\hat{\mathbf{p}}}(k) \notin U_j$, will converge to some $\mathbf{x} \in \mathcal{M}$ where $\mathbf{x} \neq \mathbf{x}_j$. This verifies (3.22). □

We have summarized Algorithm 2 in Table 3.1 which appears after a discussion of implementation issues in Section 3.1.2.4.

Given that the processes $\{\Lambda_i(k)\}$ are iid, and that at each step the subsets $\{(A_i(k), B_i(k))\}_{i=1}^n$ are chosen independently of the past shows that $\{Y_k\}$ is a Markov chain, i.e.

$$P(Y_{k+1} = \mathbf{y}_{k+1} | Y_l, l < k, Y_k = \mathbf{y}_k) = P(Y_{k+1} = \mathbf{y}_{k+1} | Y_k = \mathbf{y}_k), \quad \mathbf{y}_k, \mathbf{y}_{k+1} \in \mathcal{M} \tag{3.24}$$

Lemmas 3 and 4 imply that $\mathbf{x}_j, j = 1, 2, \cdots, L$, are transient states and $\mathbf{p}^*$ is an absorbing state for $\{Y_k\}$. Now since $L < \infty$, we conclude that with probability one the process will enter the absorbing state $\mathbf{p}^*$, i.e.,

$$P(\lim_{r \to \infty} Y_r = \mathbf{p}^*) = 1 \tag{3.25}$$

We summarize the discussion above in the following

Theorem 4. *In the absence of measurement noise, with probability one Algorithm 2 converges to the optimal solution* $\mathbf{p}^*$.

Remark 4. *We should point out that as long as each node has at least* $d + 2$ *neighbors, the convergence of the proposed method is not affected by the connectivity of the network (the number of neighbors for each node). The* $d + 2$ *neighbors are required due to the fact that at least* $d+1$ *nodes are needed to uniquely localize each node. Furthermore, since we eliminate at least one neighbor in order to "escape" a local minimum, then* $d+2$ *neighbors are required for each node. However, a higher network connectivity results in improved convergence rate. This is due the fact that*

there are more subsets $A_i(k) \subset \mathbb{G}_i$ and $B_i(k) \subset \mathbb{H}_i$ to choose in order to escape a local minimum.

3.1.2.3 Upper Bound for Cost Function under Noisy Distance Measurements

We assume that the distance measurements $\{d_{ij}\}$ in (1) are expressed as follows:

$$d_{ij} = \hat{d}_{ij}|1 + \epsilon_{ij}|, \tag{3.26}$$

where $\{\hat{d}_{ij}\}$ are the true distances between the nodes, and the ϵ_{ij}'s represent measurement errors which, as in [20, 21], are modeled as iid Gaussian random variables with zero mean and known variance σ^2.

Theorem 5. *Let $F(\underline{\mathbf{p}})$ denote the cost function defined in* (3.3) *where the distances $\{d_{ij}\}$ are given by* (3.26)*. Define*

$$v^* = \min_{\underline{\mathbf{p}}} F(\underline{\mathbf{p}}). \tag{3.27}$$

Then

$$0 \leq E(v^*) \leq \frac{1}{2}\left(\sigma^2 + 2e^{-\frac{1}{2\sigma^2}}\right) \sum_{(i,j)\in\mathcal{E}\cup\mathcal{F}} \hat{d}_{ij}^2 \tag{3.28}$$

Proof.

$$\begin{aligned}
F(\underline{\mathbf{p}}) &= \frac{1}{2}\sum_{(i,j)\in\mathcal{E}} \left(\|\mathbf{p}_i - \mathbf{p}_j\| - d_{ij}\right)^2 + \frac{1}{2}\sum_{(i,j)\in\mathcal{F}} \left(\|\mathbf{p}_i - \mathbf{a}_j\| - d_{ij}\right)^2 \\
&= \frac{1}{2}\sum_{(i,j)\in\mathcal{E}} \left(\|\mathbf{p}_i - \mathbf{p}_j\| - \hat{d}_{ij}|1 + \epsilon_{ij}|\right)^2 + \frac{1}{2}\sum_{(i,j)\in\mathcal{F}} \left(\|\mathbf{p}_i - \mathbf{a}_j\| - \hat{d}_{ij}|1 + \epsilon_{ij}|\right)^2 \\
&= \frac{1}{2}\sum_{(i,j)\in\mathcal{E}} \left(\|\mathbf{p}_i - \mathbf{p}_j\|^2 + \hat{d}_{ij}^2(1 + 2\epsilon_{ij} + \epsilon_{ij}^2) - 2\|\mathbf{p}_i - \mathbf{p}_j\| \hat{d}_{ij}|1 + \epsilon_{ij}|\right) \\
&\quad + \frac{1}{2}\sum_{(i,j)\in\mathcal{F}} \left(\|\mathbf{p}_i - \mathbf{a}_j\|^2 + \hat{d}_{ij}^2(1 + 2\epsilon_{ij} + \epsilon_{ij}^2) - 2\|\mathbf{p}_i - \mathbf{a}_j\| \hat{d}_{ij}|1 + \epsilon_{ij}|\right)
\end{aligned} \tag{3.29}$$

It follows that

$$0 \leq v^* = \min_{\underline{\mathbf{p}}} F(\underline{\mathbf{p}}) \leq \frac{1}{2} \sum_{(i,j)\in\mathcal{E}\cup\mathcal{F}} \hat{d}_{ij}^2 (2 + 2\epsilon_{ij} + \epsilon_{ij}^2 - 2|1+\epsilon_{ij}|) \tag{3.30}$$

Let $q(x)$ denote the probability density function of $\epsilon_{i,j} \sim \mathcal{N}(0, \sigma^2)$. Taking expectation in (3.30) and after some manipulations we get

$$\begin{aligned}
0 \leq E[v^*] &\leq \frac{1}{2} \sum_{(i,j)\in\mathcal{E}\cup\mathcal{F}} \hat{d}_{ij}^2 (2 + E[\epsilon_{ij}^2] - 2E[|1+\epsilon_{ij}|]) \\
&= \frac{1}{2} \sum_{(i,j)\in\mathcal{E}\cup\mathcal{F}} \hat{d}_{ij}^2 \left[2 + \sigma^2 - 2 \left(\int_{-1}^{\infty} (1+x) q(x)\, dx - \int_{-\infty}^{-1} (1+x) q(x)\, dx \right) \right] \\
&= \frac{1}{2} \sum_{(i,j)\in\mathcal{E}\cup\mathcal{F}} \hat{d}_{ij}^2 \left(\sigma^2 + 4Q(\frac{1}{\sigma}) - 2\sigma \sqrt{\frac{2}{\pi}} e^{-\frac{1}{2\sigma^2}} \right) \\
&\leq \frac{1}{2} \left(\sigma^2 + 2e^{-\frac{1}{2\sigma^2}} \right) \sum_{(i,j)\in\mathcal{E}\cup\mathcal{F}} \hat{d}_{ij}^2
\end{aligned} \tag{3.31}$$

where we have used the fact that $Q(x) \triangleq \frac{1}{\sqrt{2\pi}} \int_x^{\infty} e^{-u^2/2}\, du \leq \frac{1}{2} e^{-x^2/2}$ for $x \geq 0$. $\square$

Denoting the number of links in the network by $\mathcal{L} = |\mathcal{E} \cup \mathcal{F}|$, and noting that $\hat{d}_{ij} \leq R_r$, (3.31) implies that

$$0 \leq E[v^*] \leq \frac{1}{2} \left(\sigma^2 + 2e^{-\frac{1}{2\sigma^2}} \right) \mathcal{L} R_r^2. \tag{3.32}$$

In the case of noisy distance measurements, the minimum of the cost function $F(\underline{\mathbf{p}})$ may not be zero. More importantly, the minimum may not be known. Thus Eq. (3.32) provides an upper bound on the minimum of the cost function $F(\underline{\mathbf{p}})$ which can be used in a stopping criterion for Algorithm 2.

Remark 5. *In the presence of noisy measurements the network may not be localizable. One possibility is that the minimizing solution* $\mathbf{p}^*$ *such that* $F(\mathbf{p}^*) = 0$ *is not unique. In this case all such solutions are absorbing states of the Markov chain*

$\{Y_k\}$ described in Section Distributed Randomized Gradient Descent (DRGD) Algorithm. Therefore Algorithm 2 will converge to one of these solutions. Another possibility is that a solution $\mathbf{p}^*$ such that $F(\mathbf{p}^*) = 0$ does not exist. In this case all the local minima of $F(\mathbf{p})$ are positive recurrent states of the Markov chain. Therefore all these minima will be visited by Algorithm 2 and the global minimum among them can be selected. Therefore even in the presence of noisy measurements the proposed algorithm is guaranteed to converge to the minimum of the cost function $F(\mathbf{p})$. We should also point out that, as indicated in next Section Simulation Results, in all of our simulations, Algorithm 2 always converged where the cost function $F(\mathbf{p})$ was below the threshold in (3.32).

3.1.2.4 **Implementation Considerations**

A practical question often not discussed explicitly is how should the sensor nodes realize that a (local) minimum of $F(\underline{\mathbf{p}})$ has been reached. For this a distributed stopping criterion is required. Two such criteria are needed in Algorithm 2. One is to determine that a local minimum of $F(\underline{\mathbf{p}})$ has been reached by Algorithm 1, and next is to determine that the global minimum of $F(\underline{\mathbf{p}})$ is reached. The distributed consensus algorithm in [73] can be used in both cases. This algorithm allows the nodes to compute the average of their individual costs using a recursive procedure. Denote the cost of node i by u_i. Node i computes the sequence $\{z_i(q)\}$ as follows,

$$z_i(q+1) = z_i(q) + \mu \sum_{j \in \mathbb{G}_i} (z_j(q) - z_i(q)), \tag{3.33}$$

where $z_i(0) = u_i$ for $i \in \{1, \ldots, n\}$. It is shown that for an appropriate choice of μ, $\lim_{q \to \infty} z_i(q) = \frac{1}{n} \sum_{\ell=1}^{n} u_\ell$, for all $i \in \{1, \ldots, n\}$ [75].

We note that a local minimum is reached by Algorithm 1 when $\|\hat{\mathbf{p}}_i(k+1) - \hat{\mathbf{p}}_i(k)\| = 0$, $\forall i = 1, \ldots, n$ and $\forall k \geq k_0$, for some k_0. Thus, setting $z_i(0) = \|\hat{\mathbf{p}}_i(k) - \hat{\mathbf{p}}_i(k-1)\|$ and running the recursive procedure in (3.33), each node i can determine

that a local minimum of $F(\underline{\mathbf{p}})$ has been reached when $z_i(q) \leq \varsigma$, for some small ς and all $i = 1, \ldots, n$.

To determine that Algorithm 2 has reached the optimal solution $\mathbf{p}^*$ such that $F(\mathbf{p}^*) = 0$, we note that

$$F(\hat{\underline{\mathbf{p}}}(k)) = \frac{1}{2} MC(k), \tag{3.34}$$

where $C(k) = \frac{1}{M} \sum_{i=1}^{M} f_i(\hat{\underline{\mathbf{p}}}(k), \mathbb{G}_i, \mathbb{H}_i)$, which includes the costs at both blind and anchor nodes. Thus each node i sets $z_i(0) = f_i(\hat{\underline{\mathbf{p}}}(k), \mathbb{G}_i, \mathbb{H}_i)$ and runs the recursion in (3.33). Node i determines that the optimal solution has been reached when $z_i(q) \leq \eta$, for some small η.

Finally, if the area of deployment of the network is known, the time to convergence of our algorithm can be improved. Let Ω_F be the bounded region where the nodes are deployed. In order to reduce the time to convergence, equation (3.21) can be followed by:

$$\hat{\mathbf{p}}_i(k+1) = \begin{cases} \hat{\mathbf{p}}_i(k), & \text{if } \hat{\mathbf{p}}_i(k+1) \notin \Omega_F \\ \hat{\mathbf{p}}_i(k+1), & \text{otherwise} \end{cases} \tag{3.35}$$

Another important consideration is related to eq. 3.7. Consider the node i. In case that during the optimization algorithm described in Algorithm 2 the positions $\mathbf{p}_i(k) = \mathbf{p}_j(k)$, $j \in \mathbb{G}_i$, or $\mathbf{p}_i(k) = \mathbf{a}_j(k)$, $j \in \mathbb{H}_i$, then the gradient defined in 3.7 is undefined, and similar situation occurs with 3.9 and later defined gradients. Due to $\mathbf{p}_i \neq \mathbf{p}_j$, $\forall i, j = 1, \ldots, n$, and $\mathbf{p}_i \neq \mathbf{a}_j$, $i, j = 1, \ldots, M$, then in case that the mentioned undesired situation occurs we can deviate any of the mentioned positions in order to avoid such situation and continue with the optimization algorithm.

3.1.3 Simulation Results

In this section we present the results of the proposed localization algorithm DRGD for several network configurations and compare our results with those from

TABLE 3.1. Summary of Algorithm 2.

1- **Initialization**
  Choose initial position $\underline{\hat{\mathbf{p}}}(0)$
  Set $k = 0$
2- **Algorithm 1**
  Set $l = 0$
  Set $\underline{\tilde{\mathbf{p}}}(0) = \underline{\hat{\mathbf{p}}}(k)$.
  Do
    Estimate global $\tilde{\alpha}_l$ via (3.13)-(3.17)
    $\forall i \in \{1, \ldots, n\}$, do:
      $\tilde{\mathbf{p}}_i(l+1) = \tilde{\mathbf{p}}_i(l) - \tilde{\alpha}_l \nabla_i f_i(\underline{\tilde{\mathbf{p}}}(l); \mathbb{G}_i, \mathbb{H}_i)$
    $l = l + 1$
  While $(\|\underline{\tilde{\mathbf{p}}}(l) - \underline{\tilde{\mathbf{p}}}(l-1)\| > \iota)$
  $k = k + 1$
  $\underline{\mathbf{p}}(k) = \underline{\tilde{\mathbf{p}}}(l)$
3- **Escaping the Local Minima**
  $\forall i \in \{1, \ldots, n\}$, randomly choose $\Lambda_i(k)$, $A_i(k) \subset \mathbb{G}_i$, $B_i(k) \subset \mathbb{H}_i$
  $\forall i \in \{1, \ldots, n\}$, do:
    $\hat{\mathbf{p}}_i(k) = \mathbf{p}_i(k) - \Lambda_i(k) \nabla_i f_i(\underline{\mathbf{p}}(k); A_i(k), B_i(k))$
4- **Go step 2**

SDP in [20] (which, as mentioned previously, is a centralized algorithm) and those from SOCP in [24] and SA in [76] (which are distributed algorithms). We were unable to obtain the parameters used in the localization algorithm described in Figure 2 in [76]. The parameters we have used in the following simulations are $T = 1,000$, $\alpha = 0.75$, $\beta = 0.9$, $q = 2$ and $p = 20$. (Please see [76] for the definitions of these parameters.)

In all the examples the networks are assumed to be deployed in the plane with $\mathbf{p}_i = [x_i, y_i]^T \in \Re^2$ and satisfy the criteria for localizability discussed in [16]. Also, we assume that the nodes have the capability to estimate the distances to their neighbors. In the figures that follow the position of the anchors is shown by black squares. The true position of the blind nodes is shown with a blue circle. The red circles indicate the initial or estimated positions of the blind nodes. The simulations were carried out on a PC with a 2.2 GHz Intel Core 2 Duo and 3 GB RAM running

Matlab R2009a. Following the implementation considerations described in Section 3.1.2.4, for the proposed algorithm DRGD the value of η was chosen to be 60% of the upper bound in (3.32). We would like to note that, since our algorithm is guaranteed to converge, for smaller values of η, the localization error of DRGD will be smaller. However, the algorithm will take longer to converge.

Figure 3.1 shows a comparison of the performance of DRGD vs. SOCP, SDP and SA. Distance measurements $\{d_{ij}\}$ were considered to be error-free. Figure 3.1-(a) shows the topology of the network. The communication radio range of the nodes is assumed to be $R_r = 1.8$ units. With this radio range the blue links represent the adjacency of the nodes. The initial position of the nodes were chosen randomly and are shown in Figure 3.1-(b), where the black links represent the error between the true position and the initial positions. The estimated position using SOCP, SDP, SA and DRGD are shown in Figures 3.1-(c), 3.1-(d), 3.1-(e) and 3.1-(f), respectively. From the results in Figure 3.1 we observe that the performance of DRGD is comparable to the one obtained from SDP, which, as mentioned previously, is a centralized algorithm. On the other hand the performances of SOCP and SA are poor. Furthermore, it can be seen from this example as well as other simulations in the following that, in the case of SOCP, the estimated positions of the blind nodes are contained in the convex hull of the anchors. This is clearly undesirable as it requires that a large number of anchors be deployed in the periphery of the sensor field. Furthermore, as the simulation results below show even in such cases the performance of SOCP is not satisfactory.

We now consider the performance of the algorithms in the presence of measurement errors using the networks whose topologies are shown in Figures 3.2-(a) and 3.3-(a). The network in Figure 3.2-(a) has 6 anchor nodes and 33 blind nodes while the network in Figure 3.3-(a) has 7 anchor nodes and 85 blind nodes. The radio

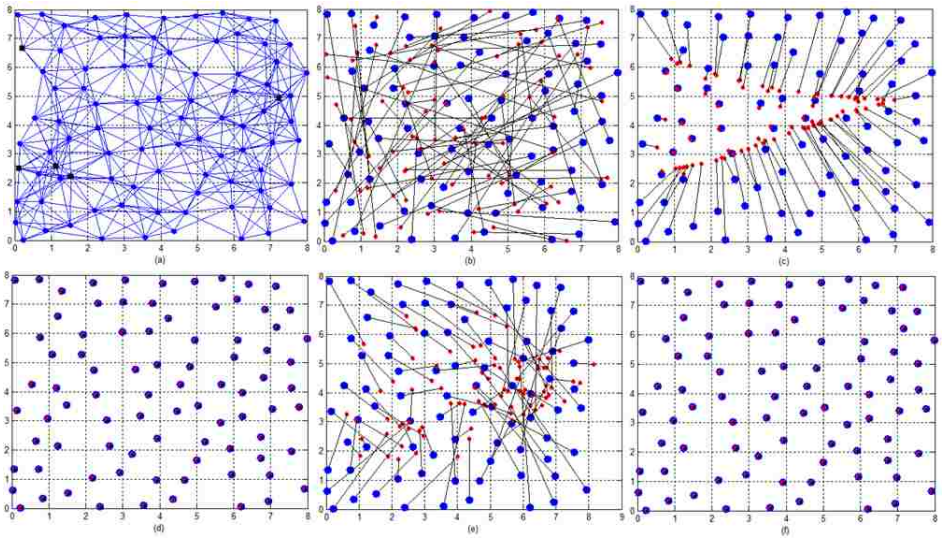

FIGURE 3.1. (a) The Network topology. (b) Initial positions for the localization algorithms. (c) Localization results using relaxation and SOCP. (d) Localization results using SDP. (e) Localization results using SA. (f) Localization results using the proposed DRGD.

range of the networks in Figures 3.2 and 3.3 are $R_r = .7$ and $R_r = 2$ and the standard deviation σ for ϵ_{ij} are equal to 0.05 and 0.1, respectively. Figures 3.2-(b) and 3.3-(b) show the estimated position of the nodes using SOCP. Figures 3.2-(c) and 3.3-(c) show the estimated position of the nodes using [20] and Figures 3.2-(d) and 3.3-(d) show the estimated position of the nodes using [76]. Finally Figures 3.2-(e) and 3.3-(e) show the estimated position of the nodes using the proposed algorithm DRGD. From the localization results, it is again evident that the performance of DRGD is comparable to SDP while the performance of SOCP and SA is not acceptable.

In Figures 3.4 and 3.5 we compare the performance of the four algorithms for 20 different networks. The networks in Figure 3.4 were generated randomly with a topology similar to that in Figure 3.2 with the same number of blind and anchor nodes and the same values for radio range R_r and standard deviation for measurement error σ. The networks in Figure 3.5 have characteristics similar to the network

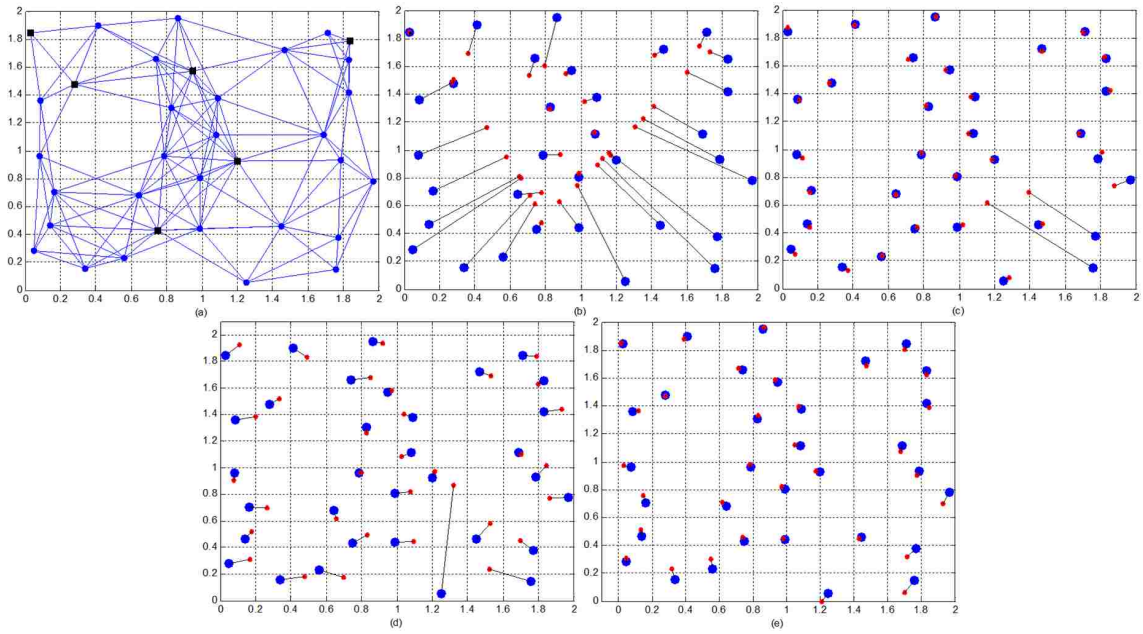

FIGURE 3.2. (a) The Network topology. (b) Localization results using relaxation and SOCP. (c) Localization results using SDP. (d) Localization results using SA. (e) Localization results using the proposed DRGD.

in Figure 3.3. In these figures we have plotted the normalized root-mean-squared error (RMSE) defined as

$$\mathcal{E} \triangleq \sqrt{\frac{1}{n}\sum_{i=1}^{n}\frac{\|\mathbf{p}_i^* - \hat{\mathbf{p}}_i\|^2}{R_r^2}}, \tag{3.36}$$

for each of the 20 networks, where $\mathbf{p}_i^*$ and $\hat{\mathbf{p}}_i$ are the true and the estimated position of node i. For reference, the RMSE of DRGD in Figures 3.2 and 3.3 is 0.0639 and 0.0949, respectively. It can be seen that DRGD significantly outperforms SOCP and SA in all the cases and its performance is close to or in many cases better than SDP.

In order to verify the effect of the position and the number of anchor nodes on the efficacy of the localization algorithms we consider four cases in Figures 3.6-3.9 where the network of blind nodes is the same but the number and the location of the anchors is varied. The distance measurements are assumed to be error-free. Figure 3.6 shows the localization performance of the four algorithms for the case

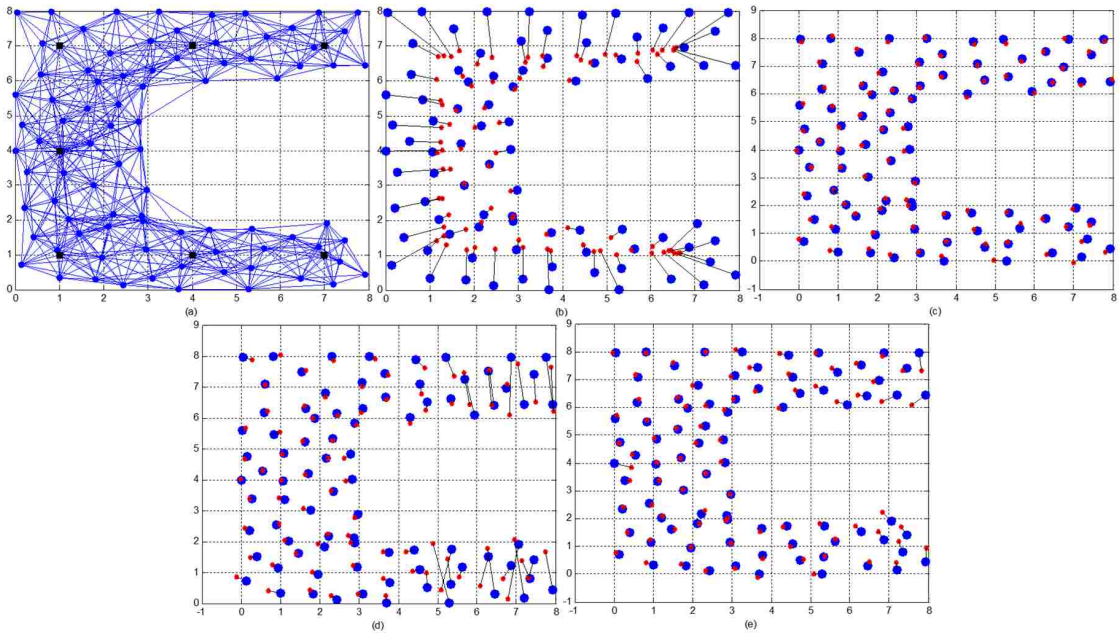

FIGURE 3.3. (a) The Network topology. (b) Localization results using relaxation and SOCP. (c) Localization results using SDP. (d) Localization results using SA. (e) Localization results using the proposed DRGD.

of five anchors deployed such that all the blind nodes are located in the convex hull of the anchors. It can be seen that the performance of SOCP and SA improves with respect to previous cases such as in Figure 3.1. In Figure 3.7 there are 10 anchors but are randomly deployed. A comparison of the results in Figures 3.6 and 3.7 shows that, in the case of SOCP and SA, the localization error for the nodes on the boundary of the network (not in the convex hull of the anchors) increases significantly even though the number of anchors has increased from five to ten. In Figures 3.8 and 3.9 we have further increased the number of anchors but ensured that some anchors are placed close to the boundary of the sensor field. The placement of the anchors in these figures is intended to ensure good performance from SOCP and SA. It can be observed that in fact the performance of SOCP and SA improves. However, even in these cases, the proposed DRGD outperforms these two algorithms.

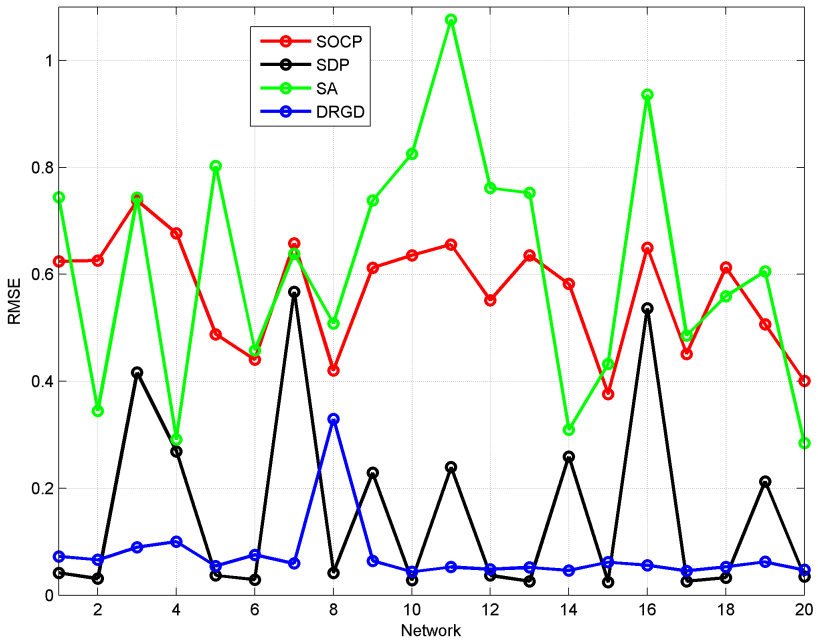

FIGURE 3.4. RMSE for the localization of 20 networks with similar characteristics to Figure 3.2-(a) using SOCP, SDP, SA and DRGD.

3.1.3.1 **Computational Complexity**

Due to the complexity of the cost function $F(\underline{\mathbf{p}})$ and the high dimension of $\underline{\mathbf{p}}$, it is difficult to determine the number of minima of $F(\underline{\mathbf{p}})$ and the geometry of their attraction basins. This implies that the number of states of the Markov chain $\{Y_k\}$ and its transition probability matrix are very difficult to compute. Therefore, an analysis of the convergence rate for the proposed DRGD algorithm is mathematically intractable.

In order to compare the complexity of DRGD with the two distributed localization algorithms SOCP and SA we have computed the average CPU time of each algorithm when run for 50 simulations on networks of Figures 3.6-3.9. The results are shown in Table 3.2. Before we discuss the results we need to point out an important issue. As mentioned previously in Section Implementation Considerations, in a truly distributed localization algorithm, a distributed algorithm such as the con-

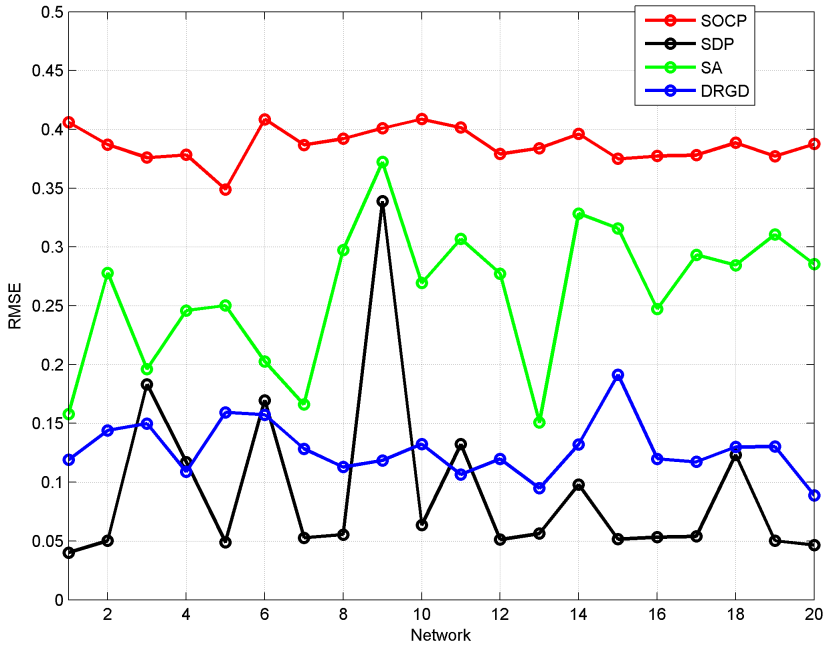

FIGURE 3.5. RMSE for the localization of 20 networks with similar characteristics to Figure 3.3-(a) using SOCP, SDP, SA and DRGD.

sensus algorithm of Section Implementation Considerations is also needed so that the sensor nodes can determine that the localization algorithm has converged. The implementations of SOCP and SA do not include such a distributed algorithm. The iterations in the localization algorithms in SOCP and SA are stopped in a centralized manner by checking the vector of positions from all the sensors. In the execution times shown in Table 3.2 the time for DRGD includes the time of the consensus algorithm while SOCP and SA do not include this time. If such a distributed convergence criteria is included for SOCP and SA, their convergence time will be increased from those in Table 3.2. It can be seen from the results in Table 3.2 that DRGD has significantly shorter convergence time than SOCP and SA in all the cases.

Another issue that we should point out is that both SOCP and SDP rely on a complex software package, namely the SeDuMi optimization package. For low cost sensor nodes with limited memory and computational resources, implementation

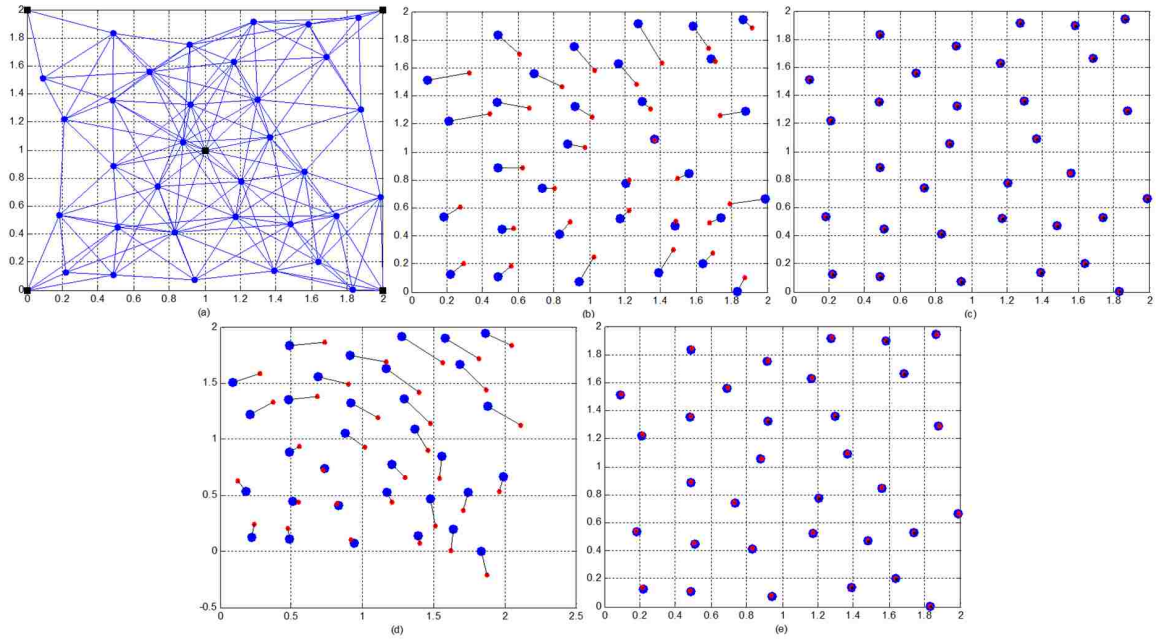

FIGURE 3.6. (a) The Network topology. (b) Localization results using relaxation and SOCP. (c) Localization results using SDP. (d) Localization results using SA. (e) Localization results using the proposed DRGD.

TABLE 3.2. Average CPU execution time (in seconds) for localization using SOCP, SA and DRGD.

	Net. Figure 3.6	Net. Figure 3.7	Net. Figure 3.8	Net. Figure 3.9
SOCP	173.052	139.418	108.483	135.815
SA	68.0944	80.044	90.3714	114.5671
DRGD	6.683	37.958	9.832	9.892

of such an optimization tool may be not be feasible. The proposed localization algorithm does not require complex computations since it is based on the gradient descent algorithm.

Finally, Figure 3.10 shows the CPU execution time-to-convergence vs. the number of anchors using DRGD. The parameters of the network are the same as those considered in Table 3.2. A significant drop in time-to-convergence is observed as the number of anchors is increased from 5 to 20 after which the time remains almost constant.

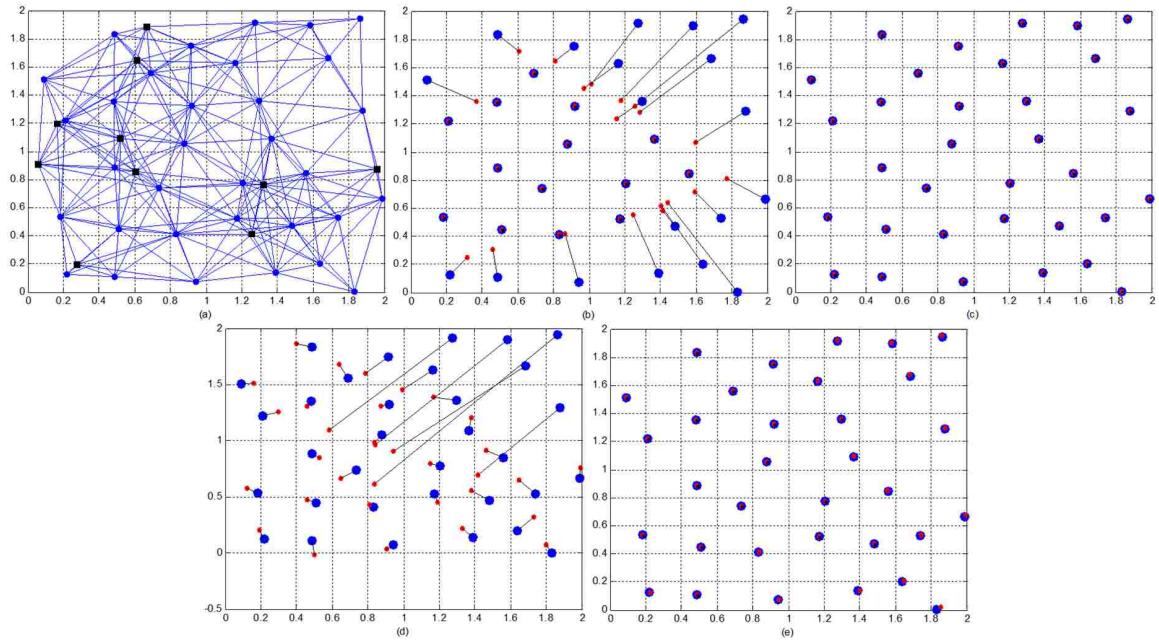

FIGURE 3.7. (a) The Network topology. (b) Localization results using relaxation and SOCP. (c) Localization results using SDP. (d) Localization results using SA. (e) Localization results using the proposed DRGD.

3.2 Distributed Mobile Nodes Localization in WSN

We now consider localization of nodes in a mobile WSN using the DRGD algorithm. Without loss of generality, we assume that $\mathbf{p}_i \in \Re^2, \forall i \in \{1, \ldots, M\}$. Assume that we desire to determine the position of the nodes every $\mathcal{T}$s, denoted as the *position sampling period* (PSP). It is easy for a sensor node to determine whether during a PSP it has moved or not, for instance by using an accelerometer. Therefore, during each PSP, only the nodes that have moved need to compute their new positions and the stationary nodes can act as anchor nodes. In the following we only need to consider a single PSP and denote by $\mathcal{N}_{\mathcal{M}} \subseteq \{1, 2, \cdots, n\}$ the set of blind nodes in the network that have traveled during this PSP. We next describe the so-called random walk mobility model for the nodes [77]. We should, however, point out that although in this section we present a modification of DRGD and

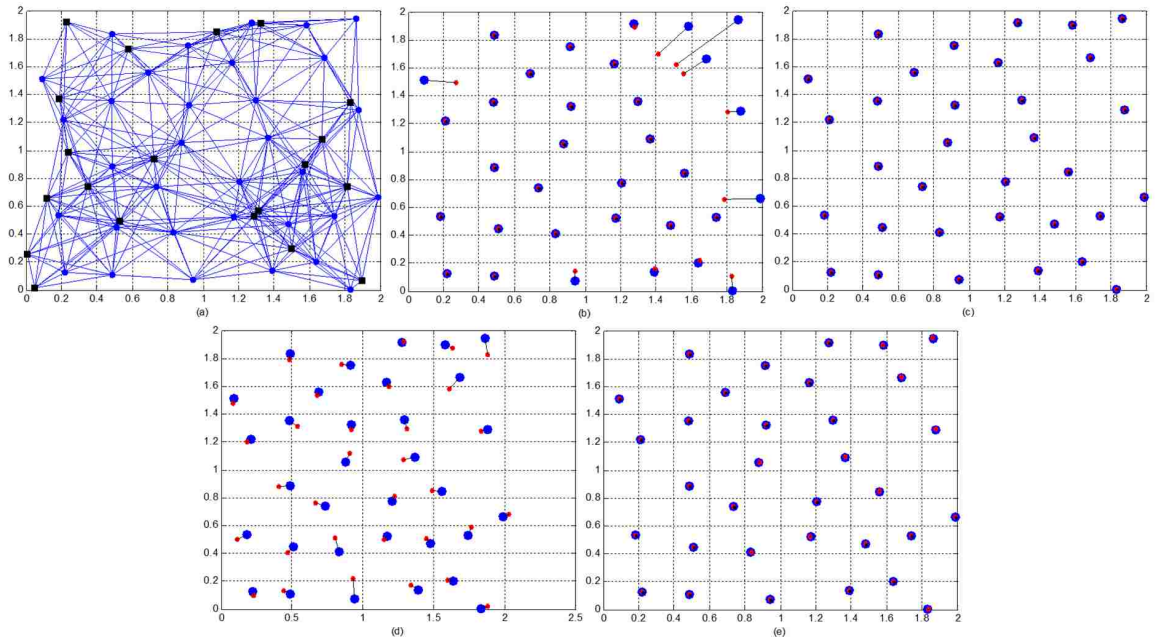

FIGURE 3.8. (a) The Network topology. (b) Localization results using relaxation and SOCP. (c) Localization results using SDP. (d) Localization results using SA. (e) Localization results using the proposed DRGD.

the subsequent simulation results for this model, DRGD can be easily tailored to, and is equally effective for any mobility model.

3.2.1 Mobility Model

We consider a maximum velocity of $V_{\max}$ for all the nodes. Therefore in a single PSP, the maximum distance a node can travel is $L_{\max} = V_{\max}\mathcal{T}$. We assume that the distance, L, traveled by any node during a single PSP is uniformly distributed in the interval $[0, L_{\max}]$.

Let $\mathbf{p}_i[w\mathcal{T}]$ denote the position of node i at time $w\mathcal{T}$, $w = 1, 2, \ldots$[3]. Let $\zeta_i(w)$ denote the angle of the vector $\mathbf{p}_i[w\mathcal{T}] - \mathbf{p}_i[(w-1)\mathcal{T}]$ with the x-axis. We assume that the direction of travel for node i at time $w\mathcal{T}$ is given by the unit vector $\mathbf{u}(w\mathcal{T}) = [\cos(\theta), \sin(\theta)]$, where θ is uniformly distributed in the interval $[\zeta_i(w) -$

[3]Note that here and in the sequel, when brackets [.] are used, we are referring to the positions of the nodes at PSPs, e.g., $\mathbf{p}_j[w\mathcal{T}]$ is the position of node j at PSP $w\mathcal{T}$. On the other hand, as before, when parentheses (.) are used, we are referring to the positions evaluated during the iterations of Algorithm 2, e.g., $\tilde{\mathbf{p}}_j(k)$ refers to the estimated position in the kth step of Algorithm 2 in Table 3.1.

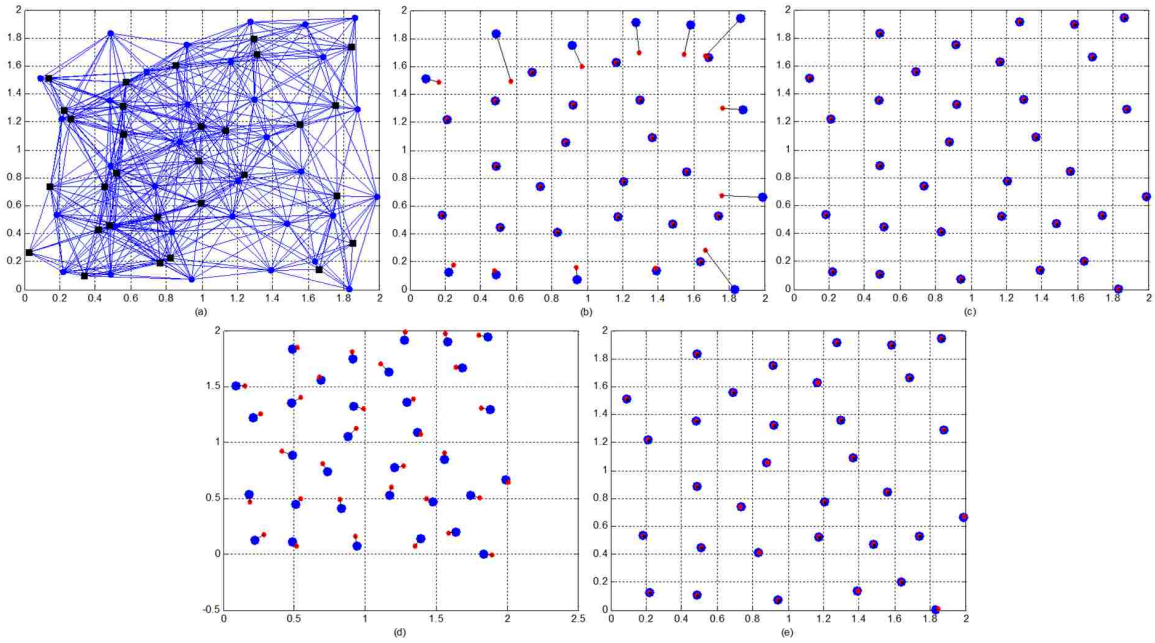

FIGURE 3.9. (a) The Network topology. (b) Localization results using relaxation and SOCP. (c) Localization results using SDP. (d) Localization results using SA. (e) Localization results using the proposed DRGD.

$\theta_{max}, \zeta_i(w) + \theta_{max}]$, and where $\theta_{max} \in [0, \pi)$. This implies that the position of node i at time $(w+1)\mathcal{T}$ is given by

$$\mathbf{p}_i[(w+1)\mathcal{T}] = \begin{cases} \mathbf{p}_i[w\mathcal{T}] & , i \notin \mathcal{N}_{\mathcal{M}} \\ \mathbf{p}_i[w\mathcal{T}] + L\mathbf{u}(w\mathcal{T}) & , i \in \mathcal{N}_{\mathcal{M}} \end{cases} \tag{3.37}$$

The mobility model described above is often referred to as the *random walk model* [77], and for small values of $\mathcal{T}$, where the traveled distance L is small compared to the dimensions of the sensor field, it is a good model.

3.2.2 Modification of DRGD for Mobile Sensors

With the mobility model of Section of Mobility Model, we modify DRGD (in Table 3.1) as follows. Note that the algorithm is now only run for the nodes in the set $\mathcal{N}_{\mathcal{M}}$ with all the other nodes treated as anchors. Suppose we wish to compute the new positions of the nodes $j \in \mathcal{N}_{\mathcal{M}}$ at time $w\mathcal{T}$. Denote by $\tilde{\mathbf{p}}_j[(w-1)\mathcal{T}]$ the position that DRGD has evaluated for node j at time $(w-1)\mathcal{T}$. The algorithm

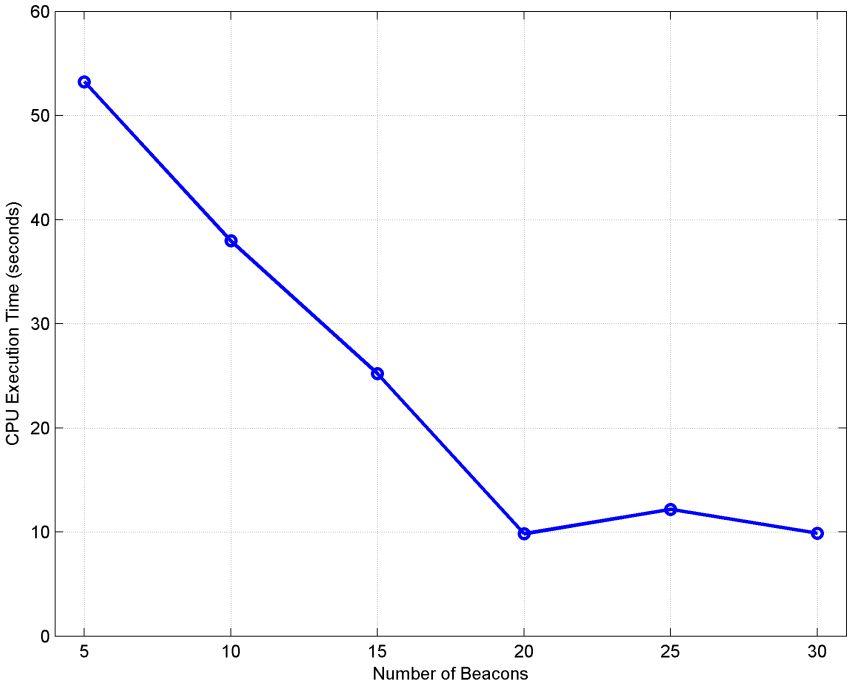

FIGURE 3.10. CPU execution time-to-convergence vs. the number of anchors using DRGD.

stores the last two positions, namely $\tilde{\mathbf{p}}_j[(w-1)\mathcal{T}]$ and $\tilde{\mathbf{p}}_j[(w-2)\mathcal{T}]$ that it has evaluated for each node j. DRGD now computes the unit vector

$$\hat{\mathbf{u}}_j((w-1)\mathcal{T}) = \frac{\tilde{\mathbf{p}}_j[(w-1)\mathcal{T}] - \tilde{\mathbf{p}}_j[(w-2)\mathcal{T}]}{\|\tilde{\mathbf{p}}_j[(w-1)\mathcal{T}] - \tilde{\mathbf{p}}_j[(w-2)\mathcal{T}]\|} \tag{3.38}$$

which represents an estimate of the direction of travel of node j in the interval $[(w-2)\mathcal{T}, (w-1)\mathcal{T}]$. To estimate the new positions $\tilde{\mathbf{p}}_j[w\mathcal{T}]$, $j \in \mathcal{N}_{\mathcal{M}}$, at time $w\mathcal{T}$, the initial positions $\hat{\mathbf{p}}_j(0)$ in Table 3.1 are set as follows.

$$\hat{\mathbf{p}}_j(0) = \tilde{\mathbf{p}}_j[(w-1)\mathcal{T}] + 0.5L_{max}\hat{\mathbf{u}}((w-1)\mathcal{T}) \tag{3.39}$$

In other words, using the two previously estimated positions for each node and the mobility model, an estimate of the current position is computed from (3.39) and used as the initial setting for Algorithm 2. The algorithm is now run until convergence is achieved. Figure 3.11 shows the mobility model and the initial position of node j given by (3.39). If the estimated positions $\tilde{\mathbf{p}}_j[(w-1)\mathcal{T}]$ and

$\tilde{\mathbf{p}}_j[(w-2)\mathcal{T}]$ are the true positions of node j, then the shaded area represents the set of possible positions of node j at $w\mathcal{T}$.

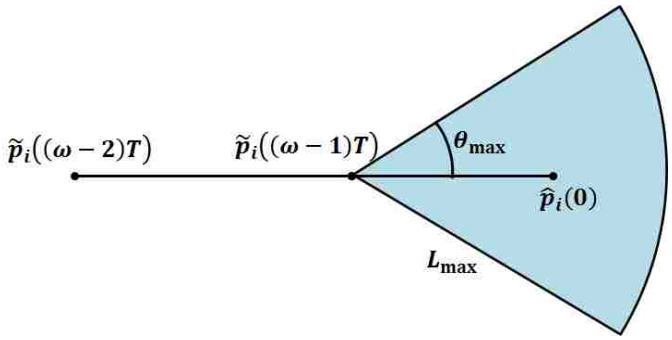

FIGURE 3.11. Depiction of the mobility model and the initial position assumed in Table 3.1 for the blind nodes.

In order to improve the convergence rate of DRDG, Eq. (3.35) is used within each iteration of Algorithm 2.

In the case of error-free measurements Ω_F can be chosen as the shaded area in Figure 3.11. This is justified by the fact that in this case the positions estimated by DRGD converge to the true positions of the nodes. Therefore, in view of our mobility model, it is guaranteed that at time $w\mathcal{T}$, node j is located in the shaded area. In case the measurements are not error-free, the shaded area must be enlarged, according to the variance of the measurement errors, to ensure that it includes the true position of the nodes.

3.2.3 Simulation Results

Simulation results are obtained for the network depicted in Figure 3.12 which consists of 50 blind nodes and 6 anchor nodes.The large number of nodes ensures that, as the nodes travel, the network remains globally rigid (uniquely localizable) and that the nodes have at least four neighbors to enable localization using DRGD. The radio range of the nodes is assumed to be $R_r = 0.7$ and the distance measurements are assumed to be error-free. We assume that all the blind nodes are mobile

and each node travels a total of 15 PSPs during the simulations. The anchors are assumed to be stationary.

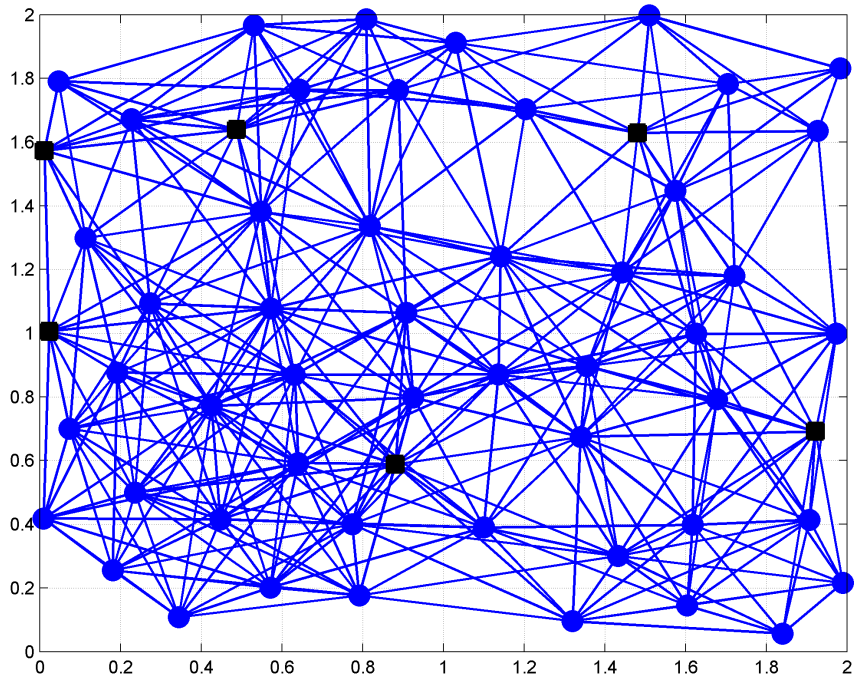

FIGURE 3.12. Topology of the network with the initial position of the blind and anchor nodes.

Figures 3.13 and 3.14 show a one-step movement of the blind nodes, where $\mathcal{T} = 1$ and $\theta_{max} = \pi/2$. For Figure 3.13 we set $V_{\max} = 0.1$ and for Figure 3.14, $V_{\max} = 0.7$. The actual starting and final positions of the nodes are shown by circles and squares, respectively. The cross shows the initial position assumed for each node according to (3.39) and + shows the estimated position. It can be seen that in both cases the algorithm converges to the correct position of the nodes.

Figures 3.15-a and 3.15-b show the trajectories of nodes $1-25$ and $26-50$, respectively, for 15 PSPs for $V_{\max} = 0.1$. The actual positions of the nodes are shown in blue circles while the estimated positions using the modified DRGD (with (3.35) and (3.39)) are shown as red crosses. Figure 3.16 shows the same results (3.16-a for nodes $1-13$, 3.16-b for nodes $14-26$, 3.16-c for nodes $27-38$, 3.16-d for

nodes $39-50$) for $V_{\max} = 0.7$. It can be seen that the algorithm accurately localizes all the mobile nodes in both cases. To provide a concrete example, consider a network deployed outdoors with the sensors having a radio range of 70 meters. Since for this example R_r was chosen to be 0.7 units, this implies that a unit corresponds to 100 meters. Therefore $V_{\max} = 0.1$ corresponds to a maximum velocity of 10 m/s or 36 km/h. On the other hand, $V_{\max} = 0.7$, chosen in Figure 3.14, corresponds to a maximum velocity of 70 m/s or 252 km/h. Although this velocity is too high for most applications, it is chosen to show the efficacy of the proposed algorithm in localizing mobile WSNs as verified by the results in Figures 3.13-3.16.

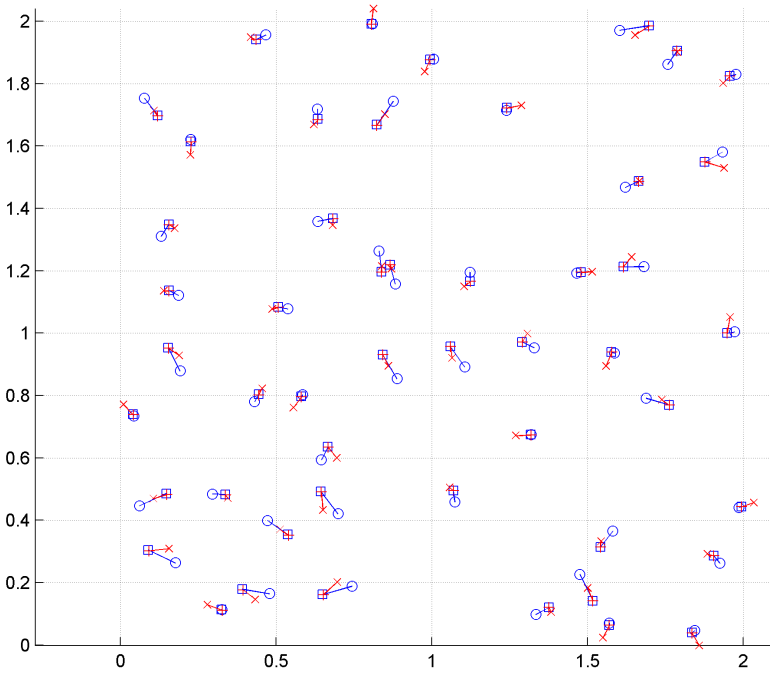

FIGURE 3.13. One-step movement of the blind nodes. Actual starting and final positions are shown by circles and squares, respectively, along with the initial position (cross) assumed for each node according to (3.39) and the final estimated position from the algorithm (+ sign) for $V_{\max} = 0.1$.

Remark 6. *Our simulation results verify that the proposed algorithm is very efficient in localizing mobile sensors. This is not surprising given the structure of the proposed algorithm. Suppose the network has been localized in its starting position.*

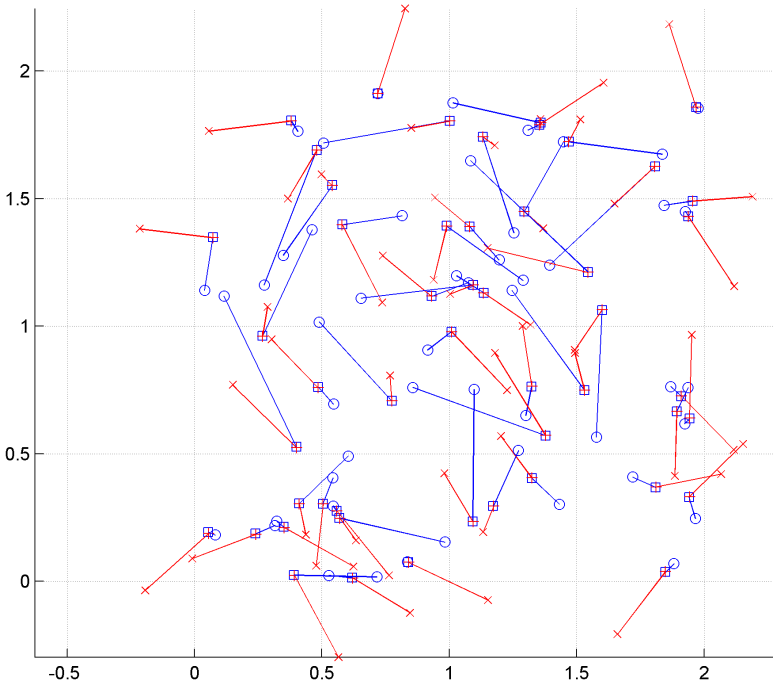

FIGURE 3.14. One-step movement of the blind nodes. Actual starting and final positions are shown by circles and squares, respectively, along with the initial position (cross) assumed for each node according to (3.39) and the final estimated position from the algorithm (+ sign) for $V_{\max} = 0.7$.

Now if the distance traveled by the nodes during the next PSP is small, it is likely that the next position vector resides in the attraction basin of the starting position. Therefore in this case, the gradient descent algorithm converges quickly and the new positions of the nodes are obtained. As the nodes travel, in some cases the new position vector does not belong to the attraction basin of the previous position. However, even in this case the algorithm converges quickly due to the fact that the next position of each node is contained in the small shaded area in Figure 3.11 and a good initial position vector is selected for the algorithm.

3.3 Centralized Node Localization in WSN with Outlier Communication Links

Due to interference or unreliable methods for distance measurement (for example using Receive Signal Strength (RSS) [44, 78]), the distances $\{d_{ij}\}$ may not

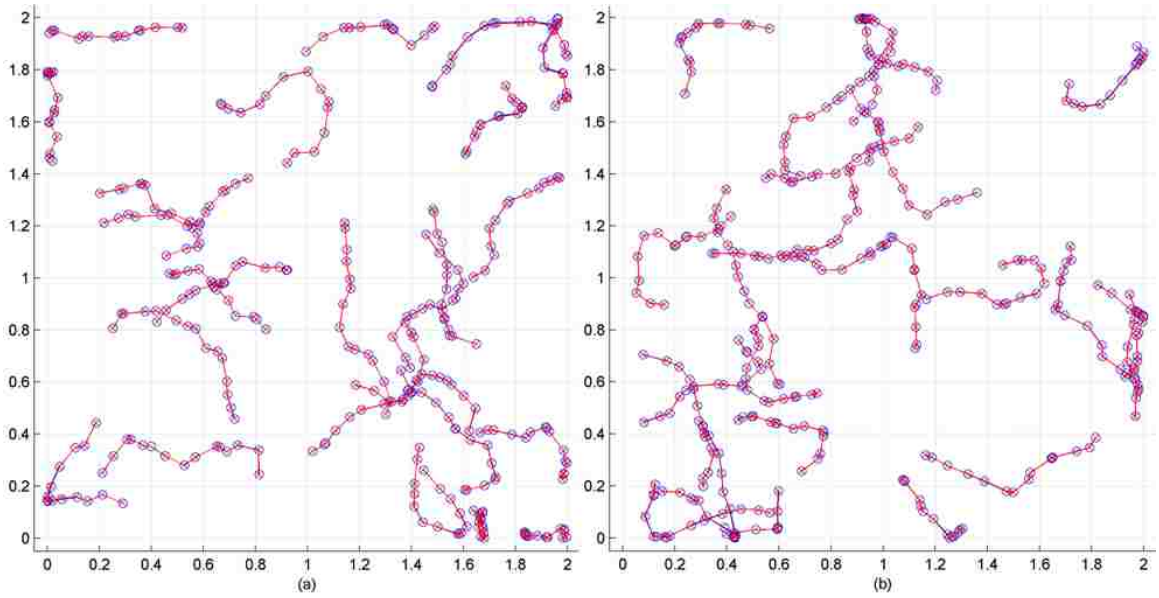

FIGURE 3.15. Trajectories of the blind nodes (blue circles) and the estimated trajectories (red crosses) using the modified DRGD algorithm, $V_{\max} = 0.1$.

correspond to the exact distance between nodes, or they may not be close to $\{\hat{d}_{ij}\}$ following certain distribution as stated in (3.26). Therefore, these measurements can be considered as outliers.

Now, we consider a centralized localization algorithm of nodes in WSNs in presence of outlier communication links. We follow the same notation used in Section 3.1.

It is assumed that each node is capable of estimating its distance to any of its neighbors. For example each node i, using a known transmit power sends a signal to all its neighbors in the set $\mathbb{G}_i \bigcup \mathbb{H}_i$. The neighbors can measure the RSS and using the appropriate channel path loss model estimate their distances to node i.

In order to localize the blind the sensor nodes, all the sensors transmit their distances to their neighbors to a Fusion Center (FC) which implements the localization algorithm. Let $d_{ij} = \|\mathbf{p}_i - \mathbf{p}_j\|$ denote the distance between nodes i and j, for $i, j = 1, 2, \cdots, M$. Note, however that, d_{ij} may be equal to the true distance between the nodes i and j, or it may it be an outlier or a falsified value. It is

assumed that if node i is falsifying its distance $d_{i,j}$ to its neighbor j, then it also ensures that $d_{j,i} = d_{i,j}$ so that the FC cannot detect the falsification by comparing the two distances reported by i and j.

The FC uses the received distance profile $\{d_{i,j}\}$ along with the position of the anchor nodes (which is assumed to be known at the FC) to estimate the position of all the blind nodes. In the absence of distance spoofing or outliers, the localization problem is to determine the positions $\{\mathbf{p}_i\}_{i=1}^n$ such that all the pairwise distance relations are satisfied. In the next section we present a localization algorithm which is robust to distance outliers/spoofing.

The implementation of distributed localization in presence of outlier distances is possible, and very similar to the algorithm described in Section 3.1. The main concern about this implementation is the time at which the distributed algorithm converges, which may increase considerably. This increasing localization time is due to the fact that we need to include the use of consensus algorithm for a distributed localization. Additionally, we need to consider the extra information shared by the nodes (such the reliability weights), and algorithms to reach a consensus about their values.

We define the following cost function:

$$\begin{aligned} F(\underline{\mathbf{p}}, \{w_{ij}\}_{(i,j)\in\mathcal{E}\cup\mathcal{F}}) &= \tfrac{1}{2}\sum_{(i,j)\in\mathcal{E}} \omega_{ij}^2 \left(\|\mathbf{p}_i - \mathbf{p}_j\| - d_{ij}\right)^2 \\ &\quad + \tfrac{1}{2}\sum_{(i,j)\in\mathcal{F}} \omega_{ij}^2 \left(\|\mathbf{p}_i - \mathbf{a}_j\| - d_{ij}\right)^2, \end{aligned} \tag{3.40}$$

where $\underline{\mathbf{p}} = \left[\mathbf{p}_1^T, \ldots, \mathbf{p}_n^T\right]^T$, and ω_{ij} is the weight associated with the distance $d_{i,j}$ (edge (i,j)).In order to deal with the uncertainties of the distance profile, we associate with each reported distance $d_{i,j}$, $(i,j) \in \mathcal{E}\cup \in \mathcal{F}$, a positive weight $\omega_{ij} \in [0,1]$. $\omega_{ij} = 0$ implies that the distance $d_{i,j}$ is completely unreliable. In this case the term corresponding to $d_{i,j}$ as well as the positions $\mathbf{p}_i, \mathbf{p}_j$ are eliminated

from the cost function. Ont he other hand $\omega_{ij} = 1$ implies that the distance $d_{i,j}$ is completely reliable. Also, it is assumed that the anchor nodes are secure and the distance information that they provide is completely reliable, i.e., for all $i, j \in \mathcal{F}$, $\omega_{ij} = 1$.

The function $F(\underline{\mathbf{p}}, \{w_{ij}\}_{(i,j)\in\mathcal{E}\cup\mathcal{F}})$ is a continuous and positive function. Moreover, in absence of outlier distances $F(\underline{\mathbf{p}}^*, \{w_{ij}\}_{(i,j)\in\mathcal{E}\cup\mathcal{F}}) = 0$, $\forall\omega_{ij} \in \mathcal{E}\cup\mathcal{F}$, where $\underline{\mathbf{p}}^*$ is the real position of the nodes. Furthermore, if $\omega_{ij} = 0$ for outliers and $\omega_{ij} > 0$ for reliable edges, then $\underline{\mathbf{p}}^*$ is the unique global minimum of $F(\underline{\mathbf{p}}, \{w_{ij}\}_{(i,j)\in\mathcal{E}\cup\mathcal{F}})$ with $F(\underline{\mathbf{p}}^*, \{w_{ij}\}_{(i,j)\in\mathcal{E}\cup\mathcal{F}}) = 0$. Thus, there may be several minimums at which the cost function (3.40) is equal to zero.

The localization problem can now be stated as a constraint optimization problem as follows:

$$\begin{aligned} \min_{\{\underline{\mathbf{p}}\},\{\omega_{ij}\}_{(i,j)\in\mathcal{E}\cup\mathcal{F}}} \quad & F(\underline{\mathbf{p}}, \{w_{ij}\}_{(i,j)\in\mathcal{E}\cup\mathcal{F}}) \\ \text{s.t.} \quad & \sum_{j\in\mathbb{G}_i\cup\mathbb{H}_i} \omega_{ij}^2 \geq K, \forall i \in \{1, \cdots, n\} \\ & \omega_{ij}^2 \leq 1, \forall (i,j) \in \mathcal{E}\cup\mathcal{F}, \end{aligned} \tag{3.41}$$

where $K \in \mathbb{N}$ is parameter to be selected. For each node i, the value of K determines the minimum number of reliable distances that the algorithm must consider in evaluating the positions. Therefore we must select $K \geq 3$. The second constraint is intended to avoid cases in which one edge alone would satisfy the first constraint.

Several approaches have been proposed in to solve constraint optimization problems as in (3.41), [79]. The most prominent is the Lagrange multipliers method. However, for large WSNs, the number of variables increases significantly. Therefore, although mathematically appealing, the complexity of this approach becomes prohibitive Another approach for solving the constraint optimization problem uses the penalty function described in [80]. An advantage of this method over methods

proposed in [79] is the fact the number of variables is lower, thereby reducing the computational cost.

We define the penalty function as follows:

$$\begin{aligned}\mathcal{L}(A,B) &= \tfrac{1}{2}\sum_{(i,j)\in\mathcal{A}}\omega_{ij}^2\left(\|\mathbf{p}_i-\mathbf{p}_j\|-d_{ij}\right)^2 \\ &\quad+\tfrac{1}{2}\sum_{(i,j)\in\mathcal{B}}\omega_{ij}^2\left(\|\mathbf{p}_i-\mathbf{a}_j\|-d_{ij}\right)^2 \\ &\quad+c\sum_{i=1}^{n}\left[\max\left(0,K-\sum_{j\in\mathbb{G}_i\cup\mathbb{H}_i}\omega_{ij}^2\right)\right]^2 \\ &\quad+c\sum_{(i,j)\in\mathcal{A}\cup\mathcal{B}}\left(\max(0,\omega_{ij}^2-1)\right)^2,\end{aligned} \tag{3.42}$$

where c is a parameter of the optimization algorithm, and $A\subseteq\mathcal{E}$ and $B\subseteq\mathcal{F}$ In the following we would like to minimize the penalty function in (3.42) with respect to the unknown positions $\{\mathbf{p}_i\}$ and the weights $\{\omega_{i,j}\}$. In this way we have converted the "hard" constraints in (3.41) to "soft" constraints in (3.42).

Let $A_i\subset\mathbb{G}_i$ and $B_i\subset\mathbb{H}_i$. The gradient of the penalty function $\mathcal{L}(A,B)$ with respect to the position $\mathbf{p}_i$ be defined as follows:

$$\begin{aligned}\nabla_{\mathbf{p}_i}\mathcal{L}(A_i,B_i) &= \sum_{j\in A_i}\omega_{ij}^2(\|\mathbf{p}_i-\mathbf{p}_j\|-d_{ij})\frac{(\mathbf{p}_i-\mathbf{p}_j)}{\|\mathbf{p}_i-\mathbf{p}_j\|} \\ &\quad+\sum_{j\in B_i}\omega_{ij}^2(\|\mathbf{p}_i-\mathbf{a}_j\|-d_{ij})\frac{(\mathbf{p}_i-\mathbf{a}_j)}{\|\mathbf{p}_i-\mathbf{a}_j\|},\end{aligned} \tag{3.43}$$

The gradient with respect to the weight $\omega_{ij}\in\mathcal{E}$ is defined as follows:

$$\begin{aligned}\nabla_{\omega_{ij}}\mathcal{L}(\mathcal{E},\mathcal{F}) &= \omega_{ij}(\|\tilde{\mathbf{p}}_i-\tilde{\mathbf{p}}_j\|-d_{ij})^2 \\ &\quad+4c\omega_{ij}\max(0,\omega_{ij}^2-1) \\ &\quad-4c\omega_{ij}\max\left(0,K-\sum_{k\in\mathcal{A}_i\cup\mathbb{H}_i}\omega_{ik}^2\right) \\ &\quad-4c\omega_{ij}\max\left(0,K-\sum_{l\in\mathcal{A}_j\cup\mathbb{H}_j}\omega_{lj}^2\right),\end{aligned} \tag{3.44}$$

Based on the algorithms described in [80] and the use of algorithm described Table 3.1, the algorithm to find the position of the blind nodes is described in

Table 3.3. The steps in this table are described as follows. The first step sets all the initial parameters of the algorithm. Using the optimization algorithm based on penalty function from [80], Step 2 finds a (local) minimum of the penalty function (3.42). It is pointed out that the Step 2 in Table 3.3 is the Gradient Descent Algorithm.

After the minimum has been reached, Step 3 checks the constraints of (3.41). If the constraints are not satisfied, then increase the penalty term c of the penalty function (3.42), and go back to Step 2 to find a new minimum.

In case that the constraints have been satisfied in Step 3, then it checks is the cost function (3.40) has reached a global minimum, at which the position of the nodes have been estimated. Otherwise, it goes to Step 4 to scape the local minimum following similar algorithm from Table 3.1.

Notice that the gradients (3.43) and (3.44) are zero at the solution of problem (3.41), which is the real position of the blind nodes and with weights equal to zero for outlier edges. Thus, the global minimums from (3.41) are absorbing states, similarly to 3.1. Thus, same arguments establish convergence to the real position of the blind nodes with probability one.

Another important issue to mention is the procedure to identify a minimum of (3.41), which is computationally time consuming. In order to verify that a minima or local minimum have been reached, variables υ and ι are used for such purposes, respectively, as it is described in Table 3.3.

Additionally, it is remarked that satisfying all the constraints from (3.41) is computationally time consuming and depending on the selected parameters of the algorithm in [80] they may not be satisfied rigorously. In order to avoid this issue, we incorporate a counter ν in order to check the number of times at which a minimum of (3.42) is reached, while all the constraints are not satisfied. Once this

counter ν has reached a threshold Φ, then algorithm considers this minimum as valid and will attempt to scape from it. This procedure is also included in Table 3.3.

Notice that eq. (3.43) is not defined if $\tilde{\mathbf{p}}_i(l) = \tilde{\mathbf{p}}_j(l)$. In order to deal with this fact, due to the positions of the sensor nodes are different, in case that the positions $\tilde{\mathbf{p}}_i(l)$ and $\tilde{\mathbf{p}}_j(l)$ are the same during the optimization algorithm, it is possible to deviate the position of one of them in order to avoid the mentioned issue.

3.3.1 Simulation Results

In order to ensure that THE unique localizability condition in [38, 41] is satisfied, the networks considered in this dissertation are assumed to be densely connected. This requirement is needed due to the fact that the position of the nodes must be estimated in the presence of unreliable distance reports. If this requirement is not satisfied, the network without the outliers distances measurements may not be localizable [16] or may not be even connected.

In this Section the algorithm described in Table 3.3 is implemented. The parameters used in Table 3.3 and (3.41) are $K = 8$, $c_0 = 0.5$, $\eta = 3$, $\Phi = 10$, $\iota = 10^{-3}$. The random variables $\Lambda_i(k)$ and $\Lambda_{ij}(k)$ are chosen from a Gaussian distribution with zero mean and unit variance, for the same reasons explained in Section 3.1.

The first network considered is shown in Figure 3.17. The network has 20 blind nodes (blue circles) and 3 anchor nodes (in black square). The radio range is equal to 4.5 units, ensuring that each node has at least 10 neighbors. The number of outlier distances is equal to 8, and no error is considered in the non-outlier distance measurements. For this case $\nu = 0.1$. The outlier distances were set in such a way as to be 5 times higher than the true distance. Figure 3.18 shows the real position of the blind nodes (blue circle), the estimated position of the blind nodes (red cross) and the edges considered non-outliers (blue links). Figure 3.19

TABLE 3.3. Localization Algorithm in Presence of Outlier Edges

1- **Initialization**

Choose initial position $\hat{\underline{\mathbf{p}}}(0)$

Choose initial weights $\{\hat{\omega}_{ij}(0)\}_{(i,j)\in\mathcal{E}}$ not satisfying all constraints.

Choose initial $c = c_0 < 1$. Set $k = 0$, and $\nu = 0$. Go to Step 2.

2- **Find minimum of Penalty Function $\mathcal{L}$**

Set $l = 0$, $\tilde{\underline{\mathbf{p}}}(0) = \hat{\underline{\mathbf{p}}}(k)$, $\tilde{\omega}_{ij}(0) = \hat{\omega}_{ij}(k)$.

Do

Estimate $\tilde{\alpha}_l$ via Armijo Algorithm [79].

$\forall i \in \{1, \ldots, n\}$, do:

$\tilde{\mathbf{p}}_i(l+1) = \tilde{\mathbf{p}}_i(l) - \tilde{\alpha}_l \nabla_{\mathbf{p}_i} \mathcal{L}(\mathcal{E}, \mathcal{F})$

$\forall (i,j) \in \mathcal{E}$, do:

$\tilde{\omega}_{ij}(l+1) = \tilde{\omega}_{ij}(l) - \tilde{\alpha}_l \nabla_{\omega_{ij}} \mathcal{L}(\mathcal{E}, \mathcal{F})$

$l = l + 1$

Set: $\mathbf{P}(s) = [\tilde{\underline{\mathbf{p}}}(s), \{\omega_{ij}(s)\}_{(i,j)\in\mathcal{E}}]$, with $s \in \{l, (l-1)\}$

While $(\mathbf{P}(l) - \mathbf{P}(l-1)\| > \iota)$

$k = k + 1$

$\underline{\mathbf{p}}(k) = \tilde{\underline{\mathbf{p}}}(l)$, $\omega_{ij}(k) = \tilde{\omega}_{ij}(l)$, $\forall (i,j) \in \mathcal{E}$

Go to Step 3.

3- **Check that constraints are satisfied.**

If all constraints are satisfied:

If $F(\underline{\mathbf{p}}(k), \{w_{ij}(k)\}_{(i,j)\in\mathcal{E}\cup\mathcal{F}}) \leq \upsilon$:

Estimated position of the nodes $\underline{\mathbf{p}}(k)$,

with link weights $\{w_{ij}(k)\}_{(i,j)\in\mathcal{E}\cup\mathcal{F}}$

Else

Go to Step 4.

End If

Else

If $(\nu \leq \Phi)$

Set $c = \eta c$ and $\nu = \nu + 1$. Go to Step 2.

Else

$\nu = 0$. Go to step 4.

End If

End If

4- **Escaping the Local Minimum**

$\forall i \in \{1, \ldots, n\}$, $\forall (i,j) \in \mathcal{E}$ do:

Randomly choose a subset $\mathcal{A}_i \subset \mathbb{G}_i$, $\mathcal{A}_j \subset \mathbb{G}_j$

Randomly choose $\Lambda_i(k)$ and $\Lambda_{ij}(k)$

$\forall i \in \{1, \ldots, n\}$, do:

$\hat{\mathbf{p}}_i(k) = \mathbf{p}_i(k) - \Lambda_i(k) \nabla_{\mathbf{p}_i} \mathcal{L}(A_i, \mathbb{H}_i)$

$\forall (i,j) \in \mathcal{E}$, do:

$\hat{\omega}_{ij}(k) = \omega_{ij}(k) - \Lambda_{\omega_{ij}}(k) \nabla_{ij} \mathcal{L}(\mathcal{E}, \mathcal{F})$

Set $c = c_0$. Go to Step 2.

shows the real position of the blind nodes (blue circle), the estimated position of the blind nodes (red cross), the edges considered outliers (in black links), and the true outlier edges (red links).

We now consider the network topology shown in Figure 3.20, keeping the same number of nodes and radio range of the network from Figure 3.17. The number of outlier links was increased to 10, with $\nu = 0.01$. Figures 3.21 and 3.22 show the similar information than Figures 3.18 and 3.19, respectively.

Simulation results in Figures 3.18 and 3.21 show that the proposed algorithm correctly estimates the position of the nodes in the presence of outlier links. On the other hand, it is possible to observe that some nodes do not satisfy the first constraint of (3.41), which is due to the optimization procedure as it was pointed out before.

Although the algorithm is capable to assign a weight equal to zero to the outlier edges, it also considers as outliers some links with correct distance. This fact is possible to observe in Figures 3.19 and 3.22. Therefore, even though the algorithm is capable of estimating the position of the nodes correctly, it is not able to identify the true outlier links.

The value of K is very important as it is possible to observe in the simulations. In some cases, for some nodes the algorithm considers the number of non-outliers edges lower than K. Thus, if the value of K is very low, then there exists a chance that the algorithm would tend to estimate the position of the node of a network not satisfying the conditions in [16] for localizability.

It was mentioned that a similar analysis to Section 3.1 could be stated in case of distances following certain distribution with mean equal to the real distances between nodes. Based on the simulation results, the upper bound for the expected minimum value of the cost function (3.40) may not be straight forward to establish

since the number of edge considered non-outlier is not predicted by the algorithm, as it can be observed in Figures 3.18 and 3.21. An alternative to address this issue is considering all the edges (outliers and non-outliers) to determine the upper bound. Anyway, based on the localization algorithm described in Table 3.3 and following the same reasoning from Section 3.1, the minimum of the problem (3.41) can be reached, estimating the position of the blind nodes with certain level of accuracy.

Simulation results in Figures 3.18 and 3.21 show that the proposed algorithm correctly estimates the position of the nodes in presence of outlier links. On the other hand, it is possible to observe that some nodes do not satisfy the first constraint of (3.41), which is due the numerical issue of the optimization process as it was pointed out before. Anyway, those Figures show that the network without the outlier communication links satisfy the conditions for localizability [16], meeting the purpose of the constraints.

Although the algorithm is capable to weight the outlier communication link with value equal to zero, it also considers outliers some links with correct distance estimations. This fact is possible to observe in Figures 3.19 and 3.22. Therefore, even though the algorithm is capable to estimate the position of the nodes correctly, it is not capable to identify the true outlier links.

The value of K is very important as it is possible to observe in the simulations. In some cases, for some nodes the algorithm considers the number of non-outliers communication links lower than K. Thus, If the value of K is very small, then there exists a chance that the algorithm would tend to estimate the position of the node of a network not satisfying the conditions in [16] for localizability.

It was mentioned that a similar analysis to Section 3.1 could be stated in case of distances following certain distribution with mean equal to the real distances between nodes. Based on the simulation results, the upper bound for the expected

minimum value of the cost function (3.40) may not be straight forward to establish since the number of communication link considered non-outlier is not predicted by the algorithm, as it can be observed in Figures 3.18 and 3.21. An alternative to address this issue is considering all the communication links (outliers and non-outliers) to determine the upper bound. Anyway, based on the localization algorithm described in Table 3.3 and following the same reasoning from Section 3.1, the minimum of the problem (3.41) can be reached, estimating the position of the blind nodes with certain level of accuracy, similarly to the results in Section 3.1.

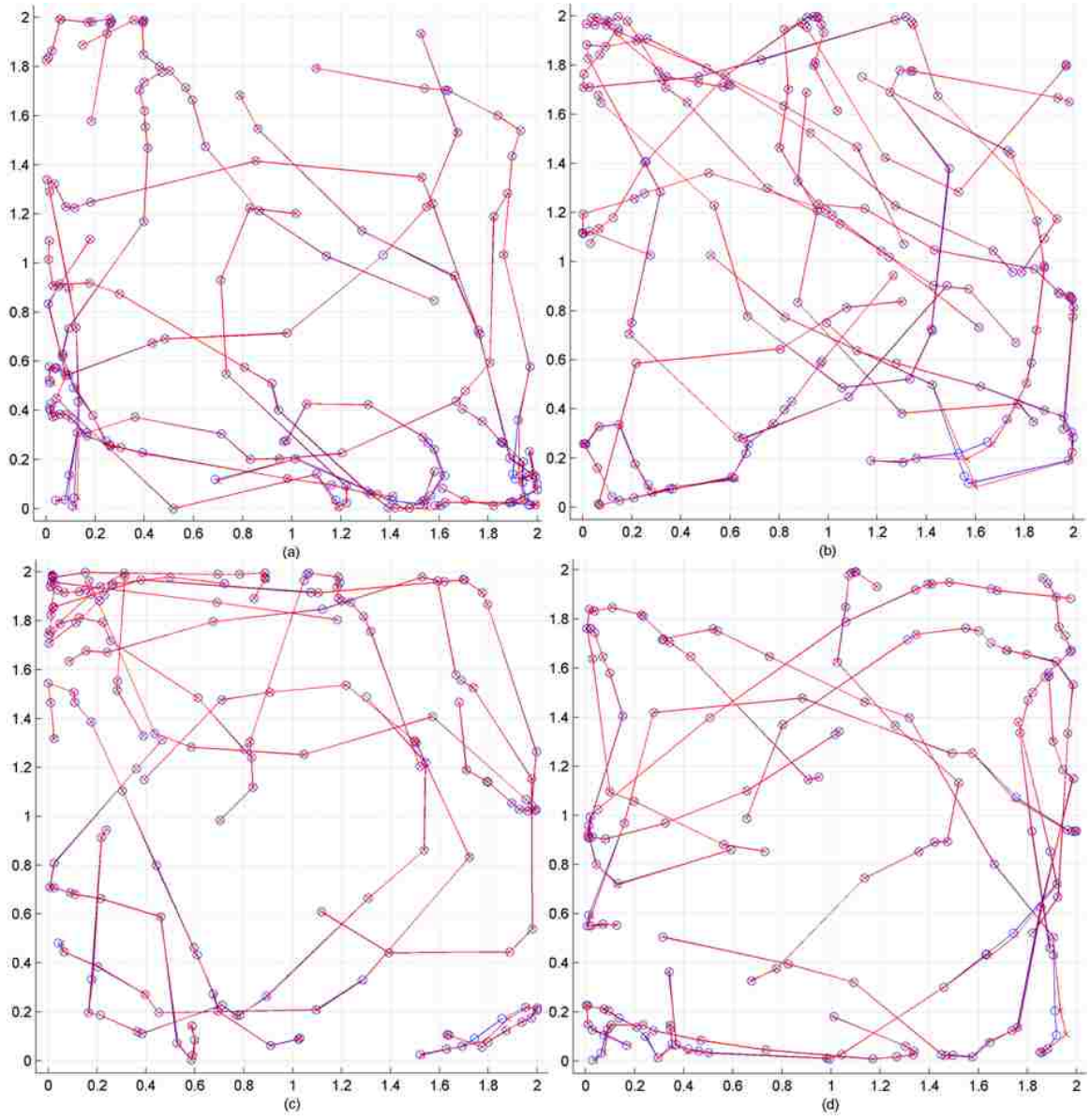

FIGURE 3.16. Trajectories of the blind nodes (blue circles) and the estimated trajectories (red crosses) using the modified DRGD algorithm, $V_{\max} = 0.7$.

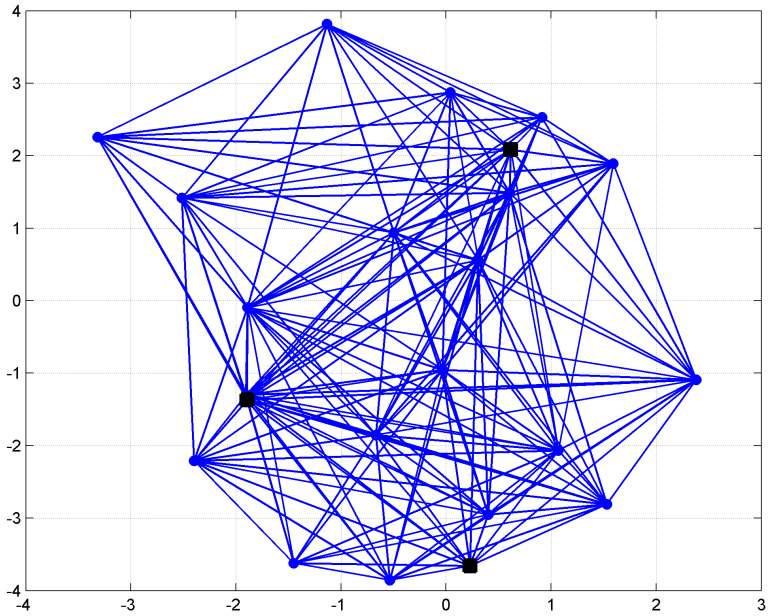

FIGURE 3.17. Topology of the sensor network, where blue links represent the edges, black squares correspond to anchor nodes, and blue circles correspond to blind nodes.

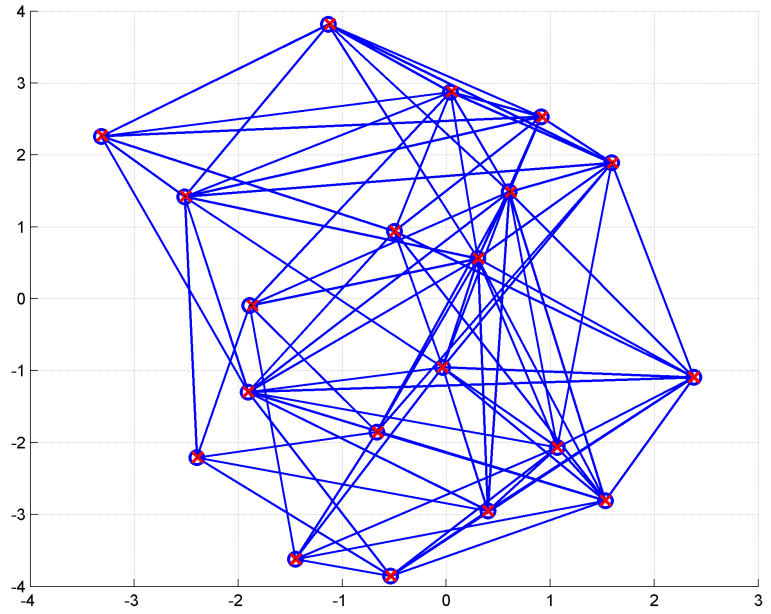

FIGURE 3.18. Real position of the blind nodes (blue circle), the estimated position of the blind nodes (red cross) and the communication links considered non-outliers (blue links)

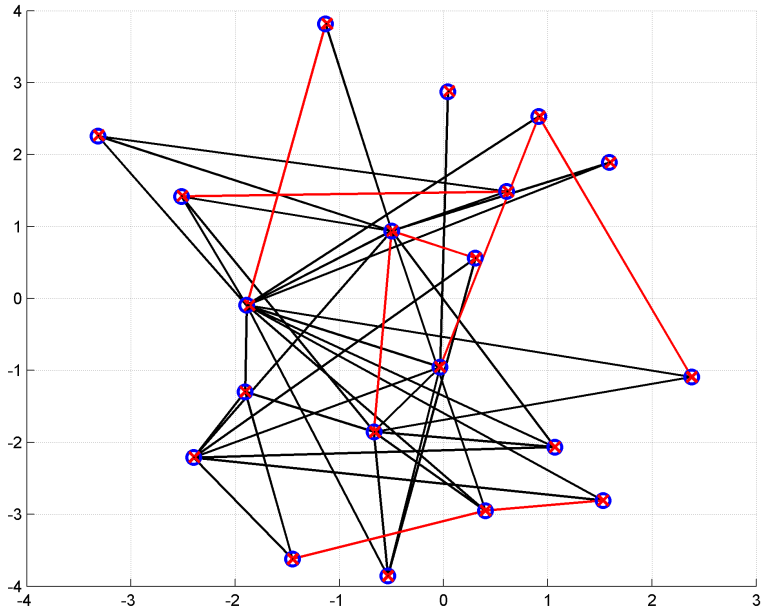

FIGURE 3.19. Real position of the blind nodes (blue circle), the estimated position of the blind nodes (red cross), the communication links considered outliers (in black links), and the true outlier communication links (red links)

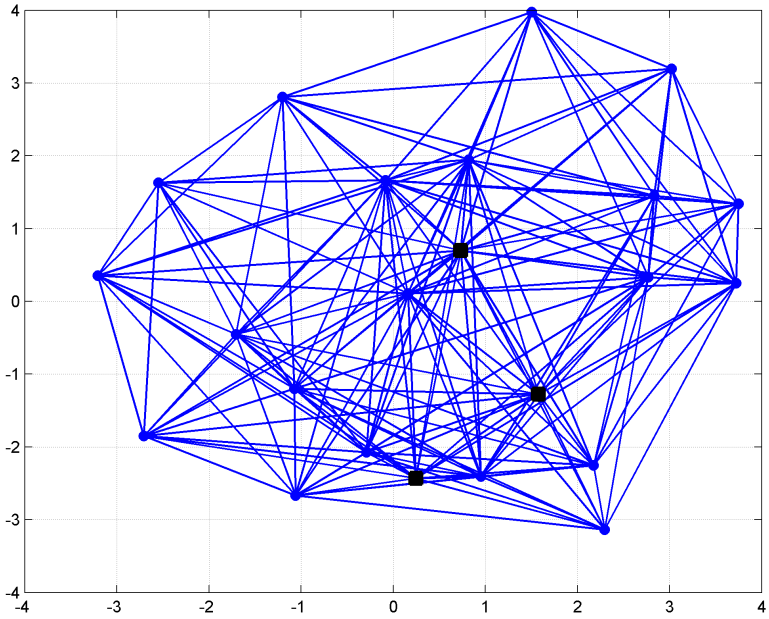

FIGURE 3.20. Topology of the sensor network, where blue links represent the edges, black squares correspond to anchor nodes, and blue circles correspond to blind nodes.

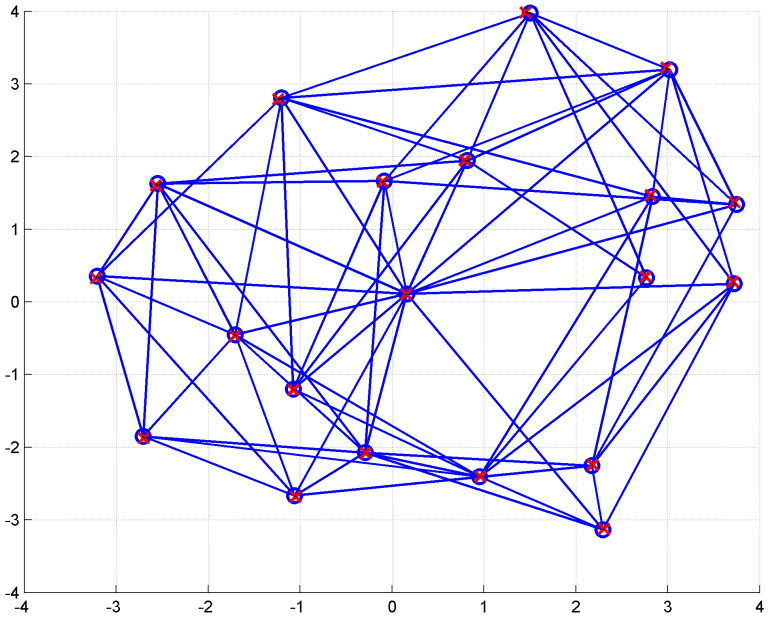

FIGURE 3.21. Real position of the blind nodes (blue circle), the estimated position of the blind nodes (red cross) and the communication links considered non-outliers (blue links)

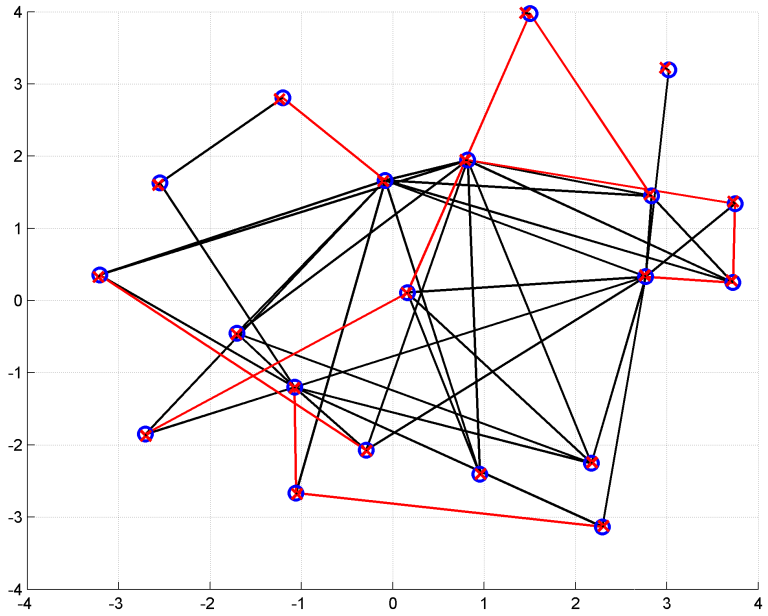

FIGURE 3.22. Real position of the blind nodes (blue circle), the estimated position of the blind nodes (red cross), the communication links considered outliers (in black links), and the true outlier communication links (red links)

Chapter 4
Conclusion

In this dissertation we present two approaches for localization of wireless devices. The algorithms are focused on systems were GPS is not available.

Firstly, we have studied the problem of localization based on narrowband signals of opportunity, and have developed a new positioning system reminiscent of GPS. This problem is important because narrowband signals are more resilient to multipath fading and are capable of penetrating common building structures, and in contrast to the wideband GPS signals. The drawback of narrowband signals lies in the difficulty in estimating TDOA, and in localizing the mobile receiver with accuracy comparable to that of GPS. Hence near optimum algorithms in the sense of MLE which are developed in this dissertation are crucial to the success of the proposed new positioning system. In fact the novelty of our proposed solution algorithms is highlighted by their excellent positioning error performance illustrated by the simulation example using the FM radio signals as an application platform. Our results demonstrate the applicability of the proposed positioning system and contribute to the existing research literature in this important field. Although our investigation has focused on narrowband signals, the results in this dissertation may have broader applications. Indeed future positioning systems will be of multi-platform, including both GPS and SOP, as well as wideband and narrowband signals. Our work presented in this dissertation provides the design algorithms for narrowband signals, and thus complements the known positioning systems available today.

While our theoretical results and simulation example are encouraging, it would be interesting to validate the proposed method as a practical positioning system. We hope to develop a prototype system in the future and to conduct the necessary field tests in order to demonstrate its viability. We believe that the novel positioning system proposed in this dissertation has great potential for applications in localizations when and where GPS is unavailable.

Next we considered range-based localization of nodes in a wireless sensor network (WSN). A distributed localization algorithm based on a novel randomization of the gradient descent method is proposed. The randomization method is tailored to and easy to implement in a WSN. It is proven that in the case of noise-free measurements and when the network is localizable, the algorithm converges and provides the true location of the nodes. In contrast to several recently proposed methods, the convergence of the algorithm does not require that the blind nodes be in the convex hull of the anchor nodes. In fact only a few anchor nodes are needed to ensure localizability of the network. Error bounds are obtained in the case of noisy distance measurements. The performance of the proposed algorithm is compared to two relaxation based methods, namely semi-definite programing (SDP) and second-order cone programing (SOCP), as well simulated annealing (SA) for several networks with and without distance errors. The results show that the proposed algorithm successfully localizes the nodes in all the cases whereas SOCP and SA fail in most of the cases. Furthermore, the computational requirements of the proposed algorithm is significantly lower than SOCP and SA. Finally the algorithm is applied for localization of mobile WSNs. Simulation results show the efficacy of the proposed algorithm in such applications.

We also extend our proposed method to localization of WSNs when some reported distances are outliers. This may arise due to the challenges of distance

measurement techniques. For example it is well known that distance estimations based on received signal strength in indoors can be highly unreliable due to multipath fading effects. Distance errors may also be due to mischief caused by an adversary who falsifies its reported distances.

Appendix A:
Proof and Discussion of Lemma 1

Without loss of generality, $\sigma^2 = 1$ and $\kappa_i > 0$ for each i are assumed. If it is not, Z_i/σ^2 can be regarded as new random variable with $|\kappa_i|/\sigma$ as the new κ_i. Hence the large ratio condition is translated into large κ_i for all i. By noting that $Z_i = (U_i - \kappa_i)^2 - (1 + \kappa_i^2)$, there holds

$$U_i = \kappa_i \pm \sqrt{Z_i + 1 + \kappa_i^2}, \qquad Z_i \geq -(1 + \kappa_i^2). \tag{4.1}$$

Since $\{U_i\}$ are jointly Gaussian distributed with mean 0 and covariance C, the random variables $\{Z_i\}$ admit joint PDF (probability density function)

$$f_Z(\{z_i\}) = \frac{\exp\left[-\frac{1}{2}\left(\underline{\kappa} - \underline{\phi}\right)' C^{-1}\left(\underline{\kappa} - \underline{\phi}\right)\right]}{\sqrt{[2\pi \det(C)]^{n-1}}\left(2^{n-1}\prod_{i=1}^{n-1}\phi_i\right)} + \cdots \tag{4.2}$$

with $\underline{\phi} = \sqrt{\underline{z} + \underline{1} + \underline{\kappa^2}}$ where $\underline{\phi}$, $\underline{z}$, $\underline{\kappa}$, $\underline{\kappa^2}$, and $\underline{1}$ are column vectors with ϕ_i, z_i, κ_i, κ_i^2, and 1 as the ith entry, respectively. By convention, square-root of a vector takes square-root of each entry. The joint PDF in (4.2) involves a summation of 2^{n-1} terms due to 2^{n-1} different $\pm$ signs in (4.1) for $1 \leq i < n$, but only the first term is shown. The $(n-1)$-integral of this first term can find to be

$$\mathcal{I}_1 = \int_{-\kappa_{n-1}}^{\infty} \cdots \int_{-\kappa_1}^{\infty} \frac{e^{-\frac{1}{2}\underline{y}' C^{-1}\underline{y}}}{\sqrt{[2\pi \det(C)]^{n-1}}}\, dy_1 \cdots dy_{n-1} \approx 1,$$

if $\kappa_i >> 1$ where $y_i = \sqrt{z_i + 1 + \kappa_i} - \kappa_i$ for $1 \leq i < n$. It follows that $f_Z(\{z_i\})$ is dominated by the first term under the condition of large κ_i in the case of $\sigma = 1$, or large ratio κ_i/σ in the case of $\sigma \neq 1$. It is also easy to see that $\mathrm{E}\{Z_i\} = 0$. In the case of $\sigma \neq 1$, the variance of Z_i is found to be

$$\sigma_{Z_i}^2 = \mathrm{E}\{|Z_i|^2\} = 2\sigma^2(2\kappa_i^2 + \sigma^2).$$

Thus $4\kappa_i^2\sigma^2$ dominates $\sigma_{Z_i}^2$ for large ratio of $\frac{|\kappa_i|}{\sigma}$. In the neighborhood of $z_i = -\sigma^2$, there holds

$$f_Z(z) \approx \frac{\exp\left[-\frac{1}{2}\left(\underline{z} + \underline{1}\sigma^2\right)'\left(D_\kappa C D_\kappa\right)^{-1}\left(\underline{z} + \underline{1}\sigma^2\right)\right]}{\sqrt{[2\pi \det(D_\kappa C D_\kappa)]^{n-1}}} \tag{4.3}$$

by $\kappa_i - \sqrt{z_i + \sigma^2 + \kappa_i^2} \approx -(z_i + \sigma^2)/2\kappa_i$, thereby concluding that Z admits an approximate joint Gaussian distribution in the neighborhood of $\underline{z} = -\underline{1}\sigma^2$. □

Although Lemma 1 states that $\{Z_i\}$ are approximately Gaussian distributed near $-\underline{1}\sigma^2$, it does not imply that its joint PDF peaks at $\underline{z} = -\underline{1}\sigma^2$. In fact it can be shown by straightforward calculation that the PDF of $\{Z_i\}$ peaks at $z_i = -3\sigma^2$ for $1 \leq i < n$. Figure 4.1 shows the approximate PDF of Z in the case of $n = 2$, given by

$$f_Z(z) \approx \frac{1}{\sqrt{2\pi\sigma^2}} \left\{ \frac{e^{-\frac{1}{2\sigma^2}\left(\kappa - \sqrt{z+(\sigma^2+\kappa^2)}\right)^2}}{2\sqrt{z + (\sigma^2 + \kappa^2)}} \right\} \tag{4.4}$$

in solid line and the PDF of Gaussian random variable with mean $-\sigma^2$ and variance $(2\kappa\sigma)^2$ in dashed line where $\kappa = 10\sigma$ is used. Therefore Z is approximately Gaussian not only in the neighborhood of $Z = -\sigma^2$ but in a much greater interval. We comment that the approximate PDF of Z and the exact of PDF of Z are indistinguishable for the case $\kappa \geq 10\sigma$.

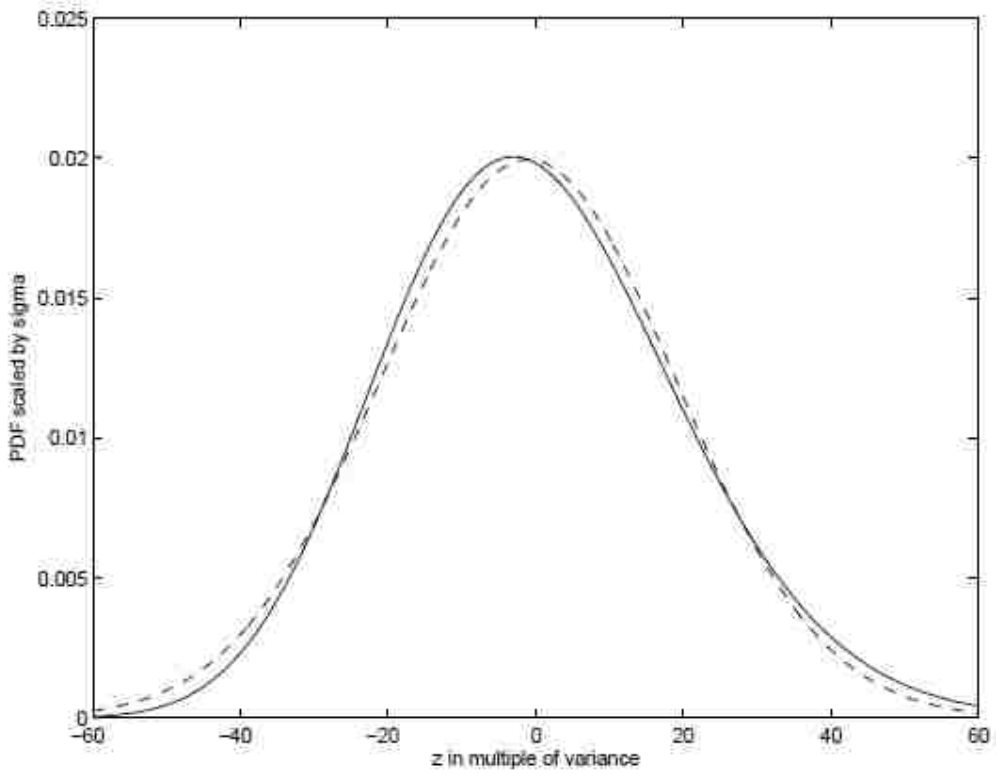

FIGURE 4.1. PDF $f_Z(z)$ versus Gaussian PDF with x-axis scaled by σ^{-1}, y-axis by σ, and $\kappa = 10\sigma$.

Appendix B: CRLB and MLE for Localization using TDOA

For localization based on SOP, the associated MLE and CRLB have some subtle differences from those based on other signals such as GPS. Recall the difference of TDOA in (2.7) where $v_{i,1} = v_i - v_1$ with $\{v_i\}_{i=1}^n$ i.i.d. Gaussian of mean zero and variance σ_v^2. Hence its joint PDF $f_{V_{i,1}}\left(\left\{\widehat{\delta}t_{i,1} - \delta_{i,1}\right\}_{i=2}^n\right)$ is given by

$$f_{V_{i,1}}(\cdots) = \frac{\exp\left[-\frac{1}{2\sigma_v^2}\left(\underline{\widehat{\delta}_d} - \underline{\delta_d}\right)' C_0^{-1}\left(\underline{\widehat{\delta}_d} - \underline{\delta_d}\right)\right]}{\sqrt{[2\pi \det(C_0)]^{n-1}}\sigma_v^{n-1}} \tag{4.5}$$

where $\underline{\widehat{\delta}_d}$ and $\underline{\delta_d}$ are column vectors of size $(n-1)$ with $\widehat{\delta}t_{i+1,1}$ and $\delta_{i+1,1}$ as the ith element, respectively, and C_0 is specified in (2.8). Recall $v_{i,1} = \widehat{\delta}_{i,1} - \delta_{i,1}$. Since $\{\delta_{i+1,1}\}_{i=1}^{n-1}$ are functions of $\mathbf{p}_m = \begin{bmatrix} x_m & y_m & z_m \end{bmatrix}'$, so is the joint PDF $f_{V_{i,1}}(\cdot)$. Denote

$$\begin{aligned}
\cos\phi_{x_i} &= \frac{x_m - x_i}{d_m(x_i, y_i, z_i)}, \\
\cos\phi_{y_i} &= \frac{y_m - y_i}{d_m(x_i, y_i, z_i)}, \\
\cos\phi_{z_i} &= \frac{z_m - z_i}{d_m(x_i, y_i, z_i)}.
\end{aligned}$$

The relation $c\delta t_i = d_m(x_i, y_i, z_i) - d_{b_i}$ with

$$d_m(x_i, y_i, z_i) = \sqrt{(x_m - x_i)^2 + (y_m - y_i)^2 + (z_m - z_i)^2}$$

yields

$$\begin{aligned}
c\frac{d\delta t_i}{dx_m} &= \frac{x_m - x_i}{d_m(x_i, y_i, z_i)} = \cos\phi_{x_i}, \\
c\frac{d\delta t_i}{dy_m} &= \frac{y_m - y_i}{d_m(x_i, y_i, z_i)} = \cos\phi_{y_i}, \\
c\frac{d\delta t_i}{dz_m} &= \frac{z_m - z_i}{d_m(x_i, y_i, z_i)} = \cos\phi_{z_i}.
\end{aligned}$$

Direct calculation gives

$$\frac{\partial \ln(f_{V_{i,1}})}{\partial \mathbf{p}_m} = -\frac{1}{c\sigma_v^2}\Phi C_0^{-1}\left(\underline{\widehat{\delta}_d} - \underline{\delta_d}\right),$$

with Φ a matrix given by

$$\Phi = \begin{bmatrix} \cos\phi_{x_2} - \cos\phi_{x_1} & \cdots & \cos\phi_{x_n} - \cos\phi_{x_1} \\ \cos\phi_{y_2} - \cos\phi_{y_1} & \cdots & \cos\phi_{y_n} - \cos\phi_{y_1} \\ \cos\phi_{z_2} - \cos\phi_{z_1} & \cdots & \cos\phi_{z_n} - \cos\phi_{z_1} \end{bmatrix}.$$

The necessary condition for optimality yields $\Phi C_0^{-1}\left(\underline{\widehat{\delta}_d} - \underline{\delta_d}\right) = 0$ at the MLE $\underline{\delta_d} = \underline{\delta_d}(\widehat{x}_m, \widehat{y}_m, \widehat{z}_m)$. A common procedure to find the MLE solution employs the Newton method and involves iterative LS. Since both Φ and $\underline{\delta_d}$ are functions of $\mathbf{p}_m$, the iterative LS can become quite complicated. For this reason the exact MLE method is not used in this dissertation.

For CRLB, we note that $\left(\underline{\widehat{\delta}_d} - \underline{\delta_d}\right)$ is a Gaussian random vector with mean zero and covariance $\sigma_v^2 C_0$ by $\{\widehat{\delta t}_{i,1} - \delta t_{i,1}\} = \{v_{i,1}\}$. The associated Fisher information matrix can be shown to be

$$\begin{aligned} \mathrm{FIM}(\mathbf{p}_m) &:= \mathrm{E}\left\{\left(\frac{\partial \ln(f_{V_{i,1}})}{\partial \mathbf{p}_m}\right)\left(\frac{\partial \ln(f_{V_{i,1}})}{\partial \mathbf{p}_m}\right)'\right\} \\ &= \frac{1}{(c\sigma_v)^2}\Phi C_0^{-1}\Phi'. \end{aligned}$$

The CRLB for the mobile position (x_m, y_m, z_m) can thus be obtained as

$$\begin{aligned} \mathrm{CRLB}(x_m, y_m, z_m) &:= [\mathrm{FIM}(\mathbf{p}_m)]^{-1} \\ &= (c\sigma_v)^2\left(\Phi C_0^{-1}\Phi'\right)^{-1}. \end{aligned}$$

For any unbiased estimate $\widehat{\mathbf{p}}_m$ to the true mobile's position $\mathbf{p}_m$, there holds

$$\mathrm{E}\left\{(\widehat{\mathbf{p}}_m - \mathbf{p}_m)(\widehat{\mathbf{p}}_m - \mathbf{p}_m)'\right\} \geq (c\sigma_v)^2\left(\Phi C_0^{-1}\Phi'\right)^{-1}.$$

References

[1] D. Li, K. Wong, Y. H. Hu, and A. Sayeed, "Detection, classification, and tracking of targets," *Signal Processing Magazine, IEEE*, vol. 19, no. 2, pp. 17–29, 2002.

[2] A. Sayed, A. Tarighat, and N. Khajehnouri, "Network-based wireless location: challenges faced in developing techniques for accurate wireless location information," *Signal Processing Magazine, IEEE*, vol. 22, no. 4, pp. 24–40, 2005.

[3] T. Hall, *Radiolocation Using AM Broadcast Signals*. Massachusetts Institute of Technology, Department of Electrical Engineering and Computer Science, 2002. [Online]. Available: http://books.google.com/books?id=XGbJNwAACAAJ

[4] C. C. C. I. Timothy D. Hall and P. N. Misra, "Radiolocation using am broadcast signals: Positioning performance," Sep. 2002, pp. 921–932.

[5] S.-H. Fang, J.-C. Chen, H.-R. Huang, and T.-N. Lin, "Metropolitan-scale location estimation using fm radio with analysis of measurements," in *Wireless Communications and Mobile Computing Conference, 2008. IWCMC '08. International*, 2008, pp. 171–176.

[6] J. Krumm, G. Cermak, and E. Horvitz, "Rightspot: A novel sense of location for a smart personal object," in *Proc. of UBICOMP 2003. Volume LNCS 2864., Springer-Verlag (2003*, 2003, pp. 36–43.

[7] A. Youssef, J. Krumm, E. Miller, G. Cermak, and E. Horvitz, "Computing location from ambient fm radio signals [commercial radio station signals],"

in *Wireless Communications and Networking Conference, 2005 IEEE*, vol. 2, 2005, pp. 824–829 Vol. 2.

[8] P. Bahl and V. N. Padmanabhan, "Radar: An in-building rf-based user location and tracking system," in *INFOCOM*, 2000, pp. 775–784.

[9] E. Chan, G. Baciu, and S. C. Mak, "Using wi-fi signal strength to localize in wireless sensor networks," in *Communications and Mobile Computing, 2009. CMC '09. WRI International Conference on*, vol. 1, 2009, pp. 538–542.

[10] R. Martin, J. Velotta, and J. Raquet, "Bandwidth efficient cooperative tdoa computation for multicarrier signals of opportunity," *Signal Processing, IEEE Transactions on*, vol. 57, no. 6, pp. 2311–2322, 2009.

[11] X. Li, B. Hua, and Y. Guo, "Study of a cost-effective localization algorithm in wireless sensor networks," in *Proceedings of the 3rd international conference on Mobile ad-hoc and sensor networks*, ser. MSN'07. Berlin, Heidelberg: Springer-Verlag, 2007, pp. 584–595. [Online]. Available: http://dl.acm.org/citation.cfm?id=1781974.1782033

[12] N. Bulusu, J. Heidemann, and D. Estrin, "Gps-less low-cost outdoor localization for very small devices," *Personal Communications, IEEE*, vol. 7, no. 5, pp. 28 –34, oct 2000.

[13] G. Mao, B. Fidan, and B. D. O. Anderson, "Wireless sensor network localization techniques," *Comput. Netw.*, vol. 51, pp. 2529–2553, July 2007. [Online]. Available: http://dl.acm.org/citation.cfm?id=1242848.1243139

[14] N. Patwari, I. Hero, A.O., M. Perkins, N. Correal, and R. O'Dea, "Relative location estimation in wireless sensor networks," *Signal Processing, IEEE Transactions on*, vol. 51, no. 8, pp. 2137 – 2148, aug. 2003.

[15] J. Aspnes, T. Eren, D. Goldenberg, A. Morse, W. Whiteley, Y. Yang, B. Anderson, and P. Belhumeur, "A theory of network localization," *Mobile Computing, IEEE Transactions on*, vol. 5, no. 12, pp. 1663 –1678, dec. 2006.

[16] T. Eren, O. Goldenberg, W. Whiteley, Y. Yang, A. Morse, B. Anderson, and P. Belhumeur, "Rigidity, computation, and randomization in network localization," in *INFOCOM 2004. Twenty-third AnnualJoint Conference of the IEEE Computer and Communications Societies*, vol. 4, march 2004, pp. 2673 – 2684 vol.4.

[17] D. Moore, J. Leonard, D. Rus, and S. Teller, "Robust distributed network localization with noisy range measurements," in *Proceedings of the 2nd international conference on Embedded networked sensor systems*, ser. SenSys '04. New York, NY, USA: ACM, 2004, pp. 50–61. [Online]. Available: http://doi.acm.org/10.1145/1031495.1031502

[18] Y. Zhang, L. Zhang, and X. Shan, "Robust distributed localization with data inference for wireless sensor networks," in *Communications, 2008. ICC '08. IEEE International Conference on*, may 2008, pp. 3125 –3129.

[19] S. Boyd and L. Vandenberghe, *Convex Optimization*. New York, NY, USA: Cambridge University Press, 2004.

[20] P. Biswas, T.-C. Liang, K.-C. Toh, Y. Ye, and T.-C. Wang, "Semidefinite programming approaches for sensor network localization with noisy distance measurements," *Automation Science and Engineering, IEEE Transactions on*, vol. 3, no. 4, pp. 360 –371, oct. 2006.

[21] P. Biswas and Y. Ye, "Semidefinite programming for ad hoc wireless sensor network localization," in *Information Processing in Sensor Networks, 2004. IPSN 2004. Third International Symposium on*, april 2004, pp. 46 – 54.

[22] L. Doherty, K. Pister, and L. El Ghaoui, "Convex position estimation in wireless sensor networks," in *INFOCOM 2001. Twentieth Annual Joint Conference of the IEEE Computer and Communications Societies. Proceedings. IEEE*, vol. 3, 2001, pp. 1655 –1663 vol.3.

[23] P. Tseng, "Second-order cone programming relaxation of sensor network localization," *SIAM J. on Optimization*, vol. 18, pp. 156–185, February 2007. [Online]. Available: http://dl.acm.org/citation.cfm?id=1272928.1272932

[24] S. Srirangarajan, A. Tewfik, and Z.-Q. Luo, "Distributed sensor network localization using socp relaxation," *Wireless Communications, IEEE Transactions on*, vol. 7, no. 12, pp. 4886 –4895, december 2008.

[25] ——, "Distributed sensor network localization with inaccurate anchor positions and noisy distance information," in *Acoustics, Speech and Signal Processing, 2007. ICASSP 2007. IEEE International Conference on*, vol. 3, april 2007, pp. III–521 –III–524.

[26] P. Biswas, T.-C. Lian, T.-C. Wang, and Y. Ye, "Semidefinite programming based algorithms for sensor network localization," *ACM Trans. Sen. Netw.*, vol. 2, pp. 188–220, May 2006. [Online]. Available: http://doi.acm.org/10.1145/1149283.1149286

[27] Q. Shi, C. He, H. Chen, and L. Jiang, "Distributed wireless sensor network localization via sequential greedy optimization algorithm," *Trans.*

Sig. Proc., vol. 58, pp. 3328–3340, June 2010. [Online]. Available: http://dx.doi.org/10.1109/TSP.2010.2045416

[28] F. Bryan Davies, "Design patterns and algorithms for small, low cost and low power tactical sensor networks," in *Military Communications Conference, 2009. MILCOM 2009. IEEE*, oct. 2009, pp. 1 –7.

[29] S. Zhu and Z. Ding, "Distributed cooperative localization of wireless sensor networks with convex hull constraint," *Wireless Communications, IEEE Transactions on*, vol. 10, no. 7, pp. 2150 –2161, july 2011.

[30] A. Abramo, F. Blanchini, L. Geretti, and C. Savorgnan, "A mixed convex/nonconvex distributed localization approach for the deployment of indoor positioning services," *Mobile Computing, IEEE Transactions on*, vol. 7, no. 11, pp. 1325 –1337, nov. 2008.

[31] B. Gidas, "Global optimization via the langevin equation," in *Decision and Control, 1985 24th IEEE Conference on*, vol. 24, dec. 1985, pp. 774 –778.

[32] M. Locatelli, D. Informatica, U. Torino, and C. Svizzera, "Simulated annealing algorithms for continuous global optimization," *Components*, pp. 1–47, 2002. [Online]. Available: http://citeseerx.ist.psu.edu/viewdoc/summary?doi=10.1.1.29.3674

[33] E. Niewiadomska-Szynkiewicz and M. Marks, "Optimization schemes for wireless sensor network localization," *Int. J. Appl. Math. Comput. Sci.*, vol. 19, pp. 291–302, June 2009. [Online]. Available: http://dx.doi.org/10.2478/v10006-009-0025-3

[34] A. Kannan, G. Mao, and B. Vucetic, "Simulated annealing based wireless sensor network localization with flip ambiguity mitigation," in *Vehicular Tech-*

nology Conference, 2006. VTC 2006-Spring. IEEE 63rd, vol. 2, may 2006, pp. 1022 –1026.

[35] P. J. Rousseeuw and B. C. V. Zomeren, "Unmasking multivariate outliers and leverage points," *Journal of the American Statistical Association*, vol. 85, no. 411, pp. 663–639, Sep. 1990.

[36] Y. Zhang, N. Meratnia, and P. Havinga, "Outlier detection techniques for wireless sensor networks: A survey," *Communications Surveys Tutorials, IEEE*, vol. 12, no. 2, pp. 159–170, Second 2010.

[37] Q. Xiao, K. Bu, Z. Wang, and B. Xiao, "Robust localization against outliers in wireless sensor networks," *ACM Trans. Sen. Netw.*, vol. 9, no. 2, pp. 24:1–24:26, Apr. 2013. [Online]. Available: http://doi.acm.org/10.1145/2422966.2422981

[38] Z. Yang, L. Jian, C. Wu, and Y. Liu, "Beyond triangle inequality: Sifting noisy and outlier distance measurements for localization," *ACM Trans. Sen. Netw.*, vol. 9, no. 2, pp. 26:1–26:20, Apr. 2013. [Online]. Available: http://doi.acm.org/10.1145/2422966.2422983

[39] Z. Yang, C. Wu, T. Chen, Y. Zhao, W. Gong, and Y. Liu, "Detecting outlier measurements based on graph rigidity for wireless sensor network localization," *Vehicular Technology, IEEE Transactions on*, vol. 62, no. 1, pp. 374–383, Jan 2013.

[40] M. Jadliwala, S. Zhong, S. Upadhyaya, C. Qiao, and J.-P. Hubaux, "Secure distance-based localization in the presence of cheating beacon nodes," *Mobile Computing, IEEE Transactions on*, vol. 9, no. 6, pp. 810–823, June 2010.

[41] S. Zhong, M. Jadliwala, S. Upadhyaya, and C. Qiao, "Towards a theory of robust localization against malicious beacon nodes," in *INFOCOM 2008. The 27th Conference on Computer Communications. IEEE*, 2008, pp. –.

[42] D. Liu, P. Ning, and W. Du, "Detecting malicious beacon nodes for secure location discovery in wireless sensor networks," in *Distributed Computing Systems, 2005. ICDCS 2005. Proceedings. 25th IEEE International Conference on*, June 2005, pp. 609–619.

[43] A. Srinivasan, J. Teitelbaum, and J. Wu, "Drbts: Distributed reputation-based beacon trust system," in *Dependable, Autonomic and Secure Computing, 2nd IEEE International Symposium on*, Sept 2006, pp. 277–283.

[44] Y.-C. Chen and J.-C. Juang, "Outlier-detection-based indoor localization system for wireless sensor networks," *International Journal of Navigation and Observation*, 2012.

[45] W. Du and L. Fang, "Lad: Localization anomaly detection for wireless sensor networks," in *In Proceedings of the 19th IEEE International Parallel & Distributed Processing Symposium (IPDPS 05*, 2005, pp. 874–886.

[46] N. Sastry, U. Shankar, and D. Wagner, "Secure verification of location claims," in *Proceedings of the 2Nd ACM Workshop on Wireless Security*, ser. WiSe '03. New York, NY, USA: ACM, 2003, pp. 1–10. [Online]. Available: http://doi.acm.org/10.1145/941311.941313

[47] W. Yang and W.-T. Zhu, "Voting-on-grid clustering for secure localization in wireless sensor networks," in *Communications (ICC), 2010 IEEE International Conference on*, May 2010, pp. 1–5.

[48] M. Maheshwari, P. Sai Ananthanarayanan, A. Banerjee, N. Patwari, and S. Kasera, "Detecting malicious nodes in rss-based localization," in *World of Wireless, Mobile and Multimedia Networks (WoWMoM), 2011 IEEE International Symposium on a*, June 2011, pp. 1–6.

[49] J. Ash and R. Moses, "Outlier compensation in sensor network self-localization via the em algorithm," in *Acoustics, Speech, and Signal Processing, 2005. Proceedings. (ICASSP '05). IEEE International Conference on*, vol. 4, March 2005, pp. iv/749–iv/752 Vol. 4.

[50] D. He, L. Cui, H. Huang, and M. Ma, "Design and verification of enhanced secure localization scheme in wireless sensor networks," *Parallel and Distributed Systems, IEEE Transactions on*, vol. 20, no. 7, pp. 1050–1058, July 2009.

[51] H. Chen, W. Lou, X. Sun, and Z. Wang, "A secure localization approach against wormhole attacks using distance consistency," *EURASIP J. Wirel. Commun. Netw.*, vol. 2010, pp. 8:1–8:11, Apr. 2010. [Online]. Available: http://dx.doi.org/10.1155/2010/627039

[52] D. Liu, P. Ning, and W. Du, "Attack-resistant location estimation in sensor networks," in *Information Processing in Sensor Networks, 2005. IPSN 2005. Fourth International Symposium on*, April 2005, pp. 99–106.

[53] L. Lazos and R. Poovendran, "Serloc: Secure range-independent localization for wireless sensor networks," in *Proceedings of the 3rd ACM Workshop on Wireless Security*, ser. WiSe '04. New York, NY, USA: ACM, 2004, pp. 21–30. [Online]. Available: http://doi.acm.org/10.1145/1023646.1023650

[54] ——, "Hirloc: high-resolution robust localization for wireless sensor networks," *Selected Areas in Communications, IEEE Journal on*, vol. 24, no. 2, pp. 233–246, Feb 2006.

[55] L. Lazos, R. Poovendran, and S. Capkun, "Rope: robust position estimation in wireless sensor networks," in *Information Processing in Sensor Networks, 2005. IPSN 2005. Fourth International Symposium on*, April 2005, pp. 324–331.

[56] Z. Li, W. Trappe, Y. Zhang, and B. Nath, "Robust statistical methods for securing wireless localization in sensor networks," in *Information Processing in Sensor Networks, 2005. IPSN 2005. Fourth International Symposium on*, April 2005, pp. 91–98.

[57] S. Capkun and J.-P. Hubaux, "Secure positioning of wireless devices with application to sensor networks," in *INFOCOM 2005. 24th Annual Joint Conference of the IEEE Computer and Communications Societies. Proceedings IEEE*, vol. 3, March 2005, pp. 1917–1928 vol. 3.

[58] S. Capkun, K. Bonne Rasmussen, M. Cagalj, and M. Srivastava, "Secure location verification with hidden and mobile base stations," *Mobile Computing, IEEE Transactions on*, vol. 7, no. 4, pp. 470–483, April 2008.

[59] K. Ho and W. Xu, "An accurate algebraic solution for moving source location using tdoa and fdoa measurements," *Signal Processing, IEEE Transactions on*, vol. 52, no. 9, pp. 2453–2463, 2004.

[60] J. Smith and J. Abel, "Closed-form least-squares source location estimation from range-difference measurements," *Acoustics, Speech and Signal Processing, IEEE Transactions on*, vol. 35, no. 12, pp. 1661–1669, 1987.

[61] I. Mellen, G., M. Pachter, and J. Raquet, "Closed-form solution for determining emitter location using time difference of arrival measurements," *Aerospace and Electronic Systems, IEEE Transactions on*, vol. 39, no. 3, pp. 1056–1058, 2003.

[62] G. Gu, "Approximate mle algorithm for source localization based on tdoa measurements," vol. 6577, 2007, pp. 657 707–657 707–9. [Online]. Available: http://dx.doi.org/10.1117/12.719865

[63] R. A. Horn and C. R. Johnson, *Matrix Analysis*. Cambridge University Press, 1990.

[64] R. Vaughan, N. Scott, and D. White, "The theory of bandpass sampling," *Signal Processing, IEEE Transactions on*, vol. 39, no. 9, pp. 1973–1984, 1991.

[65] P. P. Vaidyanathan, *Multirate systems and filter banks*. Upper Saddle River, NJ, USA: Prentice-Hall, Inc., 1993.

[66] C. Knapp and G. C. Carter, "The generalized correlation method for estimation of time delay," *Acoustics, Speech and Signal Processing, IEEE Transactions on*, vol. 24, no. 4, pp. 320–327, 1976.

[67] P. Stoica and R. Moses, *Introduction to spectral analysis*. Prentice Hall, 1997. [Online]. Available: http://books.google.com/books?id=Gh_vAAAAMAAJ

[68] B. Lathi and Z. Ding, *Modern Digital and Analog Communication Systems*, ser. The Oxford Series in Electrical and Computer Engineering. Oxford University Press, Incorporated, 2009. [Online]. Available: http://books.google.com/books?id=dltNPwAACAAJ

[69] Z. Yang and Y. Liu, "Understanding node localizability of wireless ad hoc and sensor networks," *Mobile Computing, IEEE Transactions on*, vol. 11, no. 8, pp. 1249–1260, 2012.

[70] J. Nocedal, "Theory of algorithms for unconstrained optimization," 1992.

[71] J. Barzilai and J. M. Borwein, "Two-point step size gradient methods," *IMA Journal of Numerical Analysis*, vol. 8, no. 1, pp. 141–148, 1988. [Online]. Available: http://imanum.oxfordjournals.org/cgi/doi/10.1093/imanum/8.1.141

[72] J. Tsitsiklis, D. Bertsekas, and M. Athans, "Distributed asynchronous deterministic and stochastic gradient optimization algorithms," *Automatic Control, IEEE Transactions on*, vol. 31, no. 9, pp. 803–812, 1986.

[73] R. Olfati-Saber and R. Murray, "Consensus problems in networks of agents with switching topology and time-delays," *Automatic Control, IEEE Transactions on*, vol. 49, no. 9, pp. 1520–1533, 2004.

[74] G. Calafiore, L. Carlone, and M. Wei, "A distributed gradient method for localization of formations using relative range measurements," in *Computer-Aided Control System Design (CACSD), 2010 IEEE International Symposium on*, sept. 2010, pp. 1146 –1151.

[75] A. Olshevsky and J. N. Tsitsiklis, "Convergence speed in distributed consensus and averaging," *SIAM J. Control Optim.*, vol. 48, pp. 33–55, February 2009. [Online]. Available: http://dl.acm.org/citation.cfm?id=1654147.1654158

[76] A. Kannan, B. Fidan, and G. Mao, "Analysis of flip ambiguities for robust sensor network localization," *Vehicular Technology, IEEE Transactions on*, vol. 59, no. 4, pp. 2057 –2070, may 2010.

[77] P. Wang and I. Akyildiz, "Effects of different mobility models on traffic patterns in wireless sensor networks," in *Global Telecommunications Conference (GLOBECOM 2010), 2010 IEEE*, 2010, pp. 1–5.

[78] G. Chandrasekaran, M. Ergin, J. Yang, S. Liu, Y. Chen, M. Gruteser, and R. Martin, "Empirical evaluation of the limits on localization using signal strength," in *Sensor, Mesh and Ad Hoc Communications and Networks, 2009. SECON '09. 6th Annual IEEE Communications Society Conference on*, 2009, pp. 1–9.

[79] D. P. Bertsekas and J. N. Tsitsiklis, *Parallel and distributed computation: numerical methods*. Upper Saddle River, NJ, USA: Prentice-Hall, Inc., 1989.

[80] P. A. Jensen and J. F. Bard, *Operations Research Models and Methods*. John Wiley and Sons, Inc., 2003.

Vita

Gustavo Andres Chacon Rojas was born in Chuquicamata, Chile, in 1980. He received the B.Sc. and M.Sc. in Electrical Engineering from University of Chile, Chile, in 2006. He has worked as a graduate assistant at LSU from August 2009 to May 2014. His research interests are wireless communication systems and electronic systems.